

**Molecular and Physiological
Characterization of the Photosynthetic
Mutants *prpl11-1*, *psae1-1* and *atmak3-1***

Inaugural - Dissertation
zur
Erlangung des Doktorgrades
der Mathematisch-Naturwissenschaftlichen Fakultät
der Universität zu Köln

vorgelegt von

Paolo Pesaresi

aus Jesi, Italien

Köln

2002

Die vorliegende Arbeit wurde am Max-Planck-Institut für Züchtungsforschung, Köln-Vogelsang, in der Abteilung Pflanzenzüchtung und Ertragsphysiologie (Prof. Dr. F. Salamini) in der Arbeitsgruppe von Dr. D. Leister angefertigt.

Berichterstatter: Prof. Dr. Francesco Salamini
Prof. Dr. Ulf-Ingo Flügge

Tag der mündlichen Prüfung: 16. 07. 2002

ABBREVIATIONS

<i>A. thaliana</i>	<i>Arabidopsis thaliana</i>
AIMS	amplification of insertion mutagenised sites
ATP	Adenosine triphosphate
bp	base pair
BLAST	basic local alignment search tool
cDNA	complementary deoxyribonucleic acid
Chl	chlorophyll
Ci	curie
Col-0	Columbia 0
d	day
DCMU	3-(3,4-dichlorophenyl)-1,1-dimethylurea
DNA	deoxyribonucleic acid
F	fluorescence
EST	expressed sequence tag
h	hour
<i>hcf</i>	high chlorophyll fluorescence
l	litre
LHC	light harvesting complex
M	molarity
min	minute
mol	mole
mRNA	messenger ribonucleic acid
NADP(H ⁺)	nicotinamide adenine dinucleotide phosphate (reduced/oxidised)
NPQ	non photochemical quenching
°C	degree Celsius
PAGE	polyacrylamide gel electrophoresis
<i>pam</i>	photosynthesis affected mutant
PAM	pulse amplitude modulation
PAR	photosynthetic active radiation
PCR	polymerase chain reaction
PFD	photons flux density
PSI	photosystem I
PSII	photosystem II
RNA	ribonucleic acid
rpm	revolutions per minute
s	second
SDS	sodium dodecyl sulphate
TMPD	N,N,N',N'-tetramethyl-p-phenylenediamine
w/v	weight per volume
WT	wild-type
F _{II}	effective quantum yield of photosystem II

CONTENTS

1 INTRODUCTION	1
1.1 PHOTOSYNTHETIC ELECTRON TRANSPORT	1
1.2 POLYPEPTIDE COMPOSITION OF THYLAKOID MEMBRANES	3
1.3 CHLOROPHYLL FLUORESCENCE PARAMETERS	6
1.4 PHOTOPROTECTIVE MECHANISMS: THE PHOTOSYNTHETIC STATE TRANSITIONS	7
1.5 FUNCTIONAL GENOMICS	9
1.5.1 Forward and Reverse Genetics	9
1.6 AIM OF THE THESIS	12
2. MATERIALS AND METHODS	13
2.1 THE T-DNA AND <i>En</i> -MUTAGENISED <i>A. thaliana</i> POPULATIONS	13
2.2 PLANT PROPAGATION AND GROWTH MEASUREMENTS	13
2.3 AUTOMATIC SCREENING FOR PHOTOSYNTHETIC MUTANTS OF <i>A. thaliana</i>	13
2.4 ISOLATION OF T-DNA AND <i>En</i> -TRANSPOSON FLANKING REGIONS	
2.4.1 Adapter sequences and primers (5'-3')	14
2.4.2 Amplification of insertion mutagenised sites (AIMS)	14
2.5 SEQUENCE ANALYSIS	15
2.6 ANALYSES OF NUCLEIC ACIDS	
2.6.1 cDNA single strand synthesis	16
2.6.2 Southern analysis	16
2.6.3 Northern analysis	16
2.6.4 Analysis of mRNAs associated with polysomes	17
2.7 COMPLEMENTATION OF <i>ARABIDOPSIS</i> MUTANTS	
2.7.1 <i>Agrobacterium</i> strain	18
2.7.2 <i>Agrobacterium</i> binary vectors	18
2.7.3 <i>Agrobacterium</i> -mediated transformation of <i>A. thaliana</i>	18
2.8 COMPLEMENTATION OF <i>mak3-1</i> YEAST STRAIN	19
2.9 TWO-HYBRID ANALYSIS	19

2.10 BIOCHEMICAL ANALYSES	
2.10.1 Thylakoid membrane preparation	19
2.10.2 Native and 2D PAGE	20
2.10.3 Immunoblot analysis	20
2.10.4 <i>In vivo</i> translation assay	20
2.10.5 LHCII phosphorylation analysis	21
2.10.6 Pigment composition analysis	21
2.11 BIOPHYSICAL ANALYSES	
2.11.1 Chlorophyll fluorescence measurements	22
2.11.2 Electron transport measurements	23
2.12 ELECTRON MICROSCOPY	23
2.13 INTRACELLULAR PROTEIN LOCALIZATION	23
3 FORWARD GENETICS	25
3.1 MUTANT SCREEN	25
3.2 MUTANT PHENOTYPES	26
3.3 IDENTIFICATION OF AFFECTED GENES IN <i>pam</i> MUTANTS	27
DISCUSSION	29
4. CHARACTERISATION OF THE <i>prpl11-1</i> MUTANT	31
4.1 <i>pam14</i> PHENOTYPE	31
4.2 CLONING OF THE <i>PAM14</i> LOCUS	33
4.3 COMPLEMENTATION OF <i>pam14</i>	35
4.4 LEVELS OF TRANSCRIPTS AND POLYSOME ACCUMULATION IN <i>prpl11-1</i> PLASTIDS	35
4.5 AMOUNTS OF PROTEIN COMPONENTS OF THE PHOTOSYNTHETIC APPARATUS ARE SIGNIFICANTLY ALTERED IN <i>prpl11-1</i> PLANTS	38
4.6 THE ABSENCE OF PRPL11 AFFECTS THE RATE OF PROTEIN SYNTHESIS IN PLASTIDS	39
DISCUSSION	41
5 BIOCHEMICAL AND PHYSIOLOGICAL CHARACTERISATION OF THE <i>psae1-1</i> MUTANT	44
5.1 LEVELS OF PsaH AND PsaL ARE DECREASED IN <i>psae1-1</i>	44

5.2 IN <i>psae1-1</i> STATE TRANSITIONS ARE IMPAIRED AND THE PSII ANTENNAE ARE REDUCED IN SIZE	46
5.3 A PSILHCII AGGREGATE IS PRESENT IN <i>psae1-1</i> THYLAKOIDS	48
5.4 THE LEVEL OF PHOSPHORYLATED LHCII IS INCREASED IN THE MUTANT	50
5.5 ELECTRON TRANSPORT THROUGH PSI IS ALTERED IN <i>psae1-1</i> MUTANT THYLAKOIDS	52
5.6 THE THYLAKOID ULTRASTRUCTURE IS ALTERED IN <i>psae1-1</i> CHLOROPLASTS	54
DISCUSSION	55
6 CHARACTERIZATION OF <i>atmak3-1</i> MUTANT	57
6.1 <i>pam21</i> PHENOTYPE	57
6.2 THE POLYPEPTIDE COMPOSITION OF THYLAKOID MEMBRANES IS ALTERED IN <i>pam21</i>	58
6.3 THE SYNTHESIS RATE OF D1 AND CP47 POLYPEPTIDES IS REDUCED IN MUTANT PLANTS	60
6.4 THE <i>pam21</i> MUTATION IS DUE TO A T-DNA INSERTION IN THE <i>At2g38130</i> GENE	64
6.5 THE <i>At2g38130</i> PROTEIN IS LOCATED IN THE CYTOSOL AND CAN FUNCTIONALLY REPLACE Mak3p IN YEAST	68
6.6 <i>AtMAK3</i> INTERACTS WITH THE <i>ARABIDOPSIS</i> ORTHOLOGUE OF Mak10p	70
DISCUSSION	73
SUMMARY	76
ZUSAMMENFASSUNG	77
REFERENCES	79
APPENDIX	
ERKLÄRUNG	92
LEBENS LAUF	93
ACKNOWLEDGMENTS	95

1 INTRODUCTION

Photosynthesis is the process that converts solar energy into chemical energy, and enables life on earth. A number of organisms are able to perform photosynthesis, including many types of bacteria. The most advanced photosynthetic bacteria are the cyanobacteria that use light energy to oxidize water and to build up organic compounds from atmospheric CO₂. The production of oxygen by cyanobacteria revolutionized life on earth, enabling the existence of aerobic organisms. In plants, that appeared later during evolution, photosynthesis is carried out in a specialized organelle, the chloroplast. It is generally accepted that the chloroplast originated from an ancestral cyanobacterium that was endocytosed and lived in symbiosis with primitive eukaryotic cells (Douglas, 1998). Reflecting their origin, chloroplasts have their own genome and a transcription and translation apparatus that closely resembles the one of prokaryotes. Besides photosynthesis, the chloroplast is also involved in the synthesis of amino acids, nucleotides, fatty acids and lipids, vitamins, hormones, and plays a major role in the assimilation of sulphur and nitrogen. All these functions require an extensive exchange of substrates with all the other compartments of the cell, reflecting the high level of functional integration of the ancestral cyanobacterium within the plant cell.

1.1 PHOTOSYNTHETIC ELECTRON TRANSFER REACTIONS

The transfer of reducing equivalents to NADP⁺ in order to generate NADPH, together with the net synthesis of ATP, represents the first step of photosynthesis, in both anoxygenic (photosynthetic bacteria) and oxygenic (green plants, algae and cyanobacteria) organisms. In the oxygen evolving photosynthetic organisms the transfer of electrons and protons from water to NADP⁺ is driven by a series of redox reactions powered by light energy which is absorbed by both photosystem I (PSI) and photosystem II (PSII). The two photosystems functionally interact via a number of redox components, including the plastoquinone pool, the cytochrome *b₆/f* complex and plastocyanin. Moreover, under certain conditions electrons may also cycle around PSI via the cytochrome *b₆/f* (Hill and Bendall, 1960) (Figure 1.1).

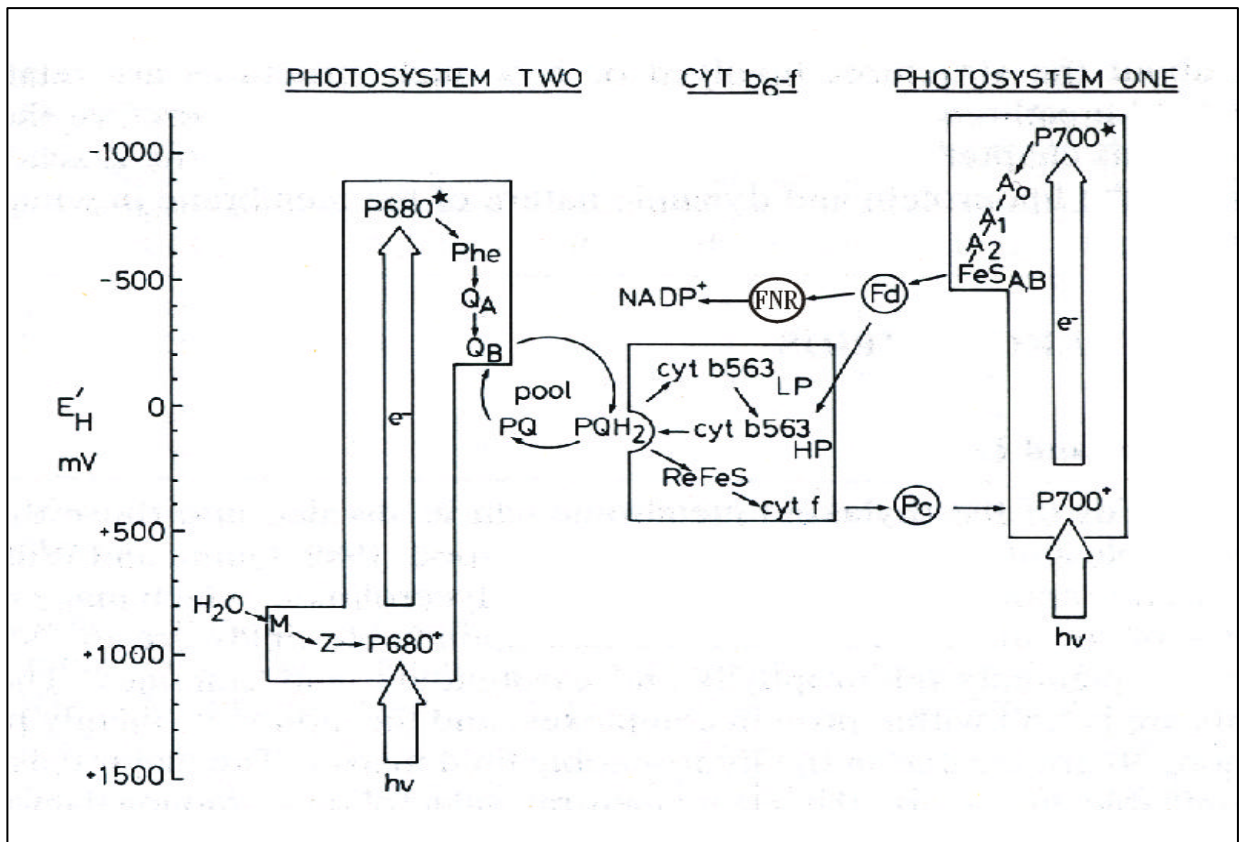


Figure 1.1 Scheme for electron transport in oxygen evolving photosynthetic organisms (Hill and Bendall, 1960). M, components of the oxygen evolving complex; Z, primary electron donor to P680, the reaction center of PSII; Phe, phaeophytin; Q_A , bound plastoquinone; Q_B , plastoquinone able to exchange with plastoquinone (PQ) pool; ReFeS, Rieske iron-sulphur center; cyt, cytochrome; Pc, plastocyanin; P700, reaction center of PSI; A_0 , A_1 , A_2 , primary and secondary electron acceptors of PSI; $FeS_{A,B}$, bound iron-sulphur centers A and B; Fd, soluble ferredoxin; FNR, ferredoxin- $NADP^+$ oxidoreductase; $NADP^+$, oxidised nicotinamide adenine dinucleotide phosphate.

The PSII complex acts as a water-plastoquinone oxidoreductase (Renger and Govindjee, 1985). The primary photochemical reaction that generates the necessary redox potential to oxidise water and reduce plastoquinone occurs in the PSII reaction center, named P680 (Joliot and Kok, 1975). When photoexcited, the reaction center chlorophyll dimer P680 reduces a bound quinone, Q_A , via a rapid oxidoreduction of a phaeophytin molecule. The electron of Q_A is transferred to a plastoquinone molecule, named Q_B . This quinone, unlike Q_A , is a two electrons acceptor, and when fully reduced, it is converted to plastoquinol (PQH_2) by the addition of two protons and no longer binds to the PSII reaction center.

The PSI complex functions as a plastocyanin-ferredoxin oxidoreductase. Within PSI, light induced charge separation occurs between the reaction center chlorophyll dimer P700 and the primary chlorophyll A acceptor, designated as A_0 (Rutherford and Heathcote, 1985).

Subsequently, the electrons flow to the secondary electron acceptors: the phylloquinone molecule named A_1 and the (4Fe-4S) center named A_2 . After reducing the terminal electron acceptors FeS_A and FeS_B the electrons are transferred from PSI to $NADP^+$ by the soluble electron carrier ferredoxin (Fd) and the Fd/ $NADP^+$ oxidoreductase (FNR). The oxidised PSI reaction center ($P700^+$) is subsequently re-reduced by plastocyanin (Gross, 1993).

The electron flow from PSII to PSI is catalysed by the cytochrome b_6/f complex that functions as a plastoquinol-plastocyanin oxidoreductase. This complex contains a two-heme cytochrome b, one heme cytochrome f and one high potential Fe_2-S_2 Rieske center (Bendall, 1982; Joliot and Joliot, 1986). Once a plastoquinol molecule is associated with the complex an electron is transferred to the Rieske center which then reduces the cytochrome f and finally an oxidised plastocyanin molecule. The second electron can be passed either to the re-oxidised Rieske center or donated to the cytochrome b_6 according to the Q-cycle scheme of Mitchell (see Bendall, 1982). As a net result of the entire process, two molecules of water are split, two molecules of NADPH synthesised and a pH gradient, used by the plastid ATPase to synthesise ATP, is built up.

1.2 POLYPEPTIDE COMPOSITION OF THYLAKOID MEMBRANES

The electron transport chain complexes are embedded in the thylakoid membranes: a lipid matrix separating an internal aqueous phase, the so-called thylakoid lumen, from the stroma (Figure 1.2). The thylakoid membranes of higher plants are not structurally homogenous, but consist of two main domains: the grana, which are stacks of thylakoids, and the stroma lamellae, which are unstacked thylakoids (Anderson, 1986). The two domains differ in protein composition and biochemical properties (Albertson, 1995). The grana are enriched in PSII polypeptides that bind chlorophyll and carotenoid molecules, responsible for the absorption of light energy and for photo-oxidation of the P680 reaction center. In particular, the chlorophyll dimer P680, together with the phaeophytin and the Q_A and Q_B quinones, is associated to the integral membrane proteins designated as D1 and D2 (Figure 1.3). These two proteins with CP47, CP43, the cytochrome b_{559} and additional small integral proteins form the core complex of PSII (Hankamer et al., 2001).

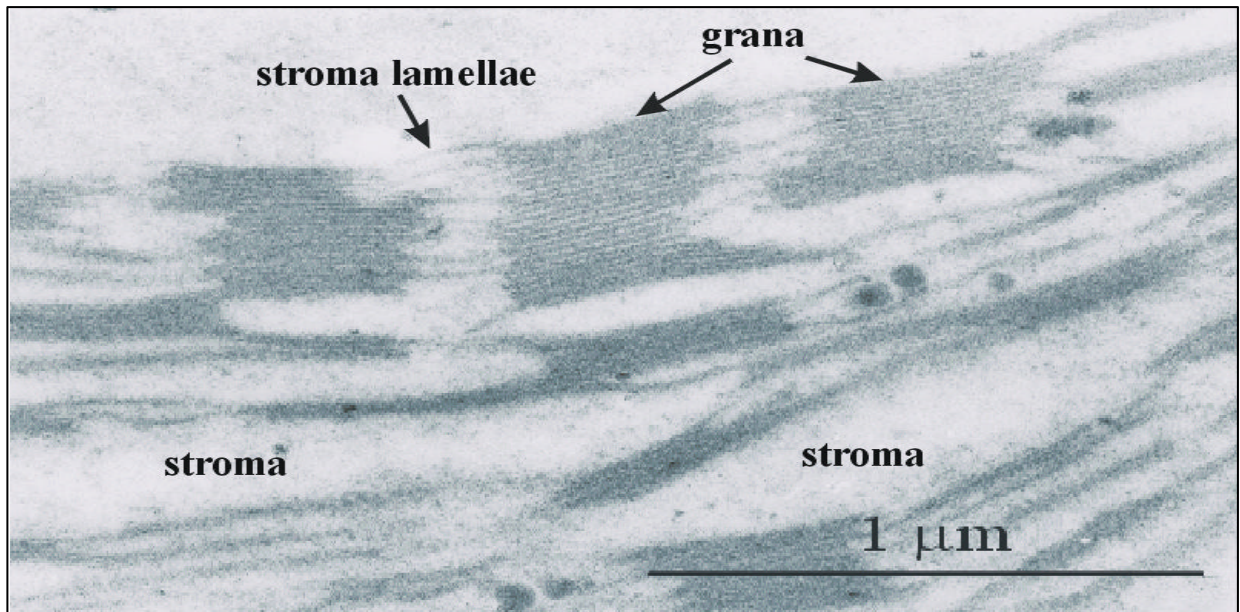


Figure 1.2 Ultrastructure of *Arabidopsis thaliana* thylakoid membranes. The chloroplast envelope is not visible.

A multi-subunit aggregate, designated as the major light harvesting complex of PSII (LHCII), surrounds the core complex and acts as the antenna of PSII (Li et al., 1986). The water-splitting process is performed by a multimeric aggregate of extrinsic proteins, named oxygen-evolving complex (OEC) that interacts directly with the D1-D2 dimer (Ghanotakis and Yocum, 1990; Nield et al., 2002).

The stroma lamellae and the surface exposed grana membranes are enriched in PSI and ATPase complexes, so that NADPH and ATP can be immediately released into the stroma. Similarly to PSII, the PSI complex consists of an inner core partially surrounded by layers of light harvesting polypeptides, the LHCI, which binds much less chlorophyll than LHCII (about 25%) (Boekema et al., 2001; Scheller et al., 2001). The inner core is formed by extrinsic and integral membrane subunits, called PsaA to PsaO (Figure 1.3). PsaA and PsaB are integral membrane subunits and bind the P700 reaction center as well as the primary and secondary electron acceptors. PsaC, together with PsaD and PsaE, forms the stromal ridge of PSI and is involved in the electron transfer to ferredoxin (Naver et al., 1995; Varotto et al., 2000). At the oxidising side of PSI the PsaN and PsaF subunits play an essential role in the docking of plastocyanin, allowing the electron flow to P700 (Haldrup et al., 1999; Haldrup et al., 2000). The association of LHCI to the inner core of PSI is mediated by PsaK and PsaG (Jensen et al., 2000; Jensen et al., 2002). The role of PsaH has been recently investigated and it appears to be involved in the

stability of PSI and in the electron transport (Naver et al., 1999). The stable association of PsaH to PSI is strictly dependent on the presence of PsaL (Lunde et al., 2000). Moreover, PsaH plays a major role in photosynthetic state transitions (Lunde et al., 2000). The functions of the PsaI, PsaJ and PsaO subunits are not known, yet.

The cytochrome *b₆f* complex is the only electron carrier exhibiting a uniform distribution between the grana and the stroma lamellae domains. The complex consists of four major polypeptides (Figure 1.3), including the cyt *f*, the cyt *b₆*, the Rieske protein and a 17 kDa polypeptide designated as subunit IV (Hauska et al., 1992; Pierre et al., 1995).

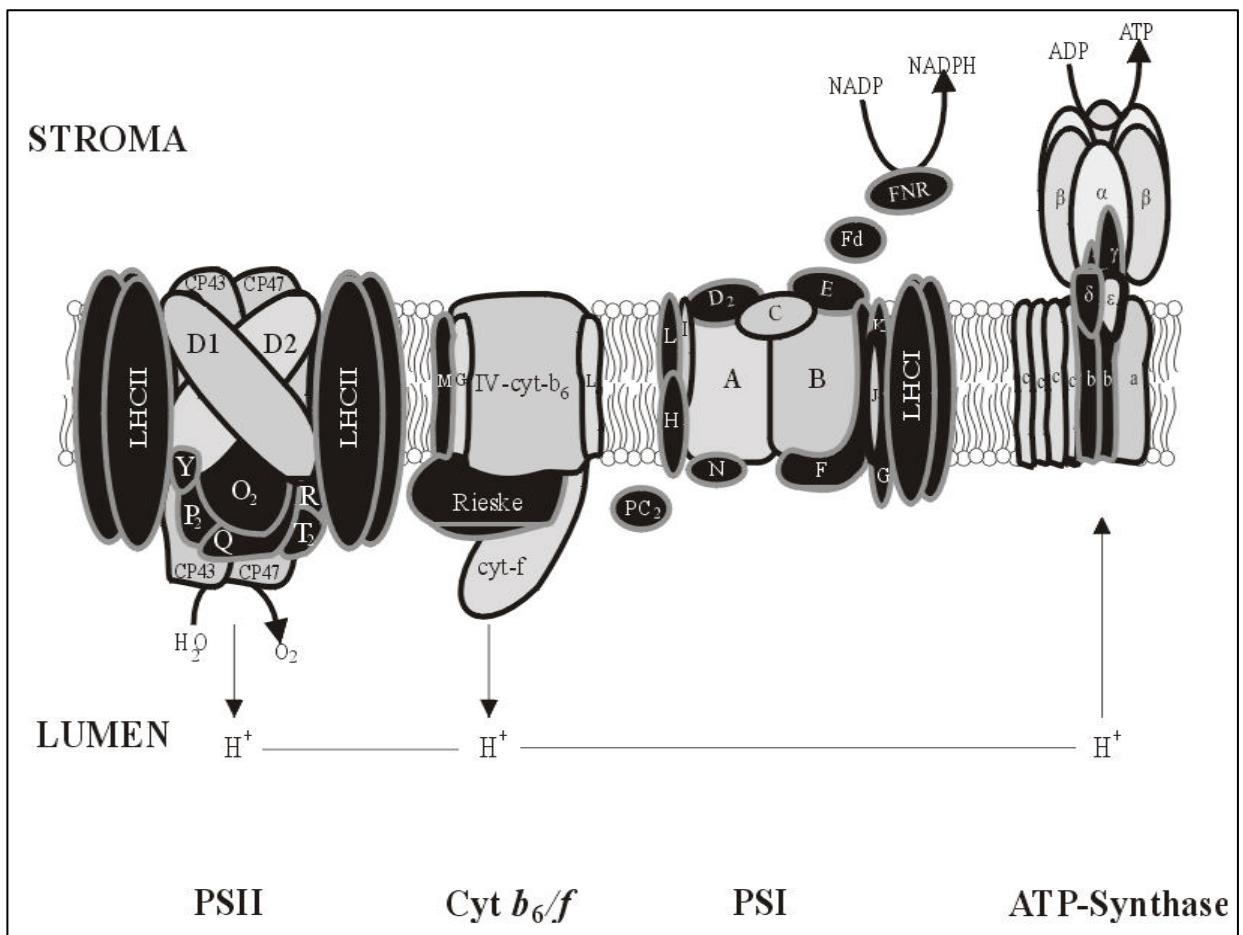


Figure 1.3 Schematic view of the thylakoid membrane complexes. PSII, photosystem II; Cyt *b₆/f*, cytochrome *b₆/f*; PSI, photosystem I. The formation of a proton (H⁺) gradient across the thylakoid membrane, essential for the formation of ATP by the ATP-synthase complex, is also shown. Nuclear encoded subunits are depicted in black, whereas the plastome encoded subunits are depicted in grey.

1.3 CHLOROPHYLL FLUORESCENCE PARAMETERS

The light energy utilised in photosynthesis is mainly absorbed by the chlorophyll molecules of the antenna complexes, which switch then to highly unstable electron-excited states. Part of the energy associated with the excited states is then used for the oxidation of the reaction centers and converted in photochemical energy, while the rest is released as fluorescence and heat (Sauer, 1975). The three different de-excitation pathways are competitive processes: the higher the fluorescence yield, the lower is the photochemical and heat conversion of light energy. Due to that, the intensity of the fluorescence emission is a valuable parameter to estimate the efficiency of photosynthesis (Clayton, 1980). To quantify chlorophyll fluorescence, the Pulse Amplitude Modulation (PAM) fluorometer system has been developed (Schreiber et al., 1986). The system is able to measure the minimal fluorescence of a dark adapted leaf (F_o) by illumination with light, designated as measuring light, whose intensity is so low that no photo-oxidation of the reaction centers takes place (Figure 1.4). After irradiating the dark-adapted leaf with a light saturating pulse the maximal fluorescence (F_m) is monitored (Krause and Weis, 1991). This fluorescence is maximal as the duration of the pulse is not long enough to allow electron transport (photochemical quenching of chlorophyll fluorescence) or heat dissipation (non-photochemical quenching of chlorophyll fluorescence). Therefore the difference between F_m and F_o (F_v) reflects the theoretical photosynthetic capacity of a leaf.

The minimal fluorescence of light-adapted leaves, recorded after a short period of dark adaptation, is called F_o' , the fluorescence emitted under light irradiation is termed transient fluorescence (F_t) and the maximal fluorescence, which is recorded after a light saturating pulse, is designated as F_m' . While the F_o' and F_t values are always higher than the F_o value, due to the presence of a portion of oxidised reaction centers in light adapted leaves, the F_m' value is reduced in comparison to the F_m value as a consequence of the activation of the heat dissipation pathway. Therefore, the difference between F_m' and F_t indicates the effective photosynthetic capacity of a leaf.

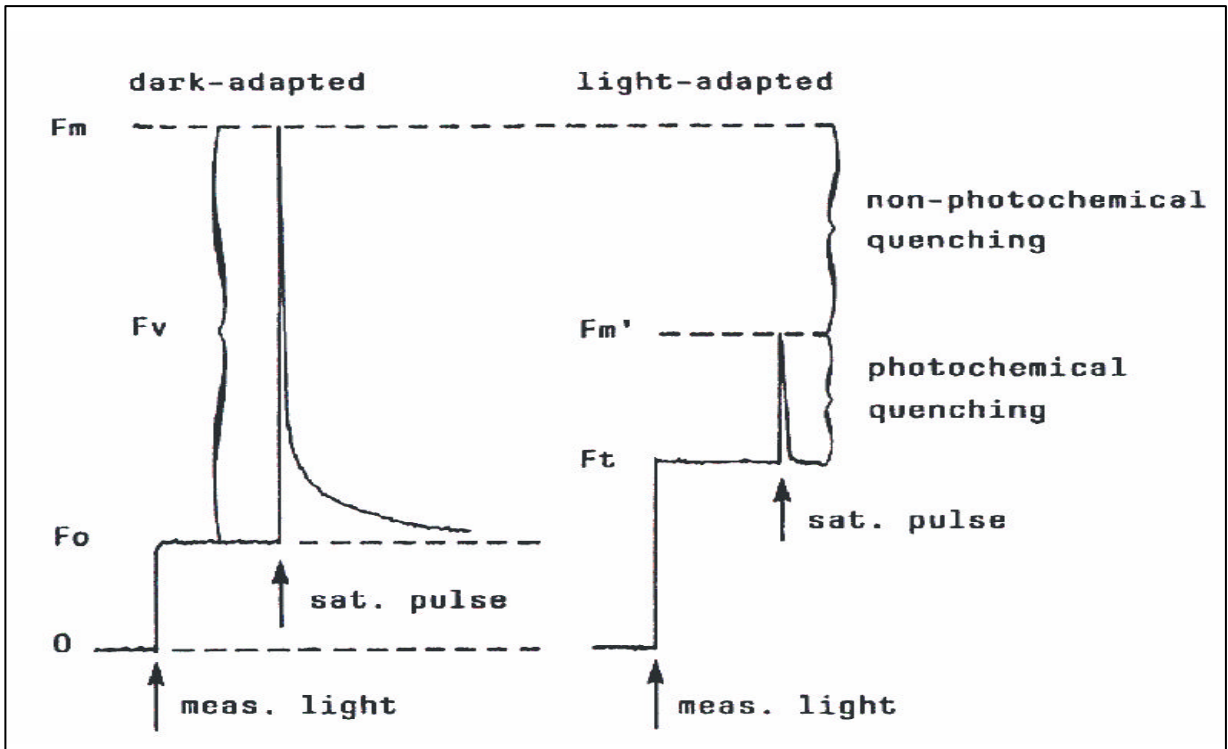


Figure 1.4 Fluorescence parameters measured by the Pulse Amplitude Modulation fluorometer system (PAM). Meas. light, measuring light; F_o , minimal fluorescence of a dark-adapted leaf; F_m , maximal fluorescence of a dark-adapted leaf; F_v , variable fluorescence; sat. pulse, light saturating pulse; F_t , transient fluorescence of a light adapted leaf; F_m' , maximal fluorescence of a light adapted leaf.

1.4 PHOTO-PROTECTIVE MECHANISMS: THE PHOTOSYNTHETIC STATE TRANSITIONS

The efficient absorption of photons by the light harvesting complexes (LHCs) of PSI and PSII is essential for photosynthesis. However, high light intensities can be harmful for plants due to saturation of the electron transport chain and consequent formation of active oxygen species (Powles, 1984; Demmig-Adams and Adams, 1992). To minimize photo-oxidative damages and optimize photosynthetic yield, plants have developed several regulatory mechanisms (Niyogi, 1999), including thermal energy dissipation (Horton et al, 1996), changes in photosystem stoichiometry (Walters and Horton, 1994; Pfannschmidt et al., 1999), and reorganization of LHCII distribution, better known as “photosynthetic state transitions” (Bennett, 1991; Allen, 1992a; Allen, 1992b; Allen and Forsberg, 2001). State transitions serve to balance the energy distribution between the two photosystems, and involve the reversible association of a mobile pool of LHCII with either PSII (state 1) or PSI (state 2) (Figure 1.5). During the transition from

state 1 to 2, induced by light (blue light) that preferentially excites PSII, a fraction of LHCII, designated as mobile pool of LHCII, becomes phosphorylated. The phosphorylated LHCII is able to diffuse from the PSII-containing grana to the PSI-rich stroma lamellae (Barber, 1986) and to attach to PSI (Samson and Bruce, 1995; Lunde et al, 2000). When PSI is preferentially excited (far-red light), LHCII is de-phosphorylated and re-attaches to PSII (state 2 \rightarrow 1 transition). The mobile LHCII pool is phosphorylated by a thylakoid-bound protein kinase (Snyders and Kohorn, 1999; Snyders and Kohorn, 2001). When PSII activity exceeds that of PSI, the plastoquinone pool becomes reduced and by interacting with the cytochrome *b₆f* activates the LHCII kinase (Gal et al., 1997; Vener et al., 1997; Vener et al., 1998; Zito et al., 1999; Wollmann, 2001). Dephosphorylation is catalyzed by a thylakoid-bound phosphatase which has a low activity (Silverstein et al., 1993; Elich et al., 1997) and is regulated by an immunophilin-like protein (Fulgosi et al., 1998).

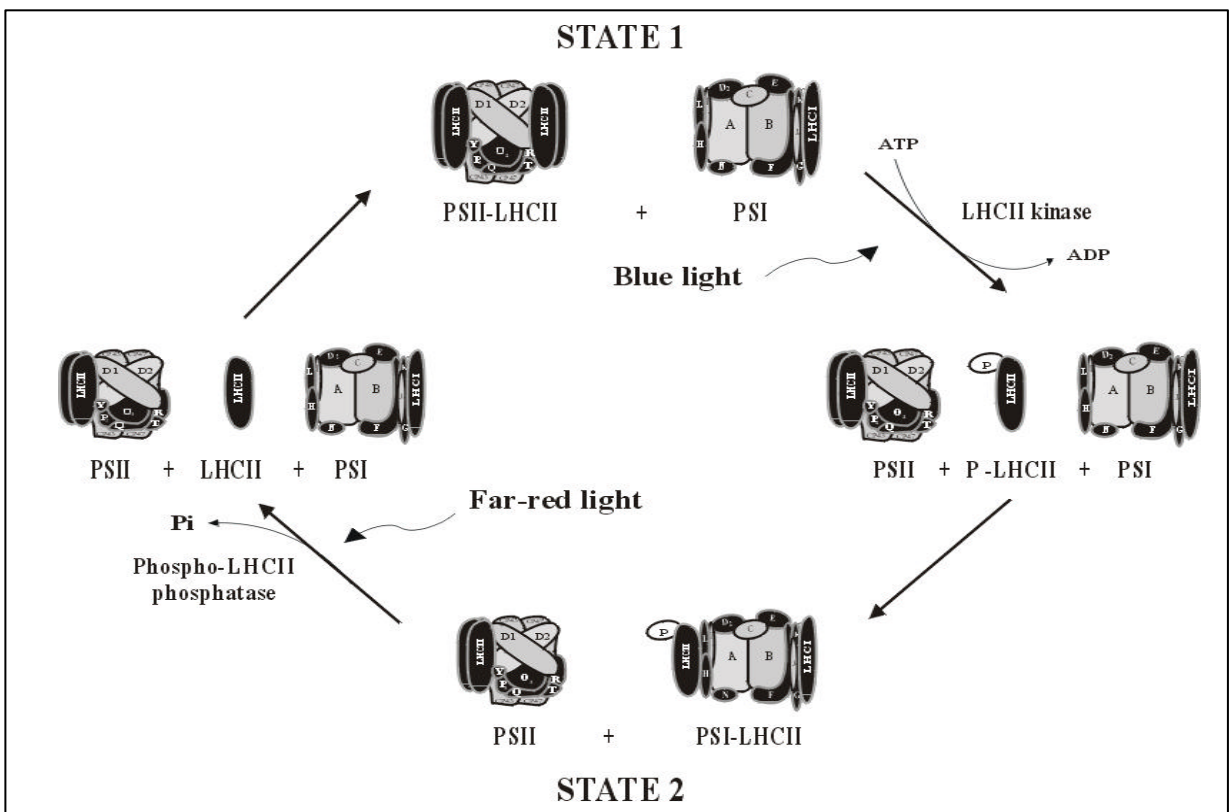


Figure 1.5 Scheme of photosynthetic state transitions. PSII-LHCII, photosystem II associated with the light harvesting complex; PSII, photosystem II without the LHCII mobile pool; P-LHCII, mobile pool of LHCII phosphorylated; PSI, photosystem I; PSI-LHCII, photosystem I associated with part of the light harvesting complex of photosystem II.

1.5 FUNCTIONAL GENOMICS

During the last decade *Arabidopsis thaliana* has become the model organism for the study of the biology of flowering plants. That was due to its short generation time, small size and large number of offspring. Moreover, its relatively small nuclear genome makes *Arabidopsis thaliana* an ideal organism for genome analysis (Meinke et al., 1998). Due to that, an international collaboration (the Arabidopsis Genome Initiative, AGI) for sequencing the *Arabidopsis* genome was established in 1996. At the end of 2000 the complete genome sequence of *A. thaliana* was reported, being the first completely sequenced plant genome and providing a novel tool for the comparison of conserved processes in eukaryotes and the identification of both plant specific genes and genes important for crop improvement (Lin et al., 1999; Mayer et al., 1999; Salanoubat et al., 2000; Tabata et al., 2000; Theologis et al., 2000). The analysis of the *Arabidopsis* genome resulted in the identification of 25 498 genes encoding proteins from 11 601 families (The Arabidopsis Genome Initiative, 2000). The functions of 69% of the genes were classified according to sequence similarity to proteins of known functions in all organisms. About 30% of the predicted gene products could not be assigned to functional categories and were classified as unknown proteins. Moreover, the information derived from sequencing and analysis of the genome significantly simplifies the identification of genes responsible of the altered phenotypes found within the mutagenised *Arabidopsis* populations, thus allowing the attribution of functions to genes. In fact, the isolation of *Arabidopsis* mutants via forward and reverse genetics has become the strategy of choice to investigate the biological processes of higher plants.

1.5.1 Forward and Reverse Genetics

The forward genetics approach to investigate photosynthesis is based on the isolation of photosynthetic mutants by using one of the several screening strategies available, such as: alteration in pigment composition of leaves, reduction of CO₂ uptake, resistance to photodynamic inhibitors of photosynthesis and alteration in chlorophyll fluorescence yield (Sommerville, 1986).

During the last 5 years, the screening method based on altered fluorescence emission has received the widest attention. This strategy is based on the evidence that any limitation of

electron transport at or beyond the primary acceptor of PSII will increase the level of fluorescence emission (Bennoun and Levine, 1967).

In 1996, Meurer et al. reported the isolation of 34 recessive photosynthetic mutants of the high-chlorophyll-fluorescence (*hcf*) phenotype by screening 7700 M₂ progenies of ethyl methane sulfonate (EMS) treated seeds of *Arabidopsis thaliana*. Most of the homozygous recessive plants were found to be seedling-lethal and with reduced chlorophyll content. On the basis of the chlorophyll fluorescence analyses and P700 absorbance changes, the *hcf* mutants were classified in different groups, including mutants with not functional PSI or PSII, and mutants with defective intersystemic electron transfer (Meurer et al., 1996).

Mutants of *Arabidopsis thaliana* that cannot dissipate excess absorbed light energy were identified by Niyogi et al. (1998). 30 000 *Arabidopsis* M₂ seeds mutagenised by EMS or fast neutron bombardment were screened by using a chlorophyll fluorescence video-imaging system. 13 independent mutants with defects in non-photochemical quenching of chlorophyll fluorescence (NPQ) were identified, including mutants defective in the xanthophyll cycle and in the energy dependent component (qE) of NPQ (Niyogi et al., 1998; Li et al., 2000).

A similar screen was performed by Toshiharu Shikanai on 21 000 *Arabidopsis* M₂ seeds resulting in the identification of 37 mutants. According to the chlorophyll fluorescence emission, mutants were classified in three groups, including plants with defective PSII, plants with altered NPQ, and plants affected in both PSI and PSII (Shikanai et al., 1999).

Photosynthetic mutants can be also identified by reverse genetics. This strategy involves the isolation of mutant plants knocked out in genes assumed to play roles in photosynthesis. This approach was made possible due to the existence of large collections of T-DNA and transposon transformants of *Arabidopsis* (Wisman et al., 1998; Parinov et al., 1999; Speulman et al., 1999; Parinov and Sundaresan, 2000). In particular, an *Arabidopsis* knockout facility has recently been established at the University of Wisconsin to provide access for the screening of 60 480 T-DNA lines (Krisan et al., 1999). The screen is based on PCR reactions primed by oligonucleotides that are complementary to the genes of interest and to the insertional mutagen. Additionally, the realisation of arrays of spotted flanking regions, at the Max-Planck-Institute for Plant Breeding Research in Cologne, has further simplified the screen, allowing the large-scale identification of transposon insertional mutants by simple hybridisation procedures (Steiner-Lange et al., 2001). In parallel, identification of about 75 000 stable insertion

positions, by sequencing and analysis of T-DNA flanking regions, has been also performed and the data are available at the Salk Institute database (<http://signal.salk.edu/cgi-bin/tdnaexpress>).

1.6 AIM OF THE THESIS

This thesis was aimed to uncover the functions of genes involved at different levels in the process of photosynthesis. Although the photosynthetic process has been extensively studied and the major enzymatic complexes identified, many aspects remain to be elucidated:

- The functions of a number of components of the photosynthetic apparatus are still unclear (see Chapter 1.2).
- Only few complexes involved in the import of proteins to the chloroplast and in sorting to the chloroplast compartments are known (Robinson et al., 2001).
- The specific signals exchanged between the nucleus and the chloroplast to co-ordinate gene expression and to accumulate the various subunits in the amount required for their proper assembly are only partially understood (Bauer et al., 2001).
- The understanding of the molecular mechanisms and the roles of the so-called photoprotective mechanisms are not fully clarified (Niyogi, 1999).

Nowadays, these and many other processes, difficult to dissect in a systematic manner by physiological studies, can be efficiently addressed by using the genetic tools provided by the collections of *Arabidopsis* mutants and the information derived from the analysis of *Arabidopsis* genome sequence.

The forward genetics approach has been used in this study by isolating a set of photosynthetic *Arabidopsis* mutants. The affected genes were identified and the phenotypes extensively characterised at physiological and molecular level in order to attribute functions to genes.

2 MATERIALS AND METHODS

2.1 THE T-DNA AND *EN*-MUTAGENISED *A. thaliana* POPULATIONS

The T-DNA mutagenised *Arabidopsis thaliana* population (ecotype Col-0), generated by Bernd Reiss (Max-Planck-Institute for Plant Breeding Research), is made up of 5 500 lines, containing random insertions of the 5.8 Kb T-DNA AC106.

The *En*-mutagenised *Arabidopsis thaliana* population (ecotype Col-0) comprises 8 000 lines carrying in total 48 000 insertions of the autonomous maize transposable element *En/Spm* (Wisman et al., 1998).

2.2 PLANT PROPAGATION AND GROWTH MEASUREMENTS

Seeds of *Arabidopsis thaliana* lines were sown in plastic trays with *Minitray* soil (Gebr. Patzer GmbH & co. KG, Sinntal-Jossa, Germany) and incubated for 3d at 2-5°C in the dark to break dormancy. Plants were grown in a greenhouse under the following conditions: day period of 16h with 20°C and PFD of 80 $\mu\text{mol photons m}^{-2} \text{s}^{-1}$; night period of 8h with 15°C. Fertilisation with “Osmocote plus” (15% N, 11% P₂ O₅, 13% K₂O, 2% MgO; Scotts Deutschland GmbH, Nordhorn, Germany) was performed according to the manufacturer’s instructions. Plant growth was measured by using an integrated digital video image analysis system (Abington Partners, Bath, UK) as reported in Leister et al. (1999).

2.3 AUTOMATIC SCREENING FOR PHOTOSYNTHETIC MUTANTS OF *A. thaliana*

The screening for mutants with altered effective quantum yield of PSII [$\Phi_{\text{II}} = (F_m' - F_t)/F_m' = \Delta F/F_m'$, (Genty et al., 1989)] was performed by using an automatic pulse amplitude modulation fluorometer system (J. Kolbowski, D-97422 Schweinfurt, Germany). A *Computerized Numerical Control* (CNC) router [Controller C116-4 and flat-bed machine FB1 (1100x750); ISEL automation, Eiterfeld, Germany] was combined with a *Pulse Amplitude Modulation* (PAM) fluorometer (one-channel version of Phyto-PAM, Walz, Effeltrich; Schreiber et al 1986). F_t was measured under photosynthetic active radiation (PAR) of 80 $\mu\text{mol m}^{-2} \text{s}^{-1}$ and 500-ms pulses of white saturating light (3 000 $\mu\text{mol m}^{-2} \text{s}^{-1}$) were used to determine F_m' and the ratio = $\Delta F/F_m'$. The sensor, which provides excitation

and measurement of fluorescence, was modified to be movable and be positioned within plant tray dimensions by an automatic steering device. The automatic PAM fluorometer system measured Φ_{II} of *A. thaliana* plants one after the other in a predefined pattern, whereby individual leaves were identified automatically (auto-focus mode) by their optimal F_t ($100 < F_t < 250$). The auto-focus mode comprised a pre-defined pattern used by the sensor to identify leaves for optimal measurement (center ? all 4 corners ? center). The sensor was positioned at a distance of less than 2 cm from leaves measured to avoid cross-illumination. 1 536 plants grown in trays (128 lines with 12 individuals) were screened per week.

2.4 ISOLATION OF T-DNA AND *En*-TRANSPOSON FLANKING REGIONS

2.4.1 Adapter sequences and primers (5'-3' orientation)

The regions flanking *AC106* T-DNA insertions were isolated by using the following adapters and primers: APL1632 (LR32 + APL16), APL1732 (LR32 + APL17), LR32 (ACTCGATTCTCAACCCGAAAGTATAGATCCCA), APL16 (*P*-TATGGGATCACATTAA-NH₂), APL17 (*P*-CGTGGGATCACATTAA-NH₂), LR26 (ACTCGATTCTCAACCCGAAAGTATAG). Left border of *AC106* T-DNA: T9750as (ATAATAACGCTGCGGACATCTACATTTT) and T9697as (CTCTTTCTTTTTCTCCATATTGACCAT); right border: T4496s (CAGGGTACCCGGGGATCAGATTGTC) and T4554s (GATCAGATTGTCGTTTCCCGCCTTCAGTTT). The regions flanking the *En* transposable element were isolated by using the following primers: right border, En8130s (GAGCGTCGGTCCCCACACTTC TATAC) and En8153s (TACGAATAAGAGCGTCCATTTTAGAGTG), left border, En230as (AGAAGCACGACGGCTGTAGAATAGGA) and En82as (ACCCACACTTTTACTTCGATTAAGAGTGT). The adapters were identical to the ones used for the isolation of the T-DNA flanking regions.

2.4.2 Amplification of insertion mutagenised sites (AIMS)

Sequences flanking the left border and the right border of both the *AC106* T-DNA and the *En*-transposon were isolated by PCR amplification of restricted and adapter-ligated plant DNA, similar to the procedure described in Frey et al. (1998). 100 ng of Arabidopsis DNA,

isolated according to Liu et al. (1995), were digested with *Csp6I* (*Hin6I*) and ligated overnight at 16°C to 12.5 pmol of adapter APL1632 (APL1732). 4 µl of the ligation were used in a linear PCR either with primer T9697as (En230as) for the T-DNA (*En*-transposon) left border or with primer T4554s (En8130s) for the T-DNA (*En*-transposon) right border. Subsequently, a 1-µl aliquot of the linear PCR was used as template for an exponential PCR with the nested primer T9750as (En82as) for the T-DNA (*En*-transposon) left border, or the nested primer T4496s (En8153s) for the T-DNA (*En*-transposon) right border and LR26. Amplifications were performed with the Advantage[®] 2 PCR kit (Clontech) and the following cycling conditions: initial denaturation for 2 min at 94 °C, followed by 30 cycles of 30 s denaturation at 94°C, 1 min annealing at 64°C and 1 min 30 s elongation at 73°C. Products of exponential PCR were separated by electrophoresis on 4% (w/v) polyacrylamide gels, bands visualized by silver staining and candidate bands were excised (Sanguinetti et al., 1994). PCR products were eluted in 50 mM KCl, 10 mM Tris-HCl pH9.0, 0.1% Triton-X 100, reamplified and directly sequenced, after gel purification, using an ABI prism 377 sequencer.

2.5 SEQUENCE ANALYSIS

Sequence data were analysed with the Wisconsin Package Version 10.0, Genetics Computer Group, Madison, Wisconsin (GCG) (Devereux et al., 1984) and amino acid sequences were aligned using the CLUSTAL-W program, (version 1.7) (Thompson et al., 1994). To infer a phylogenetic tree, protein sequences were aligned by CLUSTAL-W, bootstrapped and then subjected to parsimony and distance-matrix (observed differences and neighbour joining) analyses (PAUP, V4b5 for Unix; Swofford, 2000). Chloroplast import sequence predictions were done using the TargetP program (version 1.0; <http://www.cbs.dtu.dk/services/TargetP/#submission>; Emanuelsson et al., 2000). For the protein and nucleotide sequence comparison, the databases at the NCBI (<http://www.ncbi.nlm.nih.gov>) and MIPS (<http://mips.gsf.de>) were employed.

2.6 ANALYSES OF NUCLEIC ACIDS

2.6.1 cDNA single strand synthesis

cDNA single strand synthesis, with oligo(dT)₁₂₋₁₈ primers, was performed according to “SuperscriptTM First-Strand Synthesis System for RT-PCR” (GibcoBRL[®], Life Technologies).

2.6.2 Southern analysis

Southern analyses were performed according to Sambrook et al. (1998). Genomic DNA was digested with *SfuI* for 6 h at 37°C, and a probe complementary to the left border of the *AC106* T-DNA was used for hybridization. The following primers were used to amplify the probe: T-DNAs (ATTGAAACACGGTGCATCTGATCGGA) T-DNAs (TTCAAATAGAGGACCTAACAGAACTCG).

2.6.3 Northern analysis

Total plant RNA was extracted from fresh tissue using the TRIzol method (InvitrogenTM, life technologies). Northern analyses were performed under stringent conditions, according to Sambrook et al. (1998). Probes complementary to nuclear and chloroplast genes were used for the hybridizations. Table 2.1 lists the genes analyzed and the primers used to amplify the probes. All the probes were cDNA fragments labeled with [³²P]. Signals were quantified by using a phosphoimager (Storm 860; Molecular Dynamics) and the program IMAGE QUANT for Macintosh (version 1.2; Molecular Dynamics).

<i>Gene name</i>	<i>Sense primer (5'-3')</i>	<i>Anti-sense primer (5'-3')</i>
<i>Prpl11</i>	agaaacagtctccgcttctc	aatggctcgtgcagttcaggt
<i>AtMAK3</i>	cttaccgggtacttctctac	ggcttcataactcttggttggg
<i>atpA</i>	gacagacagaccggtaaaac	aaacatctcctgactgggtc
<i>atpB</i>	ttaggtcctgtcgatactcg	acccaataaggcggatacct
<i>psbA</i>	tgcattccgttgatgaatggc	tcggccaaaataaccgtgag
<i>psbB</i>	caattaggtggctatgggc	ggtagcgggtgaccattgaa
<i>psbC</i>	gttcttgatccaatgtggag	ttccggttagtccataaggg
<i>psbD</i>	tagctttagctggctcgtgac	gaaaggcacctacacctaac
<i>psbE</i>	ctatagtcattgggtcctcc	cagaatcgattccctacgag
<i>rbcL</i>	cgttggagagaccggttctt	caaagcccaaagtgtactcc
<i>psaA</i>	tgggctaaaccgggtcattt	ggaaccaaccagcaaaaagc
<i>psaB</i>	gtattgctaccgcacatgac	ccacgaaactcttggtttcc
<i>APT1</i>	tcccagaatcgctaagattg	cctttcccttaagctctg

Table 2.1 Primers used to generate cDNA probes are listed

2.6.4 Analysis of mRNAs associated with polysomes

Polysomes were isolated as described by Barkan (1998). 200 mg of leaf tissue were ground to a fine powder in liquid nitrogen, mortar and pestle. Subsequently, the microsomal membranes were solubilized with 1% Triton X-100 and 0.5% sodium deoxycholate. The solubilized material was layered onto 15 to 55% step sucrose gradients and centrifuged in a Beckman L7-55 ultracentrifuge (Kontron TST 60.4 rotor) at 45 000 rpm for 65 min at 4 °C. The sucrose gradients were fractionated in at least ten fractions and the mRNAs associated with polysomes were then purified by using extraction with phenol/chloroform/isoamyl

alcohol (25:24:1) followed by precipitation at room temperature with 95% ethanol. All samples were then subjected to Northern analyses as described in chapter 2.6.3.

2.7 COMPLEMENTATION OF *ARABIDOPSIS* MUTANTS

2.7.1 *Agrobacterium* strain

The *Agrobacterium* strain GV3101 was used for *Arabidopsis* transformation. The strain has a C58C1 chromosomal background marked by a rifampicin resistance mutation, and carries pMP90RK, a helper Ti plasmid encoding virulence functions for T-DNA transfer from *Agrobacterium* to plant cells (Koncz et al., 1990).

2.7.2 *Agrobacterium* binary vectors

The binary expression vector pPCV702 was used to perform the complementation test with cDNA sequences. The vector carries the cauliflower mosaic virus 35S promoter, a **b**-lactamase gene providing ampicillin and carbenicillin resistance for selection in *E.coli* and *Agrobacterium*, and a kanamycin resistance gene as plant selectable marker (Koncz et al., 1990). The expression vector pP001-VS was used to perform the complementation test with genomic sequences. The vector carries a **b**-lactamase gene providing ampicillin and carbenicillin resistance and a *pat* gene (phosphoinositrin-N-acetyltransferase) conferring resistance to the BASTA herbicide (generated by Bernd Reiss, Max-Planck-Institute for Plant Breeding Research).

2.7.3 *Agrobacterium*-mediated transformation of *A. thaliana*

Arabidopsis mutant plants were transformed as reported (Clough and Bent, 1998). Flowering plants were dipped for 15 s in an *Agrobacterium* suspension containing 5% sucrose and the surfactant Silwet L-77 (0.0005%). After dipping, plants were transferred to a growth-chamber with high humidity conditions for two days and then to the greenhouse until seeds were harvested.

2.8 COMPLEMENTATION OF *mak3-1* YEAST STRAIN

The *Saccharomyces cerevisiae* strain 2323 (*MATa*, *ura3*, *leu2*, *his3*, *aro7*, *mak3-1*) carrying a mutation in the *MAK3* gene (Tercero et al., 1992) was transformed with the empty pH7 vector (LEU2, replication origins for yeast and *E.coli*, ADH1 promoter and terminator sequences), with pH7 carrying the *Arabidopsis MAK3* gene (*AtMAK3*) and with the pJC11B vector carrying the yeast wild-type *MAK3* gene (pRS316 URA3 CEN with 5.2 Kb *MAK3* insert). To test whether *AtMAK3* could complement the strain 2323, the cytoplasm of that strain was mixed with the cytoplasm of strain 3167 (*MATa*, *kar1-1*, *arg1*, *leu1*, *thr1*) carrying the viral dsRNAs, L-A-HN and M₁. The cytoduction (cytoplasmic mixing) was performed as reported in Ridley et al. (1984). Cytoductants were tested for the killer phenotype as described in Ridley et al. (1984).

2.9 TWO-HYBRID ANALYSIS

The yeast two hybrid assays were performed by using two different yeast strains supplied by Clontech:

- Y190 (Harper et al., 1993): *MATa*, *ura3-52*, *his3-200*, *ade2-101*, *lys2-801*, *trp1-901*, *leu3-112*, *gal 4D*, *gal 80D*, *cyh^r 2*, *LYS2::GAL1_{UAS}-HIS3_{TATA}-HIS3*, *MEL1*, *URA3::GAL1-_{mers(X3)}-GAL1_{TATA}-LacZ*
- AH109 (James et al., 1996): *MATa*, *ura3-52*, *his3-200*, *ade2-101*, *lys2-801*, *trp1-901*, *leu3-112*, *gal 4D*, *gal 80D*, *LYS2::GAL1_{UAS}-GAL1_{TATA}-HIS3*, *MEL1 GAL2_{UAS}-GAL2_{TATA}-ADE2*, *URA3::MEL1_{UAS}-MEL1_{TATA}-LacZ*

The pAS2-1 vector (Harper et al., 1993) carrying the GAL4 DNA binding domain was used to express the baits and pGAD424 (Bartel et al., 1993) and pGADT7 (Harper et al., 1993), carrying the GAL4 activation domain were used to express the preys. Yeast transformation was performed following a lithium acetate procedure as described by Gietz et al. (1992).

2.10 BIOCHEMICAL ANALYSES

2.10.1 Thylakoid membrane preparation

Leaves from 4 week-old plants were harvested in the middle of the day period and thylakoids were prepared from mesophyll chloroplasts as described in Bassi et al. (1985).

Thylakoid membrane amount was calculated according to the total chlorophyll content as described in Porra et al. (1989).

2.10.2 Native and 2D PAGE

The GREEN NATIVE PAGE was performed by fractionating thylakoid membrane samples on polyacrylamide gradient gels (4-12% acrylamide) according to Peter and Thornber (1991) using lithium dodecyl sulphate (LDS) instead of lauryl β -D imminopropionidate in the upper electrophoresis buffer. The BLUE NATIVE PAGE was performed according to Schagger (1994). In particular, a 5-12% acrylamide gradient was used for the separating gel and 4% acrylamide for the stacking gel. Both native PAGEs were run at 4°C. Fractionation in the second dimension was in denaturing SDS-PA gradient (10-16% acrylamide) gels as described by Schagger and von Jagow (1987). The 2D gel was stained either with silver salts or Comassie Brilliant Blue R 250 as described in Sambrook et al. (1989). Densitometric analyses of protein gels after Comassie staining were performed by using the Lumi Analyst 3.0 (Boehringer-Mannheim).

2.10.3 Immunoblot analysis

For immunoblot analyses, thylakoid proteins separated by denaturing 1D or 2D PAGE (Schagger and von Jagow, 1987) were transferred to Immobilon-P membranes (Millipore) and incubated with antibodies specific for individual subunits of PSI (PsaA/B, C, D, E, F - G, H, L, N, LHCI), PSII (D1, CP43, CP47, D2, Cyt*b*-559, OEC, LHCII), Cyt b6/f (PetD, Cyt f), ATPase (α - and β -subunit) and RUBISCO (RbcS and RbcL). Phosphorylated threonine residues were identified using a phosphothreonine-specific antibody raised in rabbits (Zymed Laboratories Inc.). Signals were detected using the Enhanced Chemiluminescence Western-Blotting Kit (Amersham).

2.10.4 *In vivo* translation assay

Young leaves of 4 week-old wild-type and mutant plants were harvested and vacuum-infiltrated with 50 μ l of reaction medium [(1 mM KH₂PO₄, pH 6.3; 0.1 % (w/v) Tween 20; 50 μ Ci [³⁵S]methionine (specific activity >1000 Ci/mmol; Amersham Buchler, Braunschweig, Germany); with or without 20 μ g/ml cycloheximide] for 5 s. After vacuum

infiltration, leaves were illuminated ($120 \mu\text{mol photons m}^{-2} \text{ s}^{-1}$) for a variable time (10, 20 and 30 min) at 25°C , washed twice with 500 μl of wash buffer (20 mM Na_2CO_3 , 10 mM DTT), disrupted by grinding in the presence of 60 μl of 100 mM Na_2CO_3 buffer, and clarified by centrifugation (4°C ; 15 min at 15 000 rpm, Sigma 2MK, Christ, Osterode, Germany). 50- μl aliquots of the supernatant, as well as of the resuspended pellet, were collected, and the incorporated radioactivity was quantified as described in Mans and Novelli (1961). Proteins were fractionated either by SDS-PAGE or by BLUE NATIVE PAGE in the first dimension and SDS-PAGE in the second dimension and transferred to Immobilon-P membranes (Millipore). Radioactive signals were detected by using Fuji Bio imaging plates (Fuji Bio imaging analyser, BAS 2000 software package, TINA software package v2.08 beta).

2.10.5 LHCII phosphorylation analysis

The LHCII phosphorylation level was analysed both *in vivo* and *in vitro*. For both kinds of analyses, thylakoids from 4 week-old plants were prepared as described in Haldrup et al. (1999) in the presence of the phosphatase inhibitor NaF (10 mM). For determination of LHCII phosphorylation levels *in vivo*, leaves were adapted to the dark for 16 h, then allowed to take up [^{33}P]phosphate for 30 min and subsequently exposed to irradiation favouring phosphorylation ($80 \mu\text{mol photons m}^{-2} \text{ s}^{-1}$, 2 h) or dephosphorylation ($800 \mu\text{mol photons m}^{-2} \text{ s}^{-1}$, 2 h). Identical amounts of thylakoid proteins (8 μg) were separated by SDS-PAGE and incorporation of radioactivity was detected by phosphoimager (Storm 860, Molecular Dynamics).

For the *in vitro* assay, thylakoids were isolated from dark-adapted leaves and incubated with 10 μCi [γ - ^{33}P]-ATP under reducing conditions (0.5 mM NADPH, 5 μM ferredoxin from barley, 200 mM ATP and 10 mM NaF) for up to 30 min in the dark (Steinback et al., 1982). Separation and detection of thylakoid proteins were performed as described for the *in vivo* assay.

2.10.6 Pigment composition analysis

Pigment analysis was carried out by reversed-phase HPLC as described in Färber et al. (1997). For pigment extraction, leaf discs were frozen in liquid nitrogen and disrupted by

grinding in a mortar in presence of acetone. After a short centrifugation, pigment extracts were filtered through a 0.2 μm membrane filter and either used directly for HPLC analysis or stored for up to 2 days at -20°C .

2.11 BIOPHYSICAL ANALYSES

2.11.1 Chlorophyll fluorescence measurements

In vivo Chl-a fluorescence of single leaves was measured using the PAM 101/103 (Walz, Effeltrich, Germany) as described in Varotto et al., (2000). Pulses (800-ms) of white light ($6000 \mu\text{mol photons m}^{-2} \text{s}^{-1}$) were used to determine the maximum fluorescence (F_m) and the ratio $(F_m - F_o)/F_m = F_v/F_m$. A 15-min illumination with actinic light at a rate of $80 \mu\text{mol photons m}^{-2} \text{s}^{-1}$ was used to drive electron transport between the two photosystems before measuring the effective quantum yield of PSII (Φ_{II}). In addition, the fluorescence quenching parameters qP (photochemical quenching) = $(F_m' - F_t)/(F_m' - F_o')$, and qN (non-photochemical quenching) = $1 - (F_m' - F_o')/(F_m - F_o)$ were recorded (Schreiber, 1986).

Also state transitions were measured with the pulse amplitude modulation 101-103 fluorometer. After 30 min of dark incubation, the maximum fluorescence (F_m) of leaves was measured by using a saturating light pulse (0.8 s, $6000 \mu\text{mol photons m}^{-2} \text{s}^{-1}$). Leaves were subsequently illuminated for 20 min with blue light ($80 \mu\text{mol photons m}^{-2} \text{s}^{-1}$) from a Schott KL-1500 lamp equipped with a Walz BG39 filter. The maximum fluorescence (F_{m2}), in state 2, was then measured. Next, state 1 was induced by switching to far-red light (Walz 102-FR), and F_{m1} was recorded 20 min later. qT was calculated according to the equation: $qT = (F_{m1} - F_{m2})/F_{m2}$ (Jensen et al., 2000). The relative fluorescence changes of PSII (F_r) were measured as reported in Lunde et al. (2000).

Emission and excitation spectra of state 1- or state 2-adapted leaves were recorded by using a Spex-Fluorolog spectrometer as described in Holzwarth et al. (1978). All spectra were corrected for wavelength-dependent changes in detector sensitivity. After illumination for 30 minutes with state 1- or state 2-favoring light as above, 'diluted leaf particles' were prepared by dilution of frozen leaf powder with cooled quartz particles as described in Weis (1985). Leaf material corresponding to about $25 \mu\text{g}$ of Chl was frozen in liquid N_2 and ground in a mortar in presence of 0.5 ml frozen water. The frozen powder (permanently kept

in liquid N₂) was homogeneously diluted with 3 ml of pre-cooled quartz particles and an aliquot of this sample (containing leaf particles at a concentration of about 4 µg Chl ml⁻¹) was used for fluorescence measurements.

2.11.2 Electron transport measurements

Thylakoids were prepared from leaves of 4 week-old plants as described in Casazza et al. (2001). Electron transport from H₂O to NADP⁺ was measured in a dual-wavelength spectrophotometer (ZWS-II, Sigma, Munich, Germany) as the increase of absorbance at 340 nm minus 390 nm. Saturating actinic light (150 µmol photons m⁻² s⁻¹) was used to induce the electron flow. The reaction mixture contained 10 µM ferredoxin, 0.5 mM ADP, 2.5 mM orthophosphate, 0.5 mM NADP⁺ and 10-20 µl of thylakoid suspension (corresponding to a final Chl concentration of 10 µg ml⁻¹), and was adjusted to a total volume of 1 ml with a buffer containing 0.1 M sorbitol, 5 mM MgCl₂, 10 mM NaCl, 20 mM KCl, 30 mM Tricine/NaOH (pH 8.0) and 0.5% (w/v) fatty acids-free BSA. For experiments in which PSII was inhibited, the reaction mixture contained, in addition, 5 mM ascorbic acid. After 2 min of illumination, DCMU and TMPD were added to a final concentration of 1 µM and 250 µM, respectively. For measurements of ATP synthesis, the reaction mixture contained, in addition, 4 mM glucose and 4 units of hexokinase. After illumination, 5 units of glucose-6-P dehydrogenase were added and the amount of ATP formed during illumination was calculated as the increase in absorbance due to the further reduction of NADP⁺ in the dark (Forti and Elli, 1995). ATP formation was measured in the presence or absence of the adenylate kinase inhibitor, P₁,P₅-di (adenosine-5') pentaphosphate.

2.12 ELECTRON MICROSCOPY

Electron microscopy was performed as described in Haldrup et al. (2000). Leaves of 4 week-old plants were used and thin sections were examined with a Zeiss EM10 microscope.

2.13 INTRACELLULAR PROTEIN LOCALIZATION

The red fluorescence protein (RFP) from reef corals was used as reporter to determine the intracellular localization of AtMAK3 (Jach et al., 2001). The RFP gene was part of a plant expression vector carrying the 35S promoter of cauliflower mosaic virus with doubled

enhancer (pGJ1425). *AtMAK3* gene was fused 5' of RFP gene, and this construct was used to transfect protoplasts. Mesophyll protoplasts were isolated from 6 week-old *Nicotiana tabacum* Petit Havana SR1 (Maliga et al., 1975) plants according to the protocol of Negrutiu et al. (1987). For transient gene expression assays, 3.3×10^5 freshly isolated SR1 mesophyll protoplasts were transfected with 10 μ g of plasmid DNA by PEG-mediated DNA uptake (Walden et al., 1994). Protoplasts were cultured for two days at 26 °C in dark conditions and in the presence of auxin (5 μ M) and cytokinin (1 μ M). The transfected protoplasts were analyzed by using the Zeiss Axiophoto fluorescence microscope equipped with a filter set purchased from AF Analysentechnik, Tübingen, Germany. Pictures were taken using a video image system mounted on the microscope, consisting of a Hitachi CCD video camera operated by the DISKUS software package.

3 FORWARD GENETICS

The functional dissection of photosynthesis can be carried out by isolating mutants with altered photosynthetic performances. This chapter describes the device used for the screening as well as the specific phenotypes of the photosynthetic mutants isolated.

3.1 MUTANT SCREEN

The photosynthetic mutants were isolated on the basis of their altered fluorescence yield values (Φ_{II}) with respect to WT plants. In particular, it was aimed to pick up mutants carrying relatively small alterations in photosynthetic performance. As device, an automatic Pulse Amplitude Modulation fluorometer system (PAM) was used (Figure 3.1 and Materials and Methods: chapter 2.3). The instrument was able to measure the Φ_{II} of 54 *Arabidopsis* plants in about 20 min. The accuracy and reproducibility of Φ_{II} measurement was tested by analyzing 24 wild-type plants; an average value of 0.77 with a standard deviation of 0.01 was found. The screening was performed on 4 week-old plants derived from an *En*- and a T-DNA mutagenised *Arabidopsis thaliana* population (see Materials and Methods: chapter 2.1). In particular, 1093 lines of the *En*-population and 1152 lines of the T-DNA population were screened. 18 photosynthesis affected mutants (*pam*) were identified, of which 6 were derived from the *En*-population and 12 from the T-DNA tagged population.



Figure 3.1 The automatic device used in the screening of *pam* mutants.

3.2 MUTANT PHENOTYPES

In all of the isolated mutant lines the photosynthetic phenotype segregated as recessive trait. With the exception of *pam10* and *pam13*, all mutants showed a drastic reduction in growth rate and a delay in flowering time. Moreover, nearly all of them had pale green or yellow cotyledons and leaves, except *pam10* and *pam11* that showed a wild-type pigmentation of leaves. The Φ_{II} values ranged between 0.40 and 0.70. Only *pam20* showed a Φ_{II} value significantly lower than 0.40 (Table 3.1).

<i>Mutant name</i>	F_{II}	<i>Phenotype</i> (leaf colour/dimension)	<i>Population</i>
<i>pam8</i>	0.60	pale green/small	<i>En</i>
<i>pam9</i>	0.43	pale green/small	<i>En</i>
<i>pam10</i>	0.65	WT/WT	<i>En</i>
<i>pam11</i>	0.51	WT/small	<i>En</i>
<i>pam12</i>	0.60	yellow/small	<i>En</i>
<i>pam13</i>	0.64	pale green/WT	<i>En</i>
<i>pam14</i>	0.61	pale green/small	T-DNA
<i>pam15</i>	0.53	yellow/small	T-DNA
<i>pam16</i>	0.64	pale green/small	T-DNA
<i>pam17</i>	0.66	pale green/small	T-DNA
<i>pam19</i>	0.62	yellow/small	T-DNA
<i>pam20</i>	0.33	yellow/small	T-DNA
<i>pam21</i>	0.60	pale green/small	T-DNA
<i>pam22</i>	0.64	yellow/small	T-DNA
<i>pam23</i>	0.54	yellow/small	T-DNA
<i>pam24</i>	0.51	yellow/small	T-DNA
<i>pam26</i>	0.49	yellow/small	T-DNA
<i>pam27</i>	0.67	yellow/small	T-DNA

Table 3.1 Characteristics of *pam* mutants

3.3 IDENTIFICATION OF AFFECTED GENES IN *pam* MUTANTS

The identification of the *En* and T-DNA insertion sites was performed using a PCR-based approach (see Materials and Methods: chapter 2.4). For the T-DNA mutants, this analysis was carried out in the generation of plants which was used for screening, since a maximum of 2 insertions were observed per line. Contrarily, additional outcrossing and selfing steps had to be performed for the *En* lines before proceeding with the isolation of the insertion flanking regions, since they contained between 6 and 11 transposon copies. The isolation of the insertion flanking regions was performed by using DNA from 10 mutants of each segregating line. After displaying the PCR products on polyacrylamide gels, only the bands present in all the 10 mutants were eluted from the gel, reamplified and sequenced.

Subsequently, specific primers complementary to insertion flanking regions were designed and combined with *En* or T-DNA primers for segregation analyses. Of the 13 knockout genes isolated, 5 segregated with the correspondent photosynthetic phenotype (Table 3.2). Among the 5 genes responsible to alter photosynthesis, 4 encoded proteins with a chloroplast transit peptide. The *pam8* phenotype was caused by an *En*-insertion in the *psaE1* gene that encodes the E subunit of PSI. An allelic mutant, named *psae1-1*, was isolated previously by Varotto et al. (2000). *pam14* had a T-DNA insertion in the *Prpl11* gene encoding the subunit L11 of chloroplast ribosomes. The third mutant, *pam15*, was due to a T-DNA insertion in a gene responsible to encode a chloroplast prolyl tRNA synthetase. *pam20* was disrupted in the gene that encodes the chloroplast heme oxygenase 1. Also in this case an allelic mutant was identified previously (Davis et al., 1999; Muramoto et al., 1999). *pam21*, contains a T-DNA insertion in a gene that codes for a cytosolic protein, a *N*-acetyltransferase.

For 6 mutants no *Arabidopsis* genomic region flanking the T-DNA or *En* elements could be obtained, indicating a large frequency of concatemeric insertions within the two mutagenised populations.

<i>mutant</i>	<i>Knockout gene</i>	
	<i>accession number</i>	<i>description</i>
<u><i>pam8</i></u>	<u>At4g28750</u>	<u>PsaE subunit</u>
<i>pam9</i>	At5g47850 At3g21560	receptor kinase like protein UDP-glycosyltransferase
<i>pam10</i>		No knockout gene isolated
<i>pam11</i>	At4g33820	1-4-beta-xylan endohydrolase
<i>pam12</i>	At3g54990	apetala2 like protein
<i>pam13</i>	At3g54990 At1g02065	apetala2 like protein SPL8 gene
<u><i>pam14</i></u>	<u>At1g32990</u>	<u>50S ribosomal protein L11</u>
<u><i>pam15</i></u>	<u>At5g52520</u>	<u>prolyl tRNA synthetase</u>
<i>pam16</i>	At5g25590	putative protein
<i>pam17</i>	At5g39370	glycoprotein S8
<i>pam19</i>		No knockout gene isolated
<u><i>pam20</i></u>	<u>At2g26670</u>	<u>heme oxygenase 1</u>
<u><i>pam21</i></u>	<u>At2g38130</u>	<u>N-acetyltransferase</u>
<i>pam22</i>		No knockout gene isolated
<i>pam23</i>		No knockout gene isolated
<i>pam24</i>	At2g15620	nitrite reductase
<i>pam26</i>		No knockout gene isolated
<i>pam27</i>		No knockout gene isolated

Table 3.2 Genes disrupted by insertions of *En* or T-DNA elements. Genes causing photosynthesis altered phenotypes are underlined

DISCUSSION

An automated PAM fluorometer was employed to isolate mutants defective for Φ_{II} . The system was able to measure the fluorescence yield of single plants in a relatively short time, allowing the analysis of thousands of plants per week. Among 2 245 insertionally mutagenised lines screened, 18 Φ_{II} mutants were identified with a frequency of approximately one per 125 lines. This frequency is considerably different with respect to those obtained with other photosynthetic mutant screens. For instance, Niyogi et al. (1998) screened 30 000 chemically and physically mutagenised lines and isolated 13 mutants affected in non-photochemical quenching of chlorophyll fluorescence at a frequency of approximately one in 2000. The low frequency of mutants recovered has to be attributed to the fact that defects in non-photochemical quenching are more rare than Φ_{II} defects. A similar screen for *npq* mutants was performed by Shikanai et al. (1999) on 21 000 chemically mutagenised lines, and 37 mutants were isolated at a frequency of approximately one in 500. In this case, mutants with slightly altered Φ_{II} were also considered, increasing the frequency of mutants recovered. Additionally, Meurer et al. (1996) carried out a screen on 7 700 chemically mutagenised M_2 seeds looking for high chlorophyll fluorescence (*hcf*) mutants. 238 *hcf* mutants at a frequency of approximately 1/30 were isolated. The markedly high number of mutants obtained using this approach was due to the fact that most defects in thylakoid development and thylakoid electron transport can cause a *hcf* phenotype. Moreover, the screen was performed on 10 days old plants, thus allowing the identification of seedling lethal mutants.

Most of the 18 Φ_{II} mutants isolated in this thesis showed a reduction in plant size, an altered pigmentation of leaves and a delay in flowering time. These features were in common with few of the mutants isolated by Meurer and most of the mutants classified into group 3 in the Shikanai screen. However, the extent of overlap between the four systems of screening can not be defined due to the lack of reciprocal classification.

The use of tagged populations (*En*-transposon or T-DNA) in the Φ_{II} screen instead of chemically or physically mutagenised populations allowed fast and systematic gene isolation. Nevertheless, some difficulties were encountered. In particular, *En*-transposon lines had a large number of insertions as well as a large number of footprints, caused by former transposition events, that made it very difficult to isolate the disrupted genes causing

the photosynthetic phenotypes. Indeed, only one out of six genes isolated within the *En* mutants segregated with the corresponding photosynthetic phenotype. On the contrary, the T-DNA mutagenised population had a reduced number of insertions and no footprints, increasing the probability to identify the knockout gene responsible for the photosynthetic phenotype. In fact, 4 of the 7 knockout genes isolated from the T-DNA mutants segregated with the photosynthetic phenotypes. However, clustering of several copies of T-DNA, as well as rearrangements and deletions mainly in the right border, often prevented the isolation of genomic DNA flanking the insertions. Indeed, for 5 of the 12 T-DNA mutants analyzed no genomic DNA flanking sequence could be isolated. This frequency is much higher than in the *En* mutants where only in one case out of six no genomic DNA flanking region was identified.

The Φ_{II} mutant frequency in the T-DNA population was double with respect to the one of the *En*-population (one mutant every 100 lines versus one mutant every 200 lines). This was rather unexpected, since the average number of insertions in *En*-lines (from 6 to 11) was much higher compared to the one of T-DNA lines (maximum 2 insertions). A possible explanation for this apparent contradiction is that the extrapolated 48 000 insertions present in the 8 000 *En*-lines may not evenly cover the *Arabidopsis* genome. This would decrease the effective number of insertions per genome. Additionally, the *En*-tagged lines were generated following a single seed descendent strategy for more than 12 generations (Wisman et al., 1998). This procedure may result in a selection against less-vital mutants, leading to a decreased representation of mutations causing severe phenotypes. As a matter of fact, a lower fraction of albino-lethal mutants were present within the *En*-population with respect to the T-DNA population.

In total 5 knockout genes causing photosynthetic phenotypes were isolated. Two of them encoding a plastid prolyl tRNA synthetase and the plastid ribosomal protein L11 seem to play a role in the chloroplast translation machinery. The *psaE1* gene is involved in the thylakoid electron transport (Varotto et al., 2000). The heme oxygenase 1 is responsible of the biosynthesis of heme groups of phytochromes (Davis et al., 1999; Muramoto et al., 1999). The *N*-acetyltransferase was the only identified protein not imported into the chloroplast, therefore the reasons of its involvement in photosynthesis are difficult to predict.

4 CHARACTERIZATION OF THE *prpl11-1* MUTANT

Screening of the T-DNA mutagenised *Arabidopsis thaliana* population resulted in the isolation of the *photosynthesis affected mutant 14 (pam14)*. The T-DNA was inserted into the *Prpl11* gene that encodes the protein L11 of the multimeric plastid 50S ribosome subunit. Recently, the identification of the complete set of proteins that make up the chloroplast ribosome in higher plants has been accomplished (Yamaguchi and Subramanian, 2000; Yamaguchi et al., 2000). In particular, it has been shown that the 50S subunit of chloroplast ribosome from spinach contains 33 proteins of which 25, including the L11 subunit, are nucleus-encoded and are imported into the chloroplast via an *N*-terminal transit peptide. Studies on *E. coli* mutants deficient in the L11 ribosomal protein indicated a role for L11 in the elongation or termination step of translation process (Sander, 1983; Tate et al., 1983; Ryan et al., 1991). This chapter describes the characterisation of the first *Arabidopsis* mutant deficient in a chloroplast ribosome subunit.

4.1 *pam14* PHENOTYPE

pam14 showed pale green cotyledons and leaves together with a significant reduction in size (Figure 4.1a). Analysis of the growth behavior, by using non-invasive image analysis (Leister et al., 1999), indicated a reduction by up to 75% of the growth rate of mutant plants relative to wild-type (Figure 4.1b). Moreover, the mutant plants showed an alteration in the photosynthetic performances due to a reduced fluorescence yield (Φ_{II}) (Table 4.1). Other chlorophyll fluorescence parameters resulted to be altered in mutant plants, too. In particular, F_0 , the minimal chlorophyll *a* (Chl *a*) fluorescence of dark-adapted leaves, showed an increase of about 24% in mutant plants, whereas the mutant F_m , the maximal Chl *a* fluorescence, was 20% lower than in wild-type plants. The ratio F_v/F_m appeared significantly reduced in the mutant, implying a defect in energy transfer within PSII. Furthermore, the high level of non-photochemical quenching (NPQ) and the strong decrease in Φ_{II} even at low light intensities (Figure 4.2) indicated a severely impaired light utilization and increased photoinhibition in mutant plants.

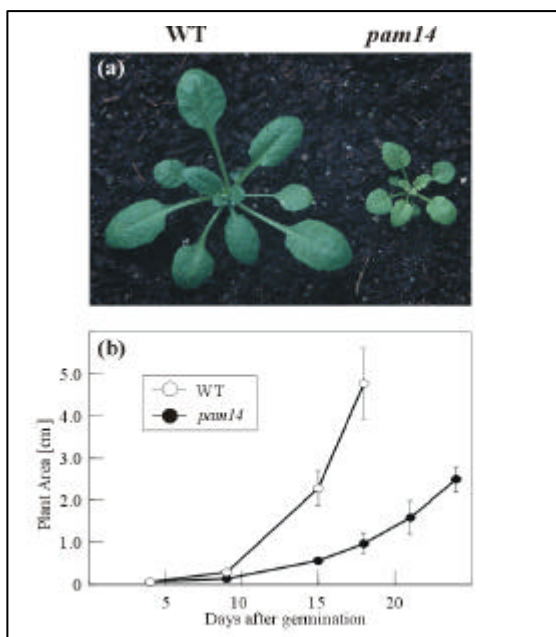


Figure 4.1 Phenotype of WT and *pam14* plants. a) 4 week-old plants grown under greenhouse conditions. b) Growth kinetics of *pam14* compared to WT plants. Leaf area was measured in the period from 4 to 24 days after germination. Bars indicate standard deviation.

	WT	<i>pam14</i>
F _o	0.19	0.25
F _m	1.03	0.82
F _v /F _m	0.81	0.69
Φ _{II}	0.78	0.55
NPQ	0.18	0.3

Table 4.1 Spectroscopic analysis of WT and *pam14* plants. The values represent the average of 20 independent measurements. Standard deviations were below 2%

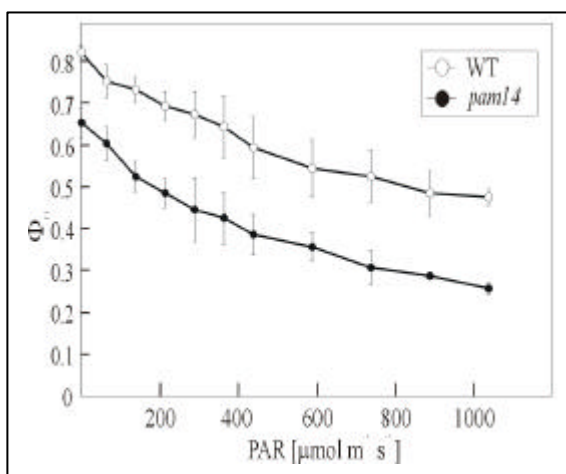


Figure 4.2 Effective quantum yield of PSII in the *pam14* mutant and WT plants illuminated at different light intensities. The value of Φ_{II} was determined in the range of 1-1039 (mol photons m⁻² sec⁻¹ photosynthetically active radiation). 5 WT and 5 *pam14* plants were incubated for 30 min in the dark prior to measurements. Φ_{II} was recorded after irradiating for 15 min with light of the appropriate intensity. Bars indicate standard deviations

4.2 CLONING OF THE *PAM14* LOCUS

Southern analysis on 4 different pools of mutant plants (10 plants per each pool) using the 5'-end of the *AC106* T-DNA as a probe revealed the presence of one T-DNA copy (Figure 4.3a). After isolating DNA from 10 mutant plants, amplification of insertion-mutagenised sites (see Material and Methods: chapter 2.4) was carried out. A DNA fragment flanking the left border of the T-DNA was isolated, and its sequence was found to be identical to that of the nuclear *Prpl1* gene of *A. thaliana* (At1g32990). *Prpl1* is located on chromosome 1 near the marker locus *mi423a*. By performing BLAST searches a second copy of the gene was identified on chromosome 5 (At5g51610); this copy lacked almost the entire second exon and it was named *Prpl1-like*. The T-DNA insertion was present in all mutant plants (Figure 4.3b) and placed in the second exon of *Prpl1*, at position +419 bp relative to the first ATG codon (Figure 4.3c).

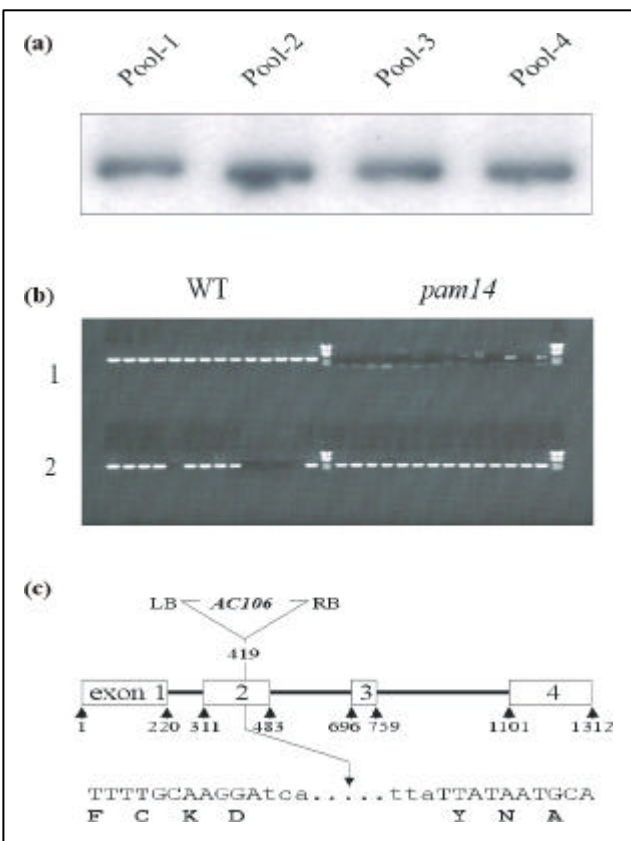


Figure 4.3 T-DNA insertion site. a) Southern analysis performed with DNA extracted from 4 different pools of mutant leaves. After digestion with *SfuI* and blotting, the filter was hybridized with a probe matching the left border of T-DNA. b) The presence of T-DNA insertion in WT and mutant plants was monitored by PCR. In row # 1 primers specific for the gene, one matching upstream and the other one downstream the T-DNA insertion, were used for the amplification. In row # 2 a primer specific for the left border of T-DNA and a primer matching upstream the T-DNA insertion were used for the amplification. All the mutants were homozygous for the T-DNA insertion while the WT plants were either heterozygous for the T-DNA insertion or without any insertion. c) The *Prpl1* gene is disrupted by the insertion of the 5.8 Kb *AC106* in the second exon. The T-DNA insertion is not drawn to scale. Upper case letters indicate plant DNA sequences flanking the T-DNA and lower case letters represent the border sequences of *AC106*. Amino acid residues, encoded by the region of *Prpl1* shown, are indicated in bold upper case letters below the first nucleotide of each codon.

4.3 COMPLEMENTATION OF *pam14*

In order to verify that the *pam14* phenotype was caused by the T-DNA insertion into *Prpl11* gene, mutant plants were transformed with the *Prpl11* cDNA fused to the 35S promoter of cauliflower mosaic virus via *A. tumefaciens* (see Materials and Methods: chapter 2.7). In all 18 transformants obtained, the wild-type phenotype was fully restored. In particular, the growth rate, the pigment composition (Figure 4.5a) and the fluorescence yield of PSII (Φ_{II}) did not differ from wild-type plants. Furthermore, all the transformants showed a large amount of *Prpl11* mRNA (Figure 4.5b). Because the *PAM14* locus corresponds to the *Prpl11* gene, we have assigned the symbol *Prpl11* to the locus and renamed the *pam14* mutant *prpl11-1*.

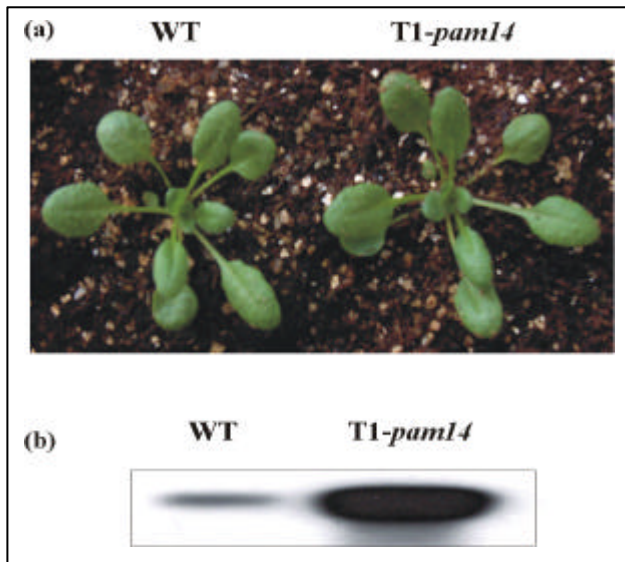


Figure 4.5 Complementation test. a) 4 week-old WT plant and T1 generation of mutant plants transformed with *Prpl11*-cDNA fused to the 35S promoter. b) Northern analysis of WT and T1 plants. The filter was hybridized with a probe complementary to *Prpl11* transcript.

4.4 LEVELS OF TRANSCRIPTS AND POLYSOME ACCUMULATION IN *prpl11-1* PLASTIDS

Northern analysis using a full-length *Prpl11* probe revealed that the T-DNA insertion drastically destabilised the *Prpl11* transcripts (Figure 4.6a). Moreover, due to the marked DNA sequence similarity to the *Prpl11-like* gene, the complete absence of *Prpl11* mRNA indicated that the *Prpl11-like* gene is not expressed. This evidence was supported by RT-PCR analysis, where specific primers for the *Prpl11-like* gene were used (Figure 4.6b), and no amplification product could be obtained either in wild-type or *prpl11-1* plants.

The effect of the *prpl1-1* mutation on plastid transcripts was studied, too (Figure 4.6c). The levels of the *psbA* transcript, which encodes the D1 protein, in wild-type and mutant plants were identical. The total amount of *psbB* transcript, encoding the CP47 protein, was also unchanged in the mutant, although accumulation of large transcripts could be detected in mutant plastids. The abundance of transcripts of the *psbD/C* operon, which codes for D2 and CP43, was actually higher in the mutant than in wild-type plants, whereas the level of *psbE* transcripts encoding Cyt-*b559* was reduced. Amounts of the *rbcL* mRNA, an indicator for the accumulation of polysomes (Barkan, 1993), were nearly identical in mutant and wild-type plants.

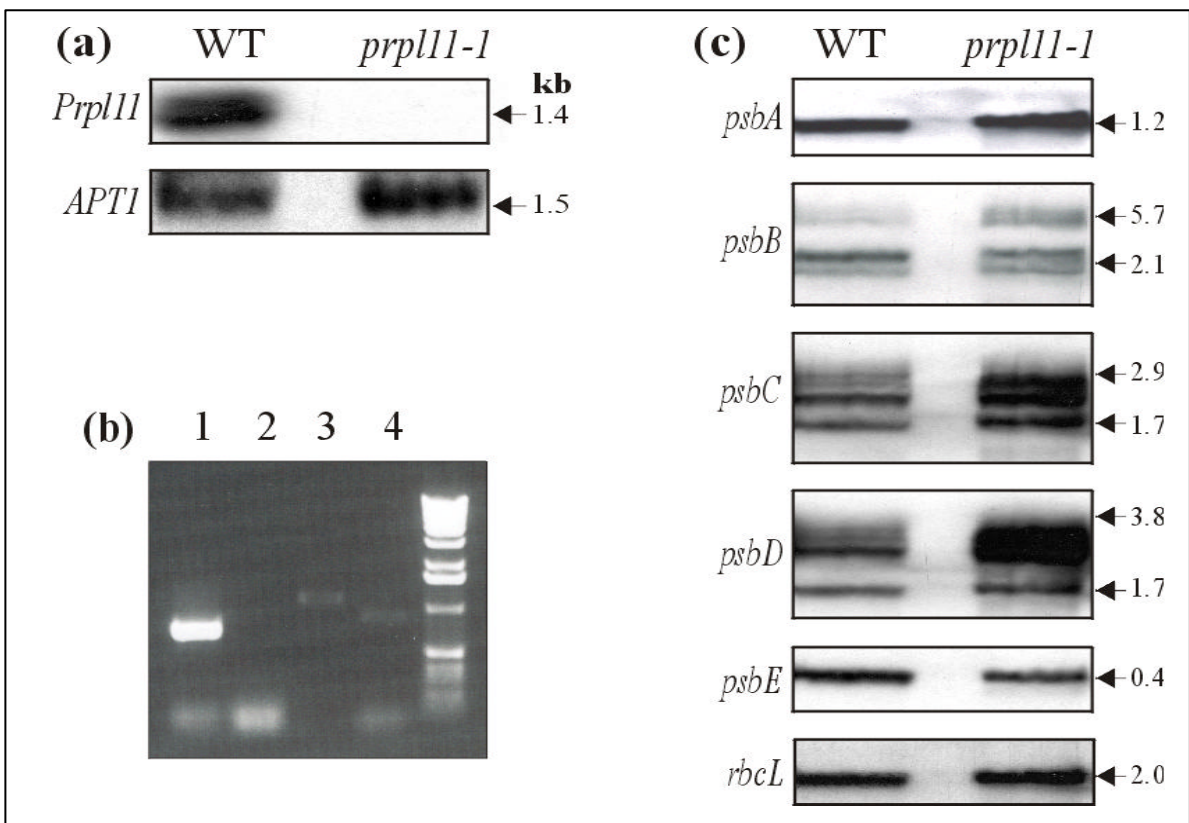


Figure 4.6 mRNA expression. The numbers at the right indicate RNA sizes that were estimated by co-electrophoresis with denatured *EcoRI/HindIII* fragments of lambda DNA. a) Northern analysis of the *Prpl11* transcript in mutant and WT plants. 30 μ g samples of total RNA were analysed using as probe a full-length *Prpl11* cDNA. To control for RNA loading, the blot was re-probed with a cDNA fragment derived from the *APT1* gene, which is expressed at a low level in all tissues of *Arabidopsis* (Moffat et al., 1994). b) RT-PCR analysis. WT (1; 3) and mutant (2; 4) single strand cDNA pools were amplified with primers specific for *Prpl11* gene (1; 2) and for *Prpl11*-like gene (3; 4). c) Transcripts of the genes *psbA*, *psbB*, *psbC-psbD*, *psbE* and *rbcL* were detected by re-probing the filter shown in (a) with the appropriate gene-specific probes.

In order to verify whether the absence of L11 subunit could affect the abundance of chloroplast ribosomes, the level of ribosomal RNAs was monitored by agarose electrophoresis (Figure 4.7a). The levels of the 1.6- and 1.15-kb plastid rRNAs were not altered in *prpl11-1* plants, suggesting that overall amounts of plastid ribosomes were not affected. Polysome formation on the *psbA*, *psbE* and *rbcL* transcripts was assessed by sucrose density-gradient fractionation (Figure 4.7b) on the basis that transcripts associated with polysomes have higher sedimentation rates than monosomes or free mRNA. The proportion of polysomes-associated to unassociated transcripts allows to estimate the efficiency of translation initiation and elongation (Barkan, 1993). No significant differences in sedimentation between wild-type and mutant plants were detected for *psbA* and *psbE*, whilst for *rbcL* slightly fewer transcripts were associated with large polysomes in the mutant. These findings indicate that the PRPL11 protein is dispensable for polysome assembly, but at least for *rbcL* transcripts, it is necessary for efficient translation initiation. Altered translation elongation would tend to result in the accumulation of large polysomes (Klaff and Gruissem, 1991; Brutnell et al., 1999).

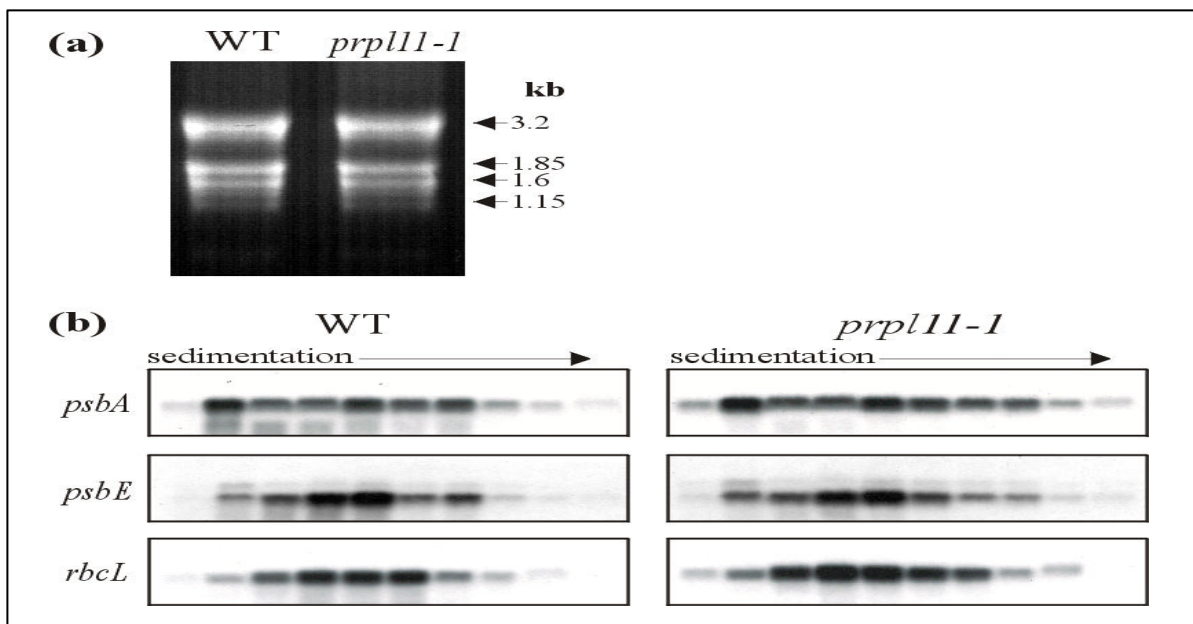


Figure 4.7 Amount of rRNAs and polysome accumulation in chloroplasts. a) Abundance of rRNAs. 2 μ g of total RNA from WT and mutant plants were denatured and run on a native 1 x MOPS gel. Cytoplasmic rRNA corresponds to the 3.2- and 1.85-kb species, whilst organelle rRNA corresponds to the 1.6- and 1.15-kb forms. b) Association of chloroplast mRNA with polysomes. Total extracts from 4 week-old WT and *prpl11-1* plants were fractionated on sucrose gradients. Ten fractions of equal volume were collected from the top to the bottom of the sucrose gradients. An equal proportion of the RNA purified from each fraction was analysed by gel-blot hybridisation. Transcripts of *psbA*, *psbE* and *rbcL* were detected with cDNA -specific probes.

4.5 AMOUNTS OF PROTEIN COMPONENTS OF THE PHOTOSYNTHETIC APPARATUS ARE SIGNIFICANTLY ALTERED IN *prp11-1* PLANTS

Thylakoids from greenhouse-grown wild-type and mutant plants were isolated and subjected to two dimensional PAGE. Individual subunits were identified by immunoblot analyses using antibodies specific for subunits of PSI, PSII and ATPase, which are components of the photosynthetic apparatus (Figure 4.8a). Densitometric analyses of protein gels after Coomassie staining indicated a decrease in the levels of PSI subunits in mutant thylakoids by 52.5% relative to wild-type (Figure 4.8a and Table 4.2), while the plastome-encoded polypeptides detected which form the core complex of PSII (D1, D2, CP43, and CP47) were reduced by 67.6%. A similar decrease (65.9%) was observed for the α - and β -subunits of the ATPase complex, whereas the nucleus-encoded peptides of LHCII were reduced by only 29.6% in *prp11-1*. The reduction of the level of the PSII core complex, detected by two-dimensional PAGE, was confirmed by Western analyses after denaturing PAGE. The amounts of both CP47 and the α -subunit of Cyt *b-559* showed the same reduction in mutant plants as found before for the entire PSII core by 2D PAGE. In addition, reduced accumulation of Cyt *f* was observed (Figure 4.8b and Table 4.2).

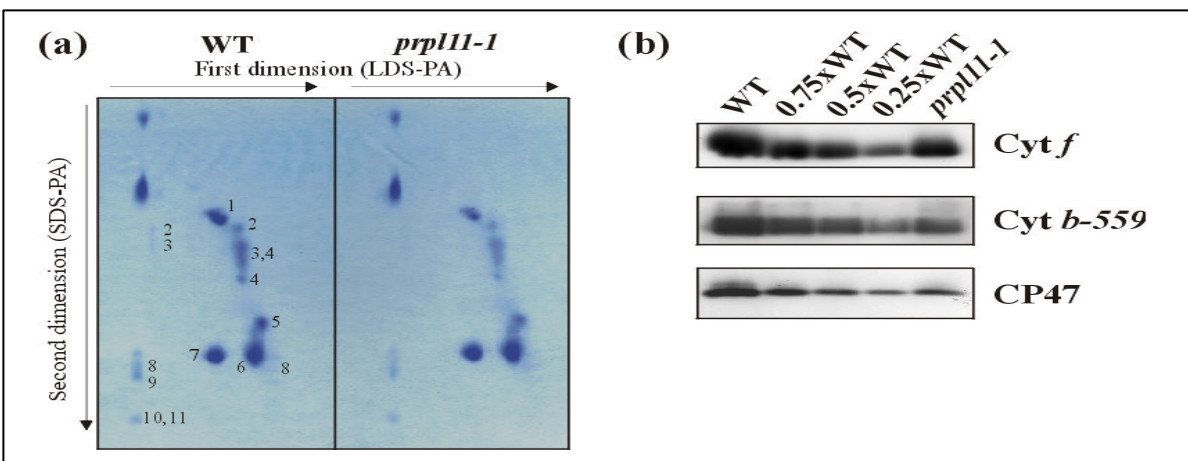


Figure 4.8 Protein composition of thylakoid membranes. a) Thylakoid membranes corresponding to 30 μ g of chlorophyll from the wild-type and the *prp11-1* were fractionated first by electrophoresis on a non-denaturing Green-PAGE, and then on a denaturing SDS-PAGE. Positions of wild-type thylakoid proteins, previously identified by Western analyses with appropriate antibodies, are indicated: 1, α - and β -subunits of the ATPase complex; 2, D1-D2 dimer; 3, CP47; 4, CP43; 5, oxygen evolving complex (OEC); 6, LHCII monomer; 7, LHCII trimer; 8, PsaD; 9, PsaF; 10, PsaC; 11, PsaH. With the exception of LHCII the amounts of all thylakoid proteins detected are significantly reduced in mutant plants. The alterations observed are quantified in Table 4.2. b) Samples of thylakoid membranes equivalent to 15 μ g of chlorophyll were loaded in lanes WT and *prp11-1*. Decreasing amounts of WT thylakoid membranes (11.25, 7.5, 3.75 μ g of chlorophyll) were loaded in the lanes marked 0.75x, 0.5x, 0.25x WT. Three replicate filters were probed with antibodies raised against Cyt *b-559*, Cyt *f* and CP47.

	<i>WT</i>	<i>prpl11-1</i>	<i>Relative level in prpl11-1 [in %]</i>
PSI	1.22	0.85	47.5
PSII core	1.85	0.88	32.4
ATPase ($\alpha + \beta$)	0.68	0.34	34.1
LHCII	2.16	2.23	70.4
Cyt <i>f</i>	1.7	1.05	42.1
CP47	2.01	1.03	34.9
Cyt <i>b-559</i>	0.96	0.45	31.9
Chl a+b	671.0	457.5	68.2

Table 4.2 Analyses of thylakoid protein levels and total chlorophyll content (in nmol Chl *a+b* per gram of fresh leaf weight) in WT and *prpl11-1* mutant plants. Values for proteins are average optical densities (OD) measured from three independent 2D protein gel analyses (see Figure 4.8a) or, in the case of Cyt *f*, CP47 and Cyt *b-559*, three independent Western analyses (see Figure 4.8b). Standard deviations were in the range below 5%. The relative values for *prpl11-1* were normalised with respect to the total chlorophyll content per gram of fresh leaf weight.

4.6 THE ABSENCE OF PRPL11 AFFECTS THE RATE OF PROTEIN SYNTHESIS IN PLASTIDS

Proteins encoded by the plastid genome, such as D1, D2, CP43, CP47, Cyt *b-559*, Cyt *f* and the α - and β -subunits of the ATPase complex, were significantly reduced in amount in mutant plants, suggesting that protein synthesis may be impaired in the plastids of the mutant. In prokaryotes a major role has been proposed for RPL11 in the elongation step of translation (Stark and Cundliffe, 1979; Stark et al., 1980; Ryan et al., 1991, Rodnina et al., 1999). In *C. reinhardtii*, McElwain et al. (1993) proposed the same role for the L23 protein, which is immunologically related to the prokaryotic L11 protein. In order to test for a similar function of PRPL11 in *Arabidopsis*, we monitored the rate of incorporation of [³⁵S]methionine into plastid proteins in mutant and wild-type leaves. Young leaves of wild-type and *prpl11-1* plants were incubated with [³⁵S]methionine in presence of light and inhibitors of cytoplasmic protein synthesis. Subsequently, organelles were disrupted to obtain the soluble protein fraction for SDS-PAGE analyses (Figure 4.9a). In three

independent experiments, the amount of the large subunit of Rubisco labelled in mutant plants was decreased on average by 65% with respect to that in wild-type plants (Figure 4.9b). This reduction in the rate of translation of *rbcL* RNA results in significantly reduced accumulation of the large subunit of Rubisco, as shown by Western analysis (Figure 4.9c). Furthermore, amounts of the nucleus-encoded small subunit of Rubisco were also decreased (Figure 4.9c), indicating that the level of the large subunit regulates the abundance of the small subunit. The converse has been demonstrated in tobacco, where a reduction in the abundance of the small subunit resulted in a decrease in translation of the large subunit (Rodermeil et al., 1996).

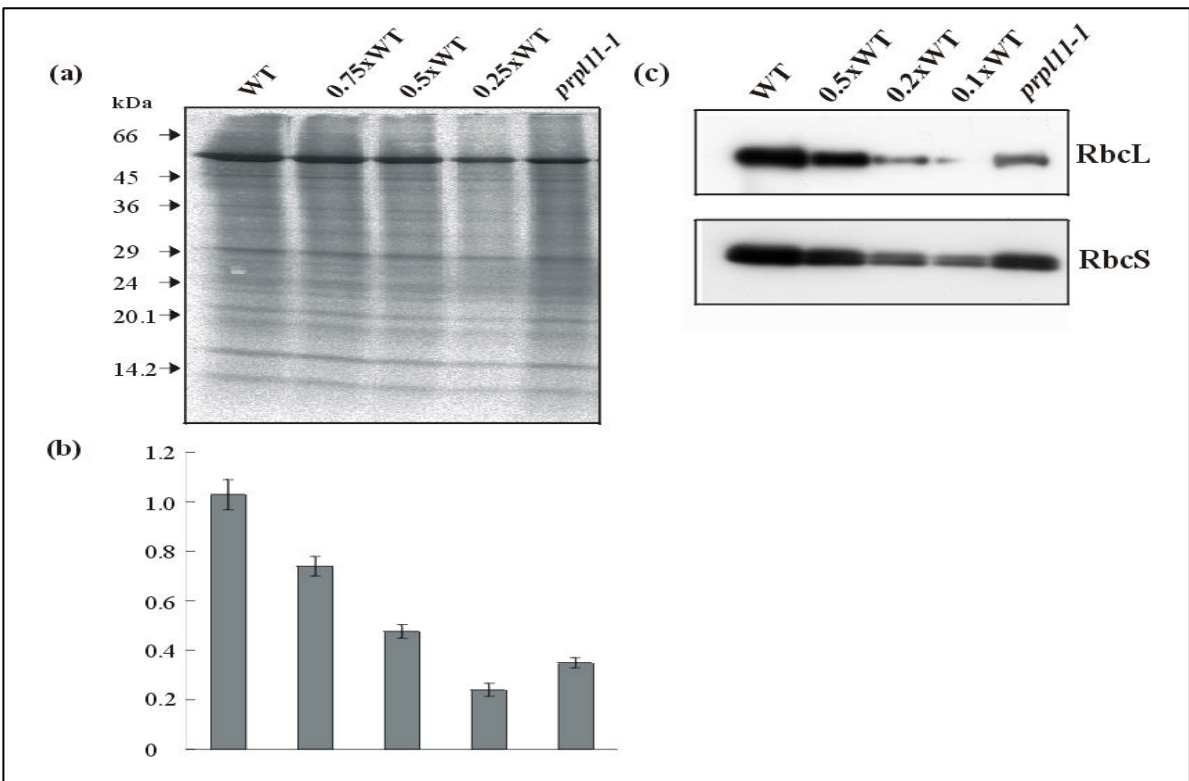


Figure 4.9 *In vivo* synthesis of soluble organelle proteins in primary leaves of 4 week-old mutant and wild-type plants. The results of one of three independent experiments are shown. a) [35 S]methionine was applied during the light period. Proteins were isolated from WT and mutant leaves, separated by SDS-PAGE, electroblotted onto a nylon membrane and analysed by fluorography. Lower amounts of WT proteins were loaded in the lanes marked 0.75x, 0.5x and 0.25x WT. The most intensely labelled band corresponds to the large subunit of Rubisco. b) Quantification (optical densities) of signals for the large subunit of Rubisco observed in (a). Bars indicate standard deviation. c) Immunoblot analysis of proteins from the *prp11-1* and WT plants. Samples of chloroplast proteins equivalent to 5 μ g of chlorophyll were loaded in lanes WT and *prp11-1*. Decreasing amounts of WT thylakoid membranes (2.5, 1 and 0.5 μ g of chlorophyll) were loaded in the lanes marked 0.5x, 0.2x, 0.1x WT. Replicate filters were probed with antibodies raised against the large and small subunit of Rubisco.

DISCUSSION

The *prpl11-1* mutation is due to a T-DNA insertion in the second exon of the *Prpl11* gene. Expression of *Prpl11* RNA could not be detected in the mutant, and transformation of the mutant plants with *Prpl11* cDNA placed under the control of the 35S promoter resulted in restoration of the wild-type phenotype. The *Prpl11* gene is present in two copies in *Arabidopsis* genome, but only one of them is transcribed. Thus, the *prpl11-1* mutation completely eliminates one of the chloroplast ribosomal proteins of *Arabidopsis*, the first such knockout mutation to be described in this species and the second in a higher plant (in addition to *hcf60* of maize; Schultes et al., 2000). The PRPL11 protein of *Arabidopsis* shows high sequence similarity to other L11 proteins from higher plants and prokaryotes, apart from the chloroplast transit peptides, which are present only in the plant proteins. Key amino acids that are important for antibiotic binding and post-translational modification of L11 are conserved in *Arabidopsis* PRPL11.

L11 proteins have been extensively characterised in prokaryotes. They are located in the 50S subunit of the ribosome and interact with the 23S rRNA (Littlechild et al., 1977). Cross-linking experiments in *E. coli* suggest that RPL11 interacts with RPL7, RPL12, RPL2, RPL4 and RPL14 (Expert-Bezançon et al., 1976; Kenny et al., 1979). An electron density map of the large 50S ribosomal subunit of *Haloarcula marismortui*, at 5.0 Å resolution, places the RPL11 protein in the “GTPase-associated site” (Ban et al., 1999). This site also includes the proteins RPL6, RPL11, RPL14, the RPL7/RPL12 stalk, and the 1055 and 1080 nucleotide region of the 23S rRNA. Ryan et al. (1991) proposed a model in which RPL11 facilitates conformational changes in the 23S rRNA backbone in *E. coli*. Furthermore, RPL11 has been implicated in the EF-G dependent hydrolysis of GTP during polypeptide elongation in *E. coli* and *B. megaterium* (Schrier and Möller, 1975; Stark and Cundliffe, 1979; Rodnina et al., 1999). Nonetheless, prokaryotic mutants lacking L11 are viable and exhibit no severe phenotypes except for an increased generation time and decreased rates of *in vitro* protein synthesis (Stark and Cundliffe, 1979). McElwain et al. (1993) reported on a *C. reinhardtii* mutant which is defective in the plastid ribosomal protein L23 which is homologous to the *E. coli* RPL11. Absence of L23 confers thiostrepton resistance, and causes a drop in growth rate and a significant reduction (more than 80%) in the rate of *in vitro* protein synthesis. Thus, while the absence of RPL11 does not result in

lethality in prokaryotes or algae, it is nonetheless necessary for the correct function of ribosomes (Stark and Cundliffe, 1979; McElwain et al., 1993).

In maize, *HCF60* encodes protein 17 of the small subunit of the chloroplast ribosome. Lack of PRPS17 causes a seedling-lethal and chlorophyll-deficient phenotype in which plastid rRNA pools are depleted (Schultes et al., 2000). Similar observations were made for the chloroplast translation mutants *hcf7*, *cps1* and *cps2* of maize (Barkan, 1993); the genes responsible have not yet been cloned. These mutants accumulate plastome transcripts to wild-type levels, while amounts of the corresponding thylakoid proteins are reduced. Interestingly, all the maize mutants cited, including *hcf60*, show a decrease in the accumulation of the *rbcL* transcript. Barkan (1993) demonstrated the existence of a strict correlation between a decrease in *rbcL* mRNA accumulation and a decrease in polysome size, suggesting that the *rbcL* transcript is destabilised as a consequence of a decrease in its ability to associate with ribosomes.

In *Arabidopsis*, the absence of PRPL11 causes a complex phenotype: plants are pale green, and show a drastic decrease in growth rate and photosynthetic efficiency. Furthermore, due to a decrease in the levels of PSI, PSII core proteins, LHCII, Cyt *f*, the α - and β -subunits of the ATPase complex, and both subunits of Rubisco, the mutants show a reduced capacity for light utilisation and an increase in photosensitivity. In contrast, transcript levels of the *psbD/C* operon actually increase suggesting an increased stability of these transcripts in mutant plants. No alteration in the abundance of *rbcL*, *psbA* and *psbB* transcripts is detectable in the *prpl11-1* mutant. Only the *psbE* transcript level was reduced in *prpl11-1* plastids, possibly due to feedback mechanisms that act to regulate the level of PSII within the thylakoid membrane (Morais et al., 1998).

Taken together, the data indicate that the primary defect in the *prpl11-1* mutant is a reduction in the efficiency of protein synthesis by plastid ribosomes. To test this hypothesis we examined the effects of absence of PRPL11 on the abundance of ribosomes, on the association of specific transcripts with polysomes and on the rate of translation in the chloroplast. Amounts of chloroplast rRNA are not altered in mutant plastids, indicating that PRPL11 plays no role in the stability of plastid ribosomes. Polysome assembly assays, performed using *psbA* and *psbE* transcripts, show no significant differences between mutant and wild-type ribosomes. These data are in accordance with the observation that the amount

of *rbcL* mRNA, which is an indicator for chloroplast ribosome content and polysome accumulation (Barkan, 1993), is unchanged in mutant plants. However, a slightly increased portion of *rbcL* mRNA seems to be associated with small polysomes suggesting that lack of PRPL11 can also affect translation initiation. *In vivo* translation assays show a decrease of about 65% in the efficiency of synthesis of the large subunit of Rubisco, demonstrating that translation efficiency in *prpl11-1* plastids is severely affected. The reduction in translation rate observed in the *in vivo* translation assays is associated with a significant reduction in the abundance of the large and the small subunit of Rubisco.

In summary, the available data suggest that neither depletion of the content of chloroplast ribosomes nor a decrease in polysome accumulation is responsible for the drop in translational efficiency in *prpl11-1* cells. The most likely explanation for the mutant phenotype is that, in the absence of PRPL11, ribosomal activity itself is impaired, as a consequence of the loss of conformational stabilisation of the GTPase-associated site in the large subunit, as has been proposed for *E. coli* mutants that lack L11 (Ryan et al., 1991, Rodnina et al., 1999).

5 BIOCHEMICAL AND PHYSIOLOGICAL CHARACTERIZATION OF THE *psae1-1* MUTANT

By screening the *En*-transposon mutagenised *Arabidopsis thaliana* population, Claudio Varotto isolated the *psae1-1* mutant, allelic to the *pam8* mutant isolated in this thesis. The mutation was caused by the insertion of the *En* transposon element into one of the two *Arabidopsis* genes (*psaE1*) that encode the subunit E of photosystem I (Varotto et al., 2000). As a consequence of the mutation, the amounts of the E, C and D subunits of PSI were significantly reduced and the photosynthetic performance was decreased. Further analyses of the *psae1-1* mutant have been performed in this study and the almost complete inhibition of photosynthetic state transitions in the mutant is described in this chapter.

5.1 LEVELS OF PsaH AND PsaL ARE DECREASED IN *psae1-1*

The knockout of *psaE1* destabilizes the stromal ridge of PSI, resulting in a decrease in the levels of PsaE, C and D subunits (Varotto et al., 2000). The residual PsaE protein present in *psae1-1* is the product of *psaE2*, which is transcribed three times less abundantly than *psaE1*. PsaF, which is necessary for energy transfer from LHCI to PSI (Haldrup et al., 2000), is not affected by the mutation (Varotto et al., 2000).

Further consequences of the mutation were studied by using antibodies directed against other thylakoid proteins (Figure 5.1) and examining leaf pigment composition by HPLC (Table 5.1). The abundance of LHCS, the PSI reaction center (PsaA and PsaB), and the overall chloroplast pigment content was not altered, indicating that the general stoichiometry of antennae and photosystems was not changed in *psae1-1* plants. The mutant contained significantly more antheraxanthin than wild-type plants, suggesting an altered activity of xanthophylls cycle enzymes. PetD levels were similar in mutant and wild-type plants, implying that the *psae1-1* mutation does not influence *cyt b₆/f*. Levels of PsaN, which is involved in the interaction between plastocyanin and PSI (Haldrup et al., 1999), and of PsaG were unchanged in *psae1-1* plants. In contrast, levels of PsaH and PsaL were decreased to 60% and 15% of wild-type values, respectively (Figure 5.1). Since PsaH was reported as the docking site for LHCII during state 2 (Lunde et al., 2000), that raised the

question whether the *psae1-1* plants showed an alteration in the photosynthetic state transition process.

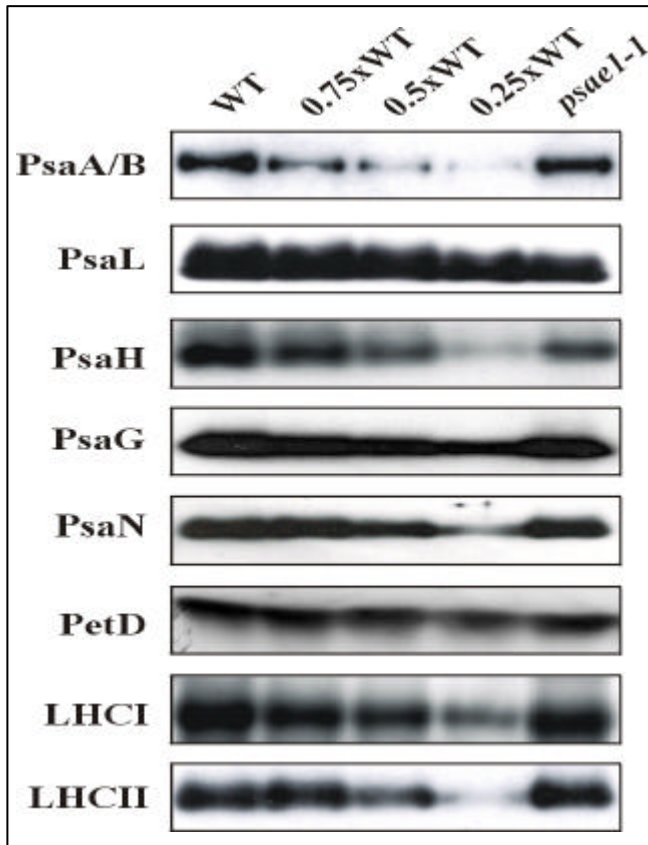


Figure 5.1 Immunoblot analysis of thylakoid membranes. 5 μg of WT and *psae1-1* thylakoid proteins were loaded in lanes WT and *psae1-1*, and decreasing amounts of WT thylakoid membranes in lanes 0.75x, 0.5x and 0.25x WT. Replicate filters were immunolabelled with antibodies raised against PsaA/B, H, L, G, N, PetD, LHCI and LHCII.

<i>Pigment</i>	<i>WT</i>	<i>psae1-1</i>
Neoxanthin	38 \pm 7	44 \pm 8
Violaxanthin	58 \pm 5	69 \pm 10
Antheraxanthin	4 \pm 1	12 \pm 4
Zeaxanthin	0	0
Lutein	163 \pm 3	176 \pm 20
Chl <i>a</i>	772 \pm 3	774 \pm 2
Chl <i>b</i>	228 \pm 3	226 \pm 2
β -Carotene	130 \pm 1	131 \pm 4

Table 5.1 Pigment composition of WT and *psae1-1* leaves. Leaf pigments from 3 plants for each genotype grown under low-light conditions (80 $\mu\text{mol photons m}^{-2} \text{s}^{-1}$) were extracted with acetone. Extracts were analyzed by HPLC as described by Färber et al. (1997). Pigment concentrations are given in mmol per mol Chl (*a+b*). Mean values (\pm SD) are shown.

5.2 IN *psae1-1* STATE TRANSITIONS ARE IMPAIRED AND THE PSII ANTENNAE ARE REDUCED IN SIZE

State transitions in wild-type and mutant plants were followed by measuring maximum PSII fluorescence signals in state 1 (Fm1) and state 2 (Fm2), after irradiating plants at wavelengths that target PSII and PSI, respectively, and normalizing these values to the maximum PSII fluorescence of dark-adapted leaves (Fm). In the wild-type, Fm1/Fm and Fm2/Fm differed significantly (0.87 ± 0.03 versus 0.77 ± 0.01), while in the *psae1-1* mutant both values were essentially the same (0.82 ± 0.03 versus 0.81 ± 0.03). This corresponds to a reduction of 85% in qT in the mutant (WT: 0.13 ± 0.01 , *psae1-1*: 0.02 ± 0.01), indicating a severe impairment in the redistribution of excitation energy between the photosystems. When instead of qT, the relative fluorescence change of PSII, F_r (Lunde et al., 2000), was monitored to measure state transitions, a similar decrease was found in mutant plants (F_r [WT]: 0.94 ± 0.01 , F_r [*psae1-1*]: 0.14 ± 0.01).

77 K fluorescence emission and excitation spectra of frozen leaf material were recorded to study in more detail the energy distribution in both genotypes (Figure 5.2). To overcome the well known distortion of the spectra by re-absorption of emitted light due to the high optical density within leaves, we used the so-called 'diluted leaf particles' method as described by Weis (1985). Prior to measurements, leaves of wild-type and mutant plants were irradiated for 30 min at state 1- or state 2-favoring wavelengths. Excitation spectra of PSII (recorded at 685 nm) of state 1-adapted leaves differed significantly in the two genotypes (Figure 5.2a): the Chl *b*-related peak (480 nm) was markedly decreased in *psae1-1* plants, revealing that energy transfer from Chl *b* to PSII, as well as the size of the functional PSII antenna (Bassi et al., 1993), was reduced. This difference in the Chl *b*-related peak for the two types of plants was decreased in state 2-adapted leaves (Figure 5.2b) due to the migration of the mobile pool of LHCII from PSII to PSI in wild-type plants. A marked difference, however, in the Chl *b*-related peak for the two genotypes persists even under the state 2-favoring conditions, indicating perturbations in the PSII antenna of mutant plants. The permanent reduction in the size of functional PSII antenna in *psae1-1* plants was confirmed by fluorescence emission analyses: emission spectra of both state 1- and state 2-adapted mutant leaves (Figures 5.2c and 5.2d, respectively) showed a reduction in the PSII-related peak (685 nm). Moreover, a 1 nm blue-shift in the emission spectra of both state 1- and state 2-

adapted *psae1-1* leaves indicate that the interaction between PSI-antenna and the PSI-core is affected by the mutation (Jensen et al., 2000).

Attachment of LHCII to PSI during state 2 should increase the size of the functional antenna of PSI. In fact, excitation spectra of PSI (recorded at 730 nm; Figures 5.2e and 5.2f) allowed to recognize state transitions as indicated by a difference in the Chl *b*-related peak (480 nm) only in wild-type plants (0.798 versus 0.812 relative fluorescence intensity in state 1- versus state 2-adapted plants), but not in mutant plants (0.792 versus 0.784 relative fluorescence).

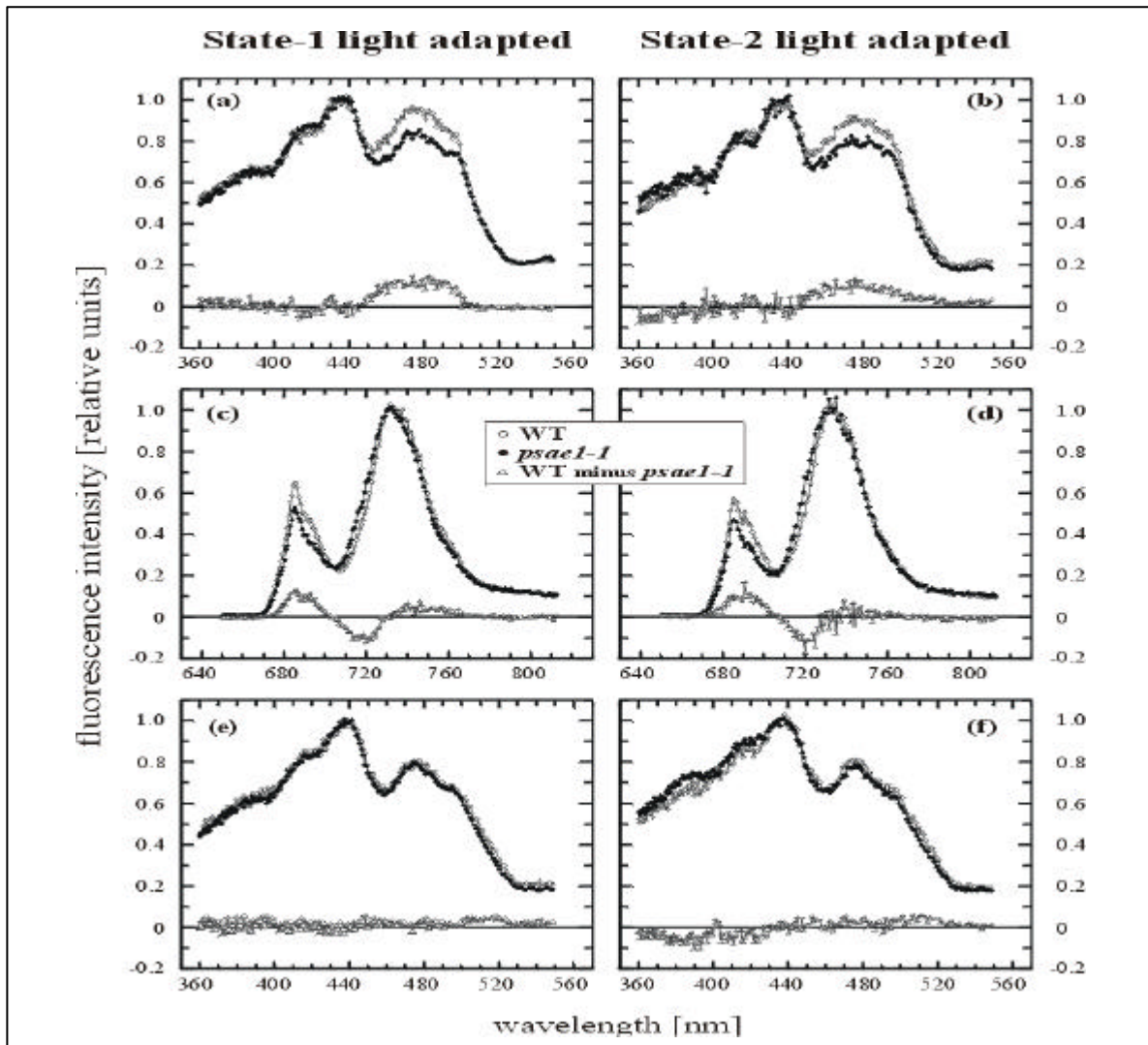


Figure 5.2 Excitation and emission spectra of PSII and PSI. 77 K fluorescence spectra were determined for plants adapted to state 1 (a, c, e) and state 2 (b, d, f). Excitation spectra were recorded at emission wavelengths specific for PSII (685 nm; a, b) or PSI (730 nm; e, f) and normalized to the maximum at 435 nm. Emission spectra (c, d) were recorded using an excitation wavelength of 480 nm, which is preferentially absorbed by Chl *b*, and normalized to the maximum emission around 732 nm. Spectra for WT plants (open circles), mutant plants (filled circles) and the respective difference (WT minus mutant: triangles) are shown.

5.3 A PSI-LHCII AGGREGATE IS PRESENT IN *psae1-1* THYLAKOIDS

In order to investigate more in detail the spectroscopic differences mentioned above, thylakoid membranes from wild-type and mutant plants grown under low-light conditions (state 2-favoring conditions) were isolated and subjected to analysis by native GREEN-PAGE to separate pigment-protein complexes (Figure 5.3a). The banding patterns obtained with the two genotypes differed in the relative intensity of the band corresponding to PSI. Strikingly, a high-molecular-weight band of about 400 kDa was present only in mutant thylakoids. This “400-kDa” band was detected under low-light conditions ($80 \mu\text{mol photons m}^{-2} \text{ s}^{-1}$), and in lower amounts in plants kept in the dark or exposed to high levels of light ($800 \mu\text{mol photons m}^{-2} \text{ s}^{-1}$) (Figure 5.3b).

The separated native pigment-protein complexes were subjected to a second fractionation by denaturing PAGE (Figure 5.4a). After silver staining, the 400-kDa complex was found to be resolved into several proteins. All its constituent polypeptides, with the exception of an abundant 27-kDa protein, were also present in the 300-kDa PSI. However, in the PSI complex obtained from *psae1-1* plants the relative abundance of polypeptides found in the 300-kDa PSI complex was less than in the wild-type, suggesting that this complex was less stable. In fact, in preparations of mutant thylakoids a larger proportion of the PSI polypeptides migrated as monomers. Immunoblot analyses confirmed the presence of several PSI subunits in the 400-kDa complex. The 27-kDa protein was identified as LHCII (Figure 5.4b), and immuno-labelling of a replicate blot with a phosphothreonine-specific antibody demonstrated that the LHCII contained in the 400-kDa complex was phosphorylated (Figure 5.4c). The spectroscopical data, together with the protein gel and immunoblot analyses, support the conclusion that in *psae1-1* plants a fraction of LHCII is permanently dissociated from PSII and linked to PSI.

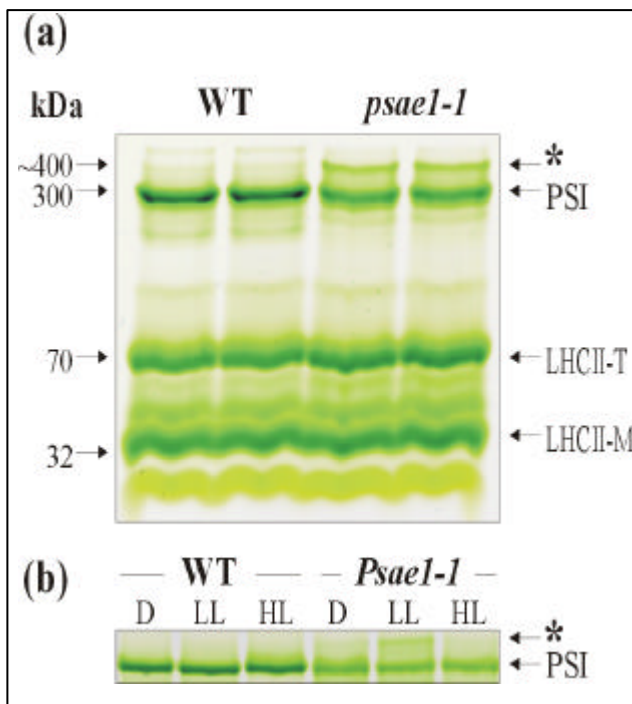


Figure 5.3 Native gel analyses. a) Thylakoid membranes were prepared in the middle of the day from WT and *psae1-1* plants grown under low-light conditions ($80 \mu\text{mol photons m}^{-2} \text{s}^{-1}$, state 2-favoring conditions). Samples from leaves pooled from ten plants were analyzed by LDS-PAGE and bands were assigned to protein-pigment complexes according to Santini et al. (1994) (PSI, photosystem I; LHCII-T, LHCII trimers; LHCII-M, LHCII monomers). The molecular weight of the mutant-specific band, indicated by an asterisk, was calculated by extrapolation (semi-logarithmic regression analysis) from the other data points. b) Thylakoid complexes from plants adapted to different light conditions and fractionated as in (a). Only the upper two bands are shown. D, plants after 2 h dark adaptation (state 1-favoring conditions); LL, plants propagated at $80 \mu\text{mol photons m}^{-2} \text{s}^{-1}$ (state 2-favoring conditions); HL, plants adapted to high light intensity (2 h of $800 \mu\text{mol photons m}^{-2} \text{s}^{-1}$, state 1-favoring conditions).

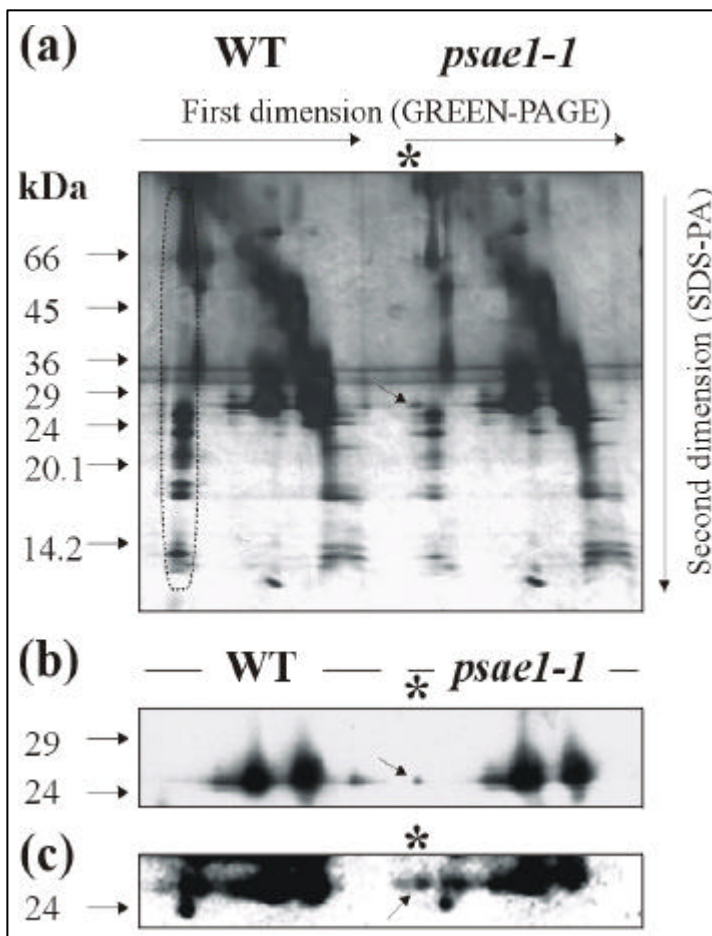


Figure 5.4 2D SDS-PAGE and immunoblot analyses a) Analysis of the 400-kDa complex by 2D gel electrophoresis. The position of the abundant 27-kDa peptide [LHCII, see (b)] is indicated by an arrow, while PSI proteins in the wild-type lane are encircled by a dotted black line. b) Western analysis of the 2D gel shown in (a) using an LHCII-specific antibody. The signal derived from the 27-kDa peptide contained in the 400-kDa complex is indicated. c) A similar filter to that shown in (b) was probed with a phosphothreonine-specific antibody. The signal derived from the LHCII contained in the 400-kDa complex is indicated.

5.4 THE LEVEL OF PHOSPHORYLATED LHCII IS INCREASED IN THE MUTANT

The phosphorylation of part of LHCII, the so-called ‘mobile pool’, is an essential requisite for the photosynthetic transition from state-1 to state-2. In order to investigate this aspect, the reversible phosphorylation of LHCII was studied *in vivo* in wild-type and *psae1-1* leaves incubated with [³³P]orthophosphate after being kept in darkness for 16 h and then exposed to different light conditions (Figure 5.5a). Low-light treatment caused a significant increase in the phosphorylation of LHCII in mutant leaves with respect to wild-type. Subsequent exposure to high-intensity light reduced the amount of phosphorylated LHCII in both genotypes, but to a lesser extent in *psae1-1* plants. When phosphorylated LHCII was monitored using a phosphothreonine-specific antibody, significantly increased levels were detected in mutant plants (Figure 5.5b). Even after prolonged dark adaptation, mutant plants had very high levels of phosphorylated LHCII, while wild-type LHCII was not phosphorylated to any significant extent. In the wild-type, illumination with high-intensity light reduced the total amount of phosphorylated LHCII to a minimum. In the mutant, the same treatment decreased the high phosphorylation level only marginally, indicating that in the mutant a large fraction of the LHCII is not accessible to dephosphorylation. The abnormal levels of phosphorylation found for *psae1-1* LHCII were not seen in other thylakoid proteins that phosphorylate in a light-dependent manner, such as CP43, D1, D2 and PSII-H.

In vitro phosphorylation of LHCII under reducing conditions (Steinback et al., 1982) was monitored in the presence of a phosphatase inhibitor in thylakoids from wild-type and mutant plants (Figure 5.5c). This measures the rate of LHCII phosphorylation under conditions of saturating electron transport, when the LHCII kinase should be maximally activated *via* the plastoquinol-cyt *b₆/f* mechanism. In mutant thylakoids, the low incorporation of [³³P]phosphate reflects the constitutively phosphorylated state of LHCII. Under non-reducing conditions, identical (low) amounts of *in vitro* phosphorylated LHCII were found in both genotypes.

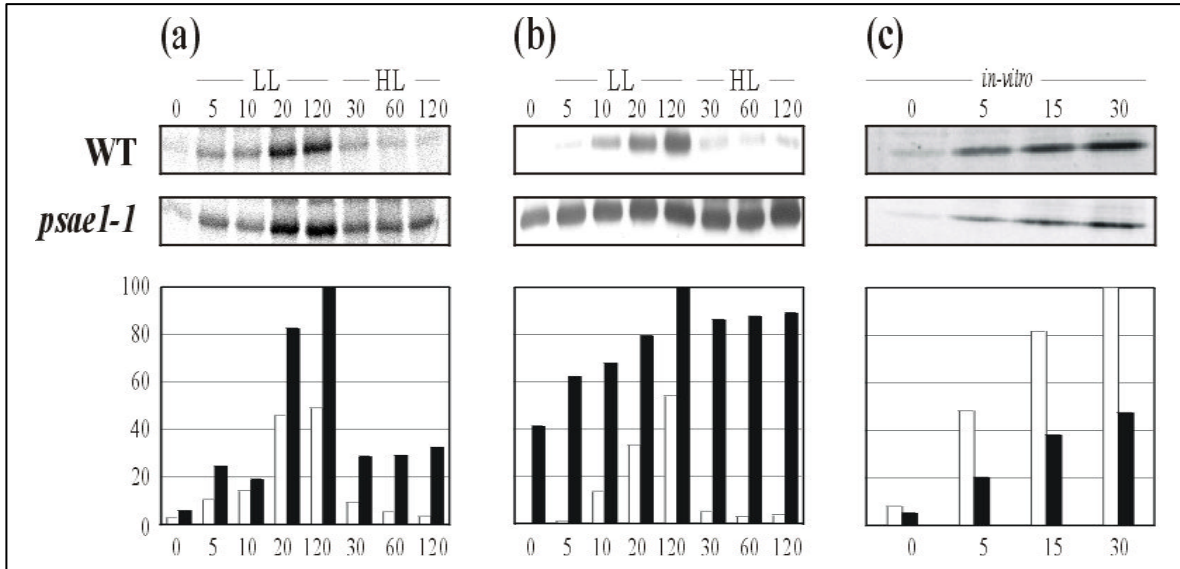


Figure 5.5 LHCII-phosphorylation in WT and mutant plants. a) *In vivo* phosphorylation of LHCII. Leaves were incubated with [^{33}P]orthophosphate, exposed to low-light (LL) and subsequently to high light (HL) (5, 10, 20 and 120 min LL or 30, 60 and 120 min HL). Identical amounts of thylakoid proteins (8 μg) were fractionated by SDS-PAGE and signals were detected by phosphoimager analysis (Molecular Dynamics). Intensities were normalized to the maximum signal obtained (120 min LL = 100%). White and black bars symbolize WT and *psae1-1* values, respectively. b) Phosphorylated LHCII detected by immunoblot analysis. Leaves were treated and thylakoid proteins fractionated by SDS-PAGE as in (a). Phosphorylated LHCII was detected by using a phosphothreonine antibody (Zymed) and signals were monitored by chemiluminescence (Amersham). c) *In vitro* phosphorylation of LHCII. To monitor the levels of *de novo* phosphorylation, thylakoids from dark-adapted leaves were incubated with [γ - ^{33}P]-ATP in the presence of the phosphatase inhibitor NaF under reducing conditions for 0, 5, 15 and 30 min in the dark. Fractionation of thylakoid proteins was done as in (a) and (b) and the levels of [^{33}P] incorporation were recorded by phosphoimager analysis (Molecular Dynamics).

The high basal level of phosphorylated LHCII evident in *psae1-1* plants raised the question whether the activity of thylakoid-bound LHCII kinase was increased, or the thylakoid-bound phosphatase activity reduced. The activity of the two enzymes was deduced from the half-life of maximum phosphorylation [$t_{1/2}(\text{phos})$] and dephosphorylation [$t_{1/2}(\text{de-phos})$] calculated from Figures 5.5a and 5.5b. Based on [^{33}P]-labelling *in vivo*, wild-type and *psae1-1* did not differ significantly (Table 5.2). When phosphorylated LHCII, detected by Western analysis, was used as the basis for calculating $t_{1/2}(\text{phos})$ and $t_{1/2}(\text{de-phos})$, wild-type plants had, for both parameters, nearly the same values as found *in vivo*. In mutant plants, however, phosphorylation and de-phosphorylation were drastically altered (Table 5.2), indicating again that a large fraction of LHCII was inaccessible to dephosphorylation.

	<i>Parameter</i>	<i>WT</i>	<i>psae1-1</i>
<i>in-vivo</i> assay	$t_{1/2}(\text{phos})$	11	9
	$t_{1/2}(\text{de-phos})$	15	13.5
Western analysis	$t_{1/2}(\text{phos})$	12.5	1.5
	$t_{1/2}(\text{de-phos})$	15	>120

Table 5.2 Half times of phosphorylation and de-phosphorylation of LHCII in WT and *psae1-1*. Half-times (min) of phosphorylation [$t_{1/2}(\text{phos})$] and dephosphorylation [$t_{1/2}(\text{de-phos})$] were derived both from values detected by phosphoimager in the *in vivo* assay (see Figure 5.5a) and from Western analysis evaluated by chemi-luminescence (see Figure 5.5b). $t_{1/2}(\text{phos})$ is the time needed to reach half-maximal values during low-light-induced phosphorylation (from $t=0$ to $t=120$ [LL]). $t_{1/2}(\text{de-phos})$ is the time needed to reduce phosphorylation to half-maximal values during the high-light-induced decrease in phosphorylation (from $t=120$ [LL] to $t=120$ [HL]). Both, $t_{1/2}(\text{phos})$ and $t_{1/2}(\text{de-phos})$ were calculated by using GraFit5 (Erithacus software).

5.5 ELECTRON TRANSPORT THROUGH PSI IS ALTERED IN *psae1-1* MUTANT THYLAKOIDS

In mutant plants, the increased level of LHCII phosphorylation under low light conditions could be caused by the drastically reduction of the amount of subunit E, involved in the electron transport (Varotto et al., 2000). In order to elucidate that aspect, the electron flow through the thylakoid membranes has been investigated.

Linear electron flow from water to NADP^+ was measured under saturating light in thylakoids from wild-type and *psae1-1* leaves. Identical amounts of NADPH were synthesized in both genotypes (Table 5.3), even when ferredoxin concentrations were varied (Figure 5.6a). This indicates that in mutant, as in wild-type plants (Haehnel, 1976), under saturating levels of light, the reduction of cyt b_6/f , but not the function of PSI, represents the rate-limiting step for linear electron flow. The addition of DCMU blocks photosynthetic electron transfer from PSII to PSI, allowing measurement of the electron flow through PSI in the presence of TMPD as electron donor for plastocyanin. Under these conditions, a decrease of 35% in NADPH production was observed in mutant leaves (Table 5.3). This difference increased to about 45% when ferredoxin concentrations were near saturation (Figure 5.6b)

The ATP/NADPH ratio was measured in the presence of an inhibitor of the adenylate kinase (Burlacu-Miron et al., 1998). No significant difference between mutant and wild-type thylakoids was detected (Table 5.3), indicating that cyclic electron flow was not increased in the mutant. Interestingly, the ATP/NADPH ratio in *psae1-1* thylakoids was higher in the absence of the inhibitor, implying an increase in adenylate kinase activity in the mutant.

Parameter	Experimental conditions	WT	<i>psae1-1</i>	
		$\mu\text{molNADPH} \times (\text{mgChl})^{-1} \times \text{h}^{-1}$	% of WT	
Electron flow	from H ₂ O to NADP ⁺ (saturating light, -DCMU, -TMPD)	53 ± 1	54 ± 1	101.9
	from TMPD to NADP ⁺ (saturating light, +DCMU, +TMPD)	102 ± 7	66 ± 4	64.7
ATP/NADPH ratio	- Pp ₅ A	0.91 ± 0.003	>2.00	>220
	+ Pp ₅ A	0.91 ± 0.002	0.91 ± 0.05	100

Table 5.3 Measurements of photosynthetic electron flow in WT and *psae1-1* thylakoids. NADPH synthesis in thylakoids was measured spectrophotometrically under saturating actinic light (150 $\mu\text{mol photons m}^{-2} \text{s}^{-1}$) and conditions favoring either electron transport from water to NADP⁺ or electron flow from the artificial electron donor TMPD via plastocyanin (PC) to NADP⁺ in the presence of DCMU (which inhibits electron flow from PSII). The ATP synthesis was indirectly measured in presence or absence of the adenylate kinase inhibitor ‘P₁,P₅-di (adenosine-5’) pentaphosphate’ (Pp₅A) by the increase of absorbance resulting from the enzymatic reactions involving glucose, hexokinase and glucose-6-P dehydrogenase at the expense of ATP (see Materials and Methods: chapter 2.11.2).

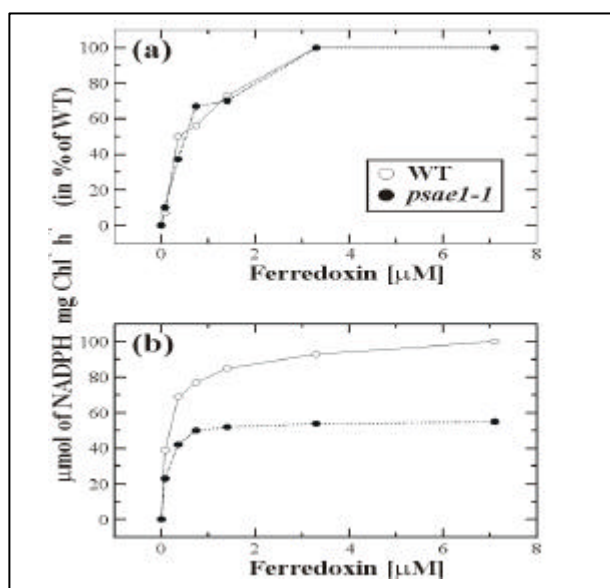


Figure 5.6 NADPH-synthesis in WT and mutant plants. a) Production of NADPH was determined spectrophotometrically as the increase of absorbance at 340 nm minus 390 nm in 3 WT and 3 *psae1-1* plants for a range of ferredoxin concentrations and under light saturating conditions. Under these conditions, the electron flow from water to NADP⁺ via PSII, cyt *b₆/f*, plastocyanin and PSI is monitored. Standard deviations are contained in the circles symbolizing values. Note that 100% of WT corresponds to 51 $\mu\text{molNADPH} \times (\text{mg Chl})^{-1} \times \text{h}^{-1}$. b) Same as (a), but measurements were done in the presence of DCMU to block electron flow from PSII and of TMPD to reduce plastocyanin. Under these conditions, the electron flow from TMPD to NADP⁺ via plastocyanin and PSI bypasses PSII, as well as cyt *b₆/f*. Note that 100% of WT corresponds to 98 $\mu\text{mol NADPH} \times (\text{mg Chl})^{-1} \times \text{h}^{-1}$.

5.6 THE THYLAKOID ULTRA-STRUCTURE IS ALTERED IN *psae1-1* CHLOROPLASTS

It has been reported that the formation of the appressed regions in thylakoid membranes is most probably due to non-phosphorylated LHCII attached to PSII (Allen, 1992b; Allen and Forsberg, 2001). In order to investigate whether the permanent phosphorylation, as well as the permanent detachment of a fraction of LHCII from PSII in mutant leaves, could perturb the thylakoid ultra-structure, electron microscopy analyses were performed (Figure 5.7). Indeed, the analyses revealed a significant decrease in the number of membrane layers in the grana stacks of state 1-adapted mutant plants (9 ± 2) with respect to the number observed in wild-type plants (15 ± 2.5), supporting previous finding in maize (Vallon et al., 1991).

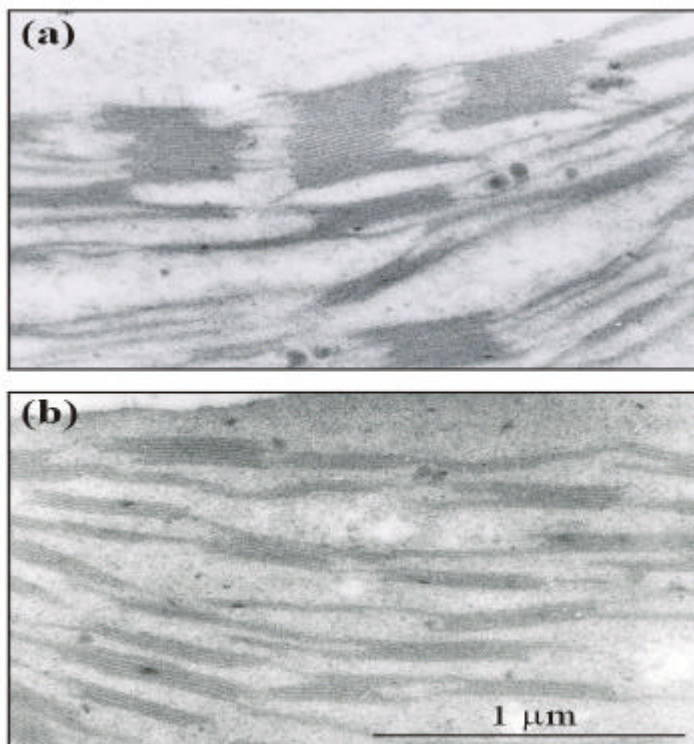


Figure 5.7 Ultrastructure of WT (a) and *psae1-1* (b) thylakoids. To quantify the difference between WT and *psae1-1*, fifty thylakoid sections obtained from dark-adapted plants of each genotype were considered. The average number of discs per grana stack is decreased in the mutant (9 ± 2) with respect to wild-type (15 ± 2.5). Magnification is 32 000; bar = 1 μm.

DISCUSSION

The inactivation of the *psae1* gene results in the almost complete suppression of state transitions. Moreover, in the mutant, the antenna size of PSII is permanently reduced, as indicated by PSII excitation and emission spectra analysis, and LHCII exists in a stable complex with PSI. Holo-complexes of LHCI and PSI can be isolated from wild-type chloroplasts, but the existence of a PSI-LHCII complex was established only on the basis of indirect evidence (Scheller et al., 2001). The high-molecular-mass complex present in *psae1-1* thylakoids represents a PSI-LHCII aggregate, as evidenced by the following observations. (i) Denaturing gel analysis reveals, in addition to PSI polypeptides, the presence of an abundant polypeptide with a molecular weight identical to LHCII in the complex. (ii) Western analysis demonstrates that this extra complex contains PSI proteins and LHCII. (iii) The molecular weight of the complex is compatible with that of a 1:1 aggregate of PSI and LHCII trimers. (iv) The aggregate is abundant in thylakoids isolated from plants grown under conditions that favor phosphorylation of LHCII. (v) The LHCII attached to PSI is phosphorylated, as expected (Allen, 1992a). Although the PSII antenna size in mutant plants is reduced to an almost identical extent under state 1- and state 2-favoring conditions, the abundance of the 400-kDa PSI-LHCII aggregate is markedly higher under low light conditions (state 2-favoring), suggesting a crucial role of light intensity on the stability of the aggregate.

Most probably, the LHCII binds to a domain of mutant PSI that differs from its normal docking site on wild-type PSI. Indeed, the PSI from mutant thylakoids showed a decrease in the abundance of PsaL and PsaH subunits. In particular, the decreased level of PsaH, the proposed attachment site for LHCII (Lunde et al., 2000), together with the destabilization of the stromal ridge (PsaC, D and E; Varotto et al., 2000) could generate a more stable, and (as indicated by PSI excitation spectra) probably non-functional, attachment site for LHCII.

The phosphorylation of LHCII, a key step in state transitions, was characterized in detail. In mutant plants, the level of phosphorylated LHCII increases dramatically. Under conditions of low light this could be attributable to an over-reduction of the plastoquinone pool and of cyt *b₆f*, as indicated by the altered 1-qP value (WT: 0.06; *psae1-1*: 0.26; Varotto et al., 2000), while the activities of LHCII kinase and phosphatase were not altered. In addition, the decrease in phosphorylation during treatment with high-intensity light proves that the ferredoxin/thioredoxin-mediated down-regulation of LHCII-kinase activity is functional in

the mutant. High levels of phosphorylated LHCII were detected even under conditions of minimal kinase activity (16 h dark or 2 h high-intensity light). Moreover, under reducing conditions and in the presence of a phosphatase inhibitor, only 50% of the mutant LHCII was accessible to de novo phosphorylation, the rest presumably being already phosphorylated. Taken together, the data on LHCII phosphorylation suggest the existence of a large pool of LHCII, probably the fraction attached to PSI, that is inaccessible to dephosphorylation in mutant thylakoids.

Electron microscopy revealed a decrease in the number of membrane layers in the grana stacks of state 1-adapted mutant thylakoids. This is in agreement with the model of Allen (1992b; Allen and Forsberg, 2001), which suggests that the formation of stacked domains in thylakoid membranes is due to the tendency of non-phosphorylated LHCII to aggregate, thereby forming large, connected, antenna. In *psae1-1* thylakoids, the high level of phosphorylated LHCII alone could be responsible for the destacking of the appressed regions. In maize and *Chlamydomonas reinhardtii*, destacking is associated with the redistribution of cyt *b_{6/f}* into the PSI-enriched stromal lamellae, a condition that stimulates cyclic electron flow (Vallon et al., 1991; Wollmann, 2001). In *psae1-1*, cyclic electron flow is, however, not increased. Interestingly, in the absence of an inhibitor of adenylate kinase, the ATP/NADPH ratio is significantly higher in the mutant, implying that adenylate kinase activity in *psae1-1* is higher than in wild-type. In mutant plants, high levels of photoinhibition have been observed (Varotto et al., 2000), possibly leading to additional PSII damage, which would require a higher rate of ATP synthesis for its repair.

In summary, evidences for the presence of two populations of PSI in the mutant plants have been shown. The 300-kDa fraction contains a wild-type-like PSI, which, although deficient for one of the two forms of PsaE, is most probably still capable of supporting state transitions, including the reversible association of LHCII, to some extent. The 400-kDa PSI fraction, on the other hand, has a significantly different subunit stoichiometry. This results (i) in the abnormal stability of the novel aggregate, (ii) in the constitutively phosphorylated state of LHCII, and (iii) in the depletion of LHCII from the PSII antenna. Together with the noted modification of the membrane layers in the grana stacks of thylakoids, all biochemical and physiological alterations described for mutant plants contribute to the unique imbalance in excitation energy distribution between photosystems.

6 CHARACTERIZATION OF THE *atmak3-1* MUTANT

The *photosynthesis affected mutant 21 (pam21)* was identified among a collection of T-DNA tagged lines on the basis of a decrease in the effective quantum yield of photosystem II. The T-DNA insertion was localised in *At2g38130*, a single-copy gene encoding for a protein orthologous to the *N*-terminal acetyltransferase Mak3p of *S. cerevisiae* (Tercero and Wickner, 1992). In yeast, Mak3p is associated with Mak10p and Mak31p forming a trimeric complex designated as *N*-terminal acetyltransferase C (NatC) (Polevoda and Sherman, 2001). The *MAK3* gene was first identified from *mak3-Δ* strains that did not assemble or maintain the L-A-HN, M₁ dsRNA viral particles (Tercero and Wickner, 1992). This defect was due to the incapacity of the mutant to acetylate the *N*-terminal of the GAG viral protein. Yeast strains mutated in *MAK10* and *MAK31* genes were also identified and their phenotypes were identical to the one of *mak3-D* strain, indicating that each subunit is essential for the NatC complex functionality (Polevoda and Sherman, 2001). This chapter reports on the detailed characterisation of *pam21* phenotype.

6.1 *pam21* PHENOTYPE

pam21 showed a slightly pale green phenotype together with a reduction in size (Figure 6.1a). Comparison of the growth behaviour, by using non invasive image analysis (Leister et al., 1999), indicated a reduction of the growth rate of mutant plants of about 40% relative to wild-type (Figure 6.1b). Additionally, 3-4 week-old mutant plants, were affected in photosynthetic performances as indicated by the reduction of both Fv/Fm and fluorescence yield (Φ_{II}) with respect to wild-type plants (Table 6.1). A slight decrease of Chl a/b ratio and chlorophyll content could be also observed in 3-4 week-old mutant plants suggesting alterations in thylakoid polypeptide composition. Interestingly, the altered photosynthetic phenotype and the slightly pale green colour of leaves disappeared in 5-6 week-old plants, suggesting that the disrupted gene plays a major role in young developing seedlings.

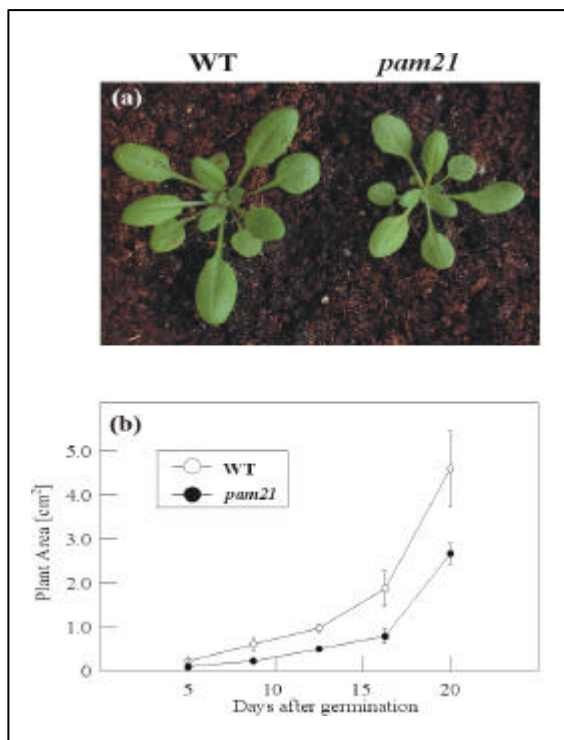


Figure 6.1 Phenotype of WT and *pam21* plants. a) 4 week-old plants grown under greenhouse conditions. b) Growth kinetics of *pam21* compared to WT plants. Leaf area was measured in the period from 5 to 20 d after germination. Bars indicate standard deviation.

	<i>WT</i> (3-4 week-old)	<i>pam21</i> (3-4 week-old)	<i>WT</i> (5-6 week-old)	<i>pam21</i> (5-6 week-old)
Fv/Fm	0.83 ± 0.004	0.73 ± 0.002	0.82 ± 0.01	0.81 ± 0.01
Φ _{II}	0.77 ± 0.004	0.66 ± 0.037	0.77 ± 0.002	0.75 ± 0.01
Chla/b	3.78 ± 0.09	3.11 ± 0.01	3.47 ± 0.09	3.23 ± 0.17
Chla+b	1.54 ± 0.04	1.42 ± 0.07	1.07 ± 0.1	1.17 ± 0.1

Table 6.1 Fluorescence parameters and pigment content (µg of chlorophyll per gram of fresh leaf weight) of WT and *pam21* plants at different developmental stages. Values (± SD) are means of 5 independent measurements.

6.2 THE POLYPEPTIDE COMPOSITION OF THYLAKOID MEMBRANES IS ALTERED IN *pam21*

Thylakoid from greenhouse-grown wild-type and mutant plants were isolated and subjected to two-dimensional PAGE (Figure 6.2a). Individual subunits of the photosynthetic apparatus were resolved and assigned to PSI, PSII core, ATPase (α-, β-subunits), the oxygen evolving complex and the major light harvesting complex of PSII (LHCII) as described in Pesaresi et al. (1995). Densitometric analyses of the 2D protein gel after Coomassie staining showed a

reduction of the PSII core in mutant thylakoids by 40% relative to wild-type, while the levels of PSI subunits were reduced by 30% (Table 6.2). A large reduction in the amount of the α - and β -subunits of ATPase could be also observed, whereas the LHCII levels were identical in mutant and wild-type thylakoids. The reduction in the amounts of PSII core and PSI polypeptides, detected by two-dimensional PAGE were confirmed by Western analyses (Figure 6.2b). The D1 subunit of PSII core and the PsaA and PsaB subunits of PSI (CP1) in mutant thylakoids showed a decrease of about 40% and 25%, respectively, in comparison to wild-type values (Table 6.2).

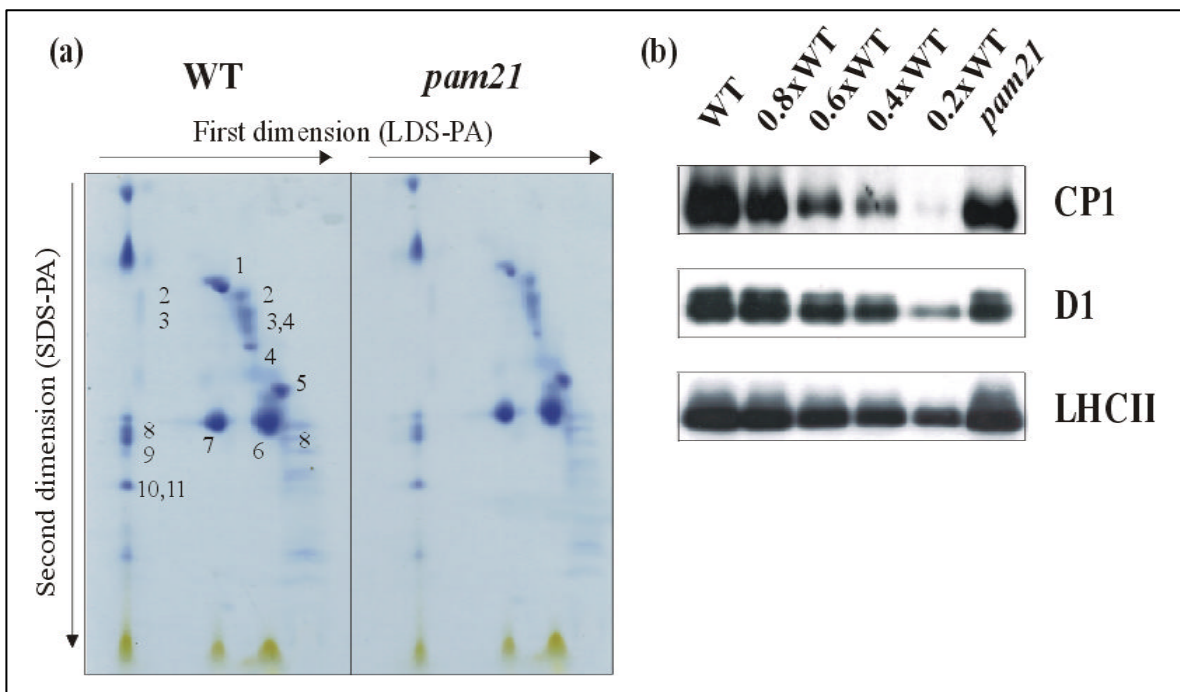


Figure 6.2 Protein composition of thylakoid membranes. a) Identical amount of thylakoid proteins from WT and *pam21* were fractionated first by electrophoresis on a non-denaturing Green-PAGE, and then on a denaturing SDS-PAGE. Positions of WT thylakoid proteins previously identified by Western analyses with appropriate antibodies are indicated: 1, α - and β -subunits of the ATPase complex; 2, D1-D2 dimer; 3, CP47; 4, CP43; 5, oxygen-evolving complex (OEC); 6, LHCII monomer; 7, LHCII trimer; 8, PsaD; 9, PsaF; 10, PsaC; 11, PsaH. b) Identical amounts of thylakoid proteins were loaded in lanes WT and *pam21*. Decreasing levels of WT thylakoid proteins were loaded in the lanes marked 0.8x, 0.6x, 0.4x, 0.2x WT. Three replicate filters were probed with antibodies raised against CP1 (PsaA/B), D1 and LHCII.

	<i>WT</i>	<i>pam21</i>	<i>Relative level in pam21 [%]</i>
PSI	1.36	0.97	71.32
PSII core	0.83	0.52	62.65
ATPase ($\alpha + \beta$)	0.59	0.34	57.62
LHCII	2.27	2.22	97.79
CP1 (western analysis)	7.9	6.02	76.20
D1 (western analysis)	3.24	1.99	61.41
LHCII (western analysis)	3.7	3.68	99.45

Table 6.2 Analyses of thylakoid protein levels in WT and *pam21* mutant plants. Values for proteins are average optical densities (OD) measured from three independent 2D protein gel analyses (see figure 6.2a) or in the case of CP1, D1 and LHCII, three independent Western analyses (see figure 6.2b). Standard deviations were in the range below 8%.

6.3 THE SYNTHESIS RATE OF D1 AND CP47 POLYPEPTIDES IS REDUCED IN MUTANT PLASTIDS

The transcript amounts of PSII core, PSI and ATPase subunits were monitored by Northern analyses (Figure 6.3). The level of the *psbA* transcript (which encodes the D1 protein) was identical in wild-type and *pam21* plants. Identical amount of mRNA was also observed for the *psbC* transcript, which codes the CP43 subunit. The total amount of *psbB* transcript, encoding the CP47 protein, was also unchanged, although accumulation of large transcripts could be detected in mutant plastids. The transcripts of *psaA* and *psaB* genes, encoding the A and B subunits of PSI, did not show any significant difference in the total amount between wild-type and mutant plants. However, for the *psaA* transcripts a slightly increased amount of the band at 5.2 kb and a decreased amount of the bands smaller than 2.0 kb could be observed in mutant plants, indicating an alteration in the mRNA maturation process. Increased amount of the *atpA* transcript, encoding the α -subunit of ATPase, was observed in *pam21* plants, while no significant change was observed in the amount of the *atpB* transcripts, encoding the β -subunit of ATPase.

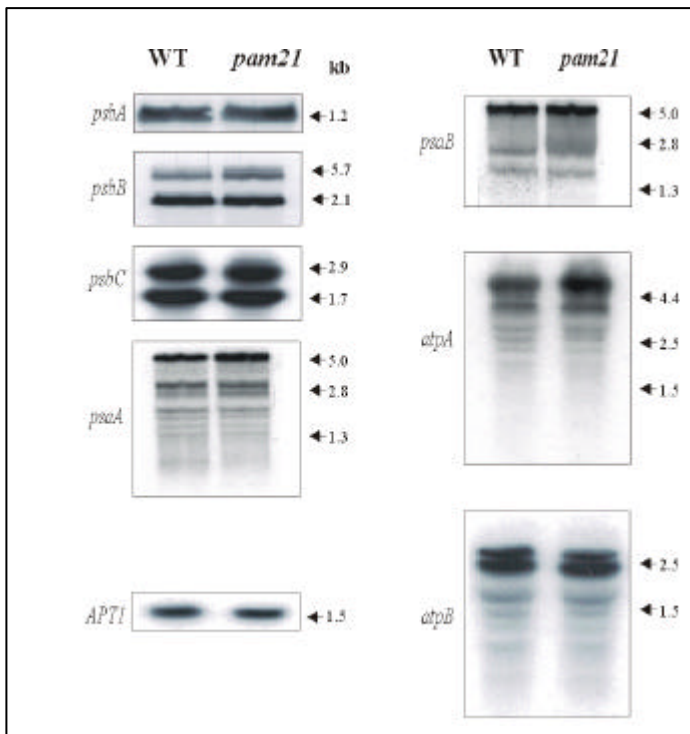


Figure 6.3 mRNA expression. The numbers at the right indicate RNA sizes that were estimated by co-electrophoresis with denatured *EcoRI/HindIII* fragments of lambda DNA. 30 µg of WT and *pam21* total RNA were transferred to a nitrocellulose filter and hybridised with cDNA fragment probes of the following genes: *psbA*, *psbB*, *psbC*, *psaA*, *psaB*, *atpA* and *atpB*. To control for RNA loading, the filter was re-probed with a cDNA fragment derived from the *APT1* gene, which is expressed at a low level in all tissues of *Arabidopsis* (Moffat et al., 1994).

Since no marked decrease in the amounts of plastome transcripts was observed in mutant plants, the possibility that the reduced levels of thylakoid polypeptides were due to a defect in protein synthesis was tested. For this purpose, the association of *psbA*, *psbB*, *psbC* and *psaA* transcripts with polysomes was analysed (Figure 6.4). Total leaf lysates were fractionated on sucrose gradients under conditions that maintain polysome integrity (Barkan, 1998). Specific mRNAs were localised in the gradients by performing Northern analyses with RNA purified from gradient fractions. The distribution of the *psbC* mRNAs was similar in the gradients containing mutant and wild-type samples, whereas *psbB* transcripts were associated with slightly smaller particles in the mutant samples. On the contrary, the *psbA* transcripts of mutant plants were more abundant in the heavier sucrose gradient fractions in comparison to wild-type samples. The *psaA* transcript distribution was similar between wild-type and mutant samples although reduced amounts of low molecular weight mRNAs could be observed in *pam21* samples, reflecting the altered transcript maturation observed with the mRNA quantification analyses (see Figure 6.3).

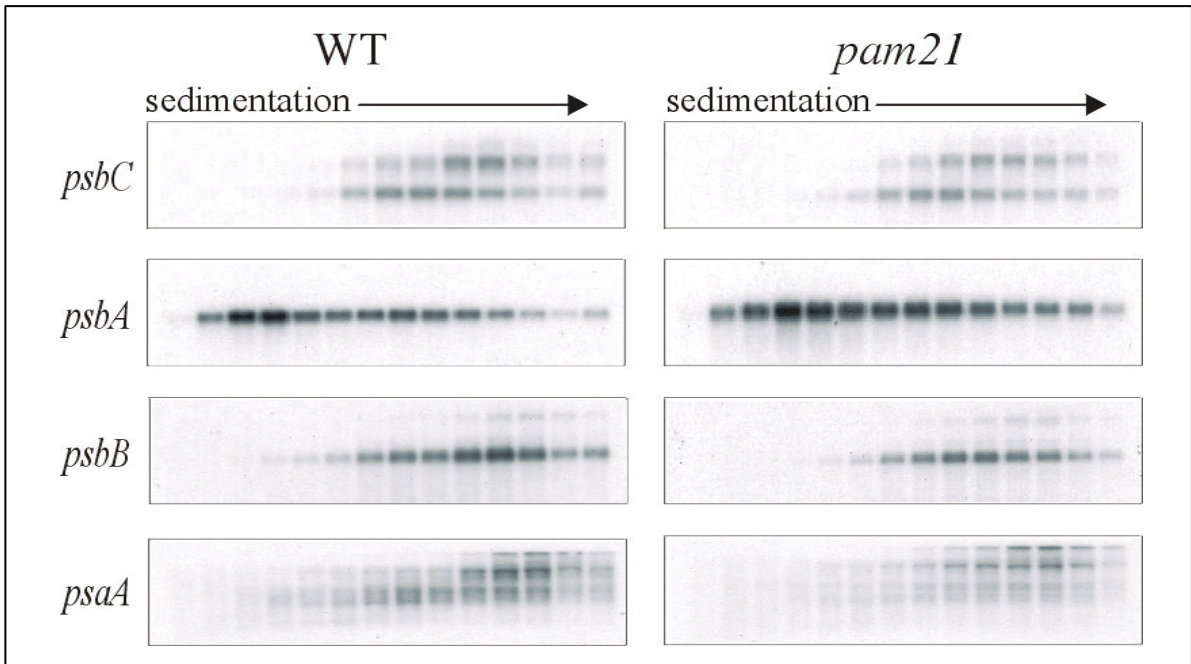


Figure 6.4 Association of chloroplast mRNAs with polysomes. Total extracts from 4 week-old WT and *pam21* plants were fractionated on sucrose gradients. 14 fractions of equal volume were collected from the top to the bottom of the sucrose gradients. An equal proportion of the RNA purified from each fraction was analysed by gel-blot hybridisation. Transcripts of *psbA*, *psbB*, *psbC* and *psaA* were detected with cDNA-specific probes.

To test whether the altered polysome association with the *psbA* and *psbB* transcripts could reduce the rate of protein synthesis, *in vivo* translation assays were performed. Young leaves of wild-type and *pam21* plants were incubated with [³⁵S]methionine in presence of light for 10 minutes. Subsequently, thylakoid membranes were isolated and polypeptides were fractionated by using a Blue-Native PAGE in the first dimension and a denaturing SDS-PAGE in the second dimension. Accumulation of labelled D1 subunit was markedly reduced in mutant leaves, whereas LHCIII accumulated to a similar extent in wild-type and mutant plants (Figure 6.5a-b) (Table 6.3). To assess the rate of synthesis of the other thylakoid proteins, the labelling was performed for a longer period (30 min) (Figure 6.5c-d). In this case, a reduced accumulation of radiolabelled CP47 could be also observed in mutant samples, while CP43, as well as most of the other thylakoid proteins, accumulated to wild-type levels (Table 6.3). These results, together with the altered polysome association, demonstrated that *psbA* and *psbB* transcripts are translated inefficiently in *pam21* plants.

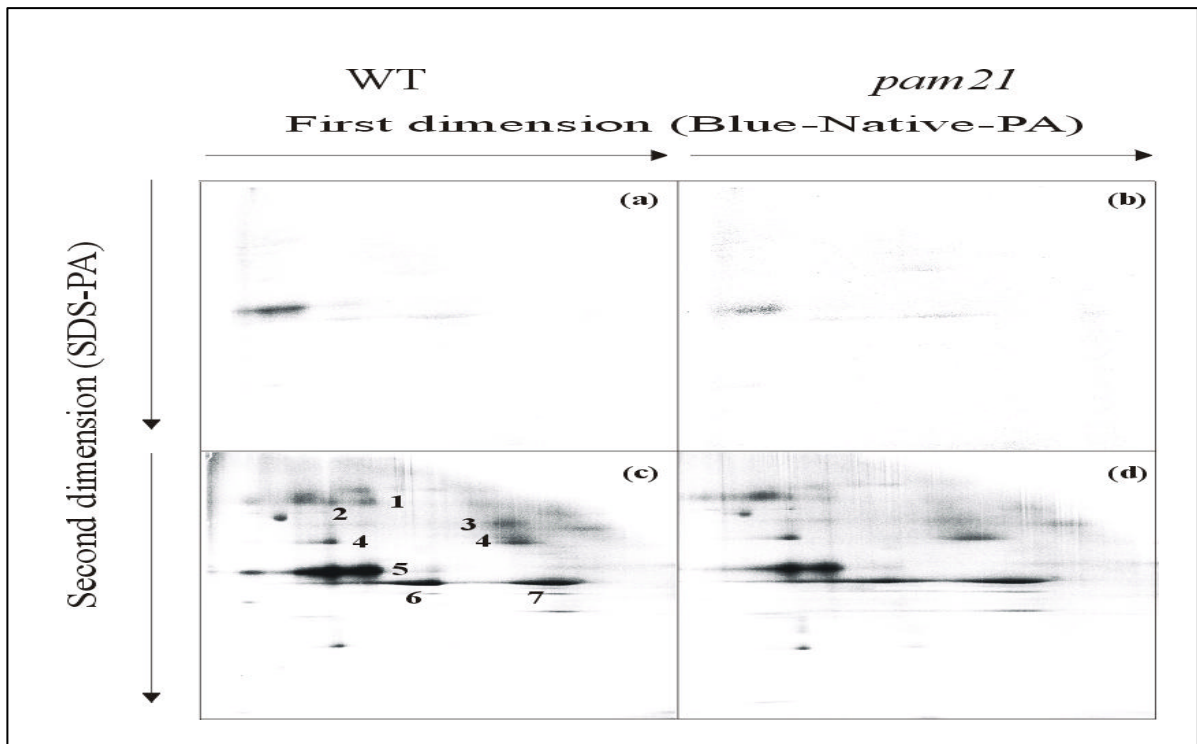


Figure 6.5 *In vivo* synthesis of thylakoid proteins in primary leaves of 3 week-old mutant and WT plants. The results of one of three independent experiments are shown. 100 mg of leaves were incubated with [³⁵S]methionine for 10 (a-b) or 30 min (c-d) under illumination. Thylakoid proteins were isolated from WT and mutant leaves, separated by Blue-Native PAGE in the first dimension and SDS-PAGE in the second dimension, electro-blotted onto a nylon membrane and analysed by fluorography. The labelled bands correspond to the following proteins as identified by Mass-spectrometry analyses: 1, PsaA-B; 2, ATP α - β ; 3, CP47; 4, CP43; 5, D1; 6 LHCII trimer; 7 LHCII monomer.

		<i>WT</i>	<i>pam21</i>	<i>Relative level in pam21 (%)</i>
D1	(10 min labelling)	0.72	0.31	50
LHCII	(10 min labelling)	0.052	0.051	98
D1	(30 min labelling)	4.6	2.5	54
CP47	(30 min labelling)	0.4	0.23	57
CP43	(30 min labelling)	0.69	0.71	102.9
LHCII	(30 min labelling)	2.6	2.57	98.8
PsaA-B	(30 min labelling)	0.8	0.74	92.5

Table 6.3 Quantification (optical densities) of signals of the labelled proteins observed in Figure 6.5. Standard deviation is in the range below 8%.

6.4 THE *pam21* MUTATION IS DUE TO A T-DNA INSERTION IN THE *At2g38130* GENE

Southern analysis of six different pools of mutant plants (10 plants per each pool) using the 5'-end of the *AC106* T-DNA as a probe revealed the presence of one T-DNA copy (Figure 6.6a). The T-DNA copy co-segregated with the *pam21* phenotype (Figure 6.6b). Isolation of genomic sequences flanking both termini of the T-DNA was performed (see Materials and Methods: chapter 2.4) and yielded in the identification of the insertion site. The T-DNA insertion was located in the third intron of the *At2g38130* gene at position 1 077 bp relative to the first ATG codon (Figure 6.6c). Northern analysis using an *At2g38130* cDNA specific probe revealed that the T-DNA insertion drastically destabilised the *At2g38130* transcript (Figure 6.6d).

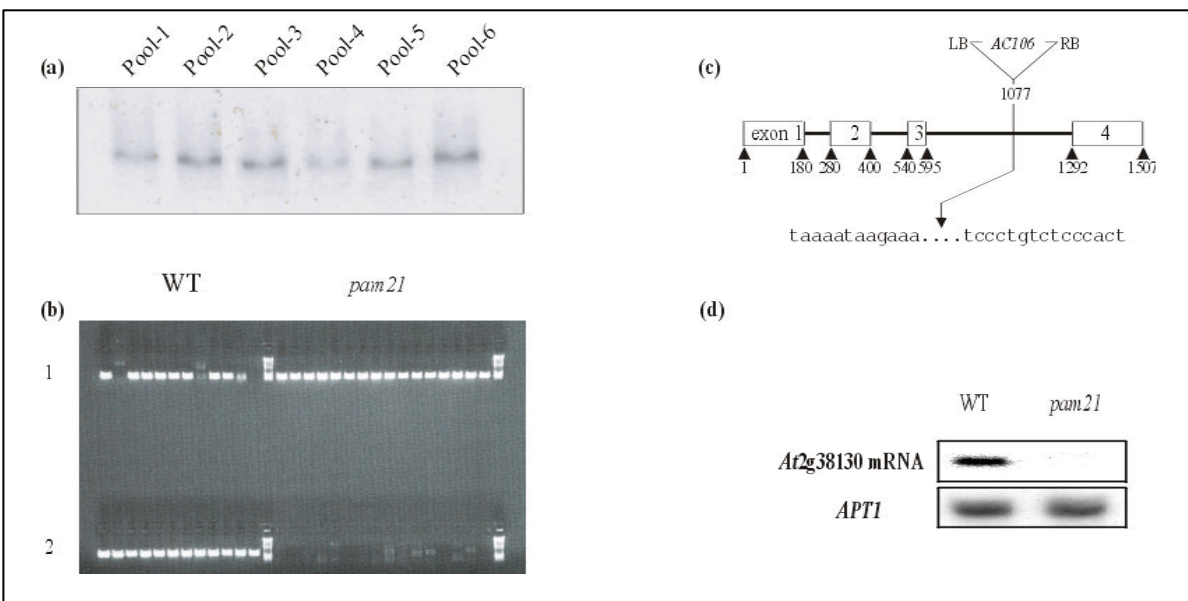


Figure 6.6 T-DNA insertion site. a) Southern analysis performed with DNA extracted from 6 different pools of mutant leaves. After digestion with *Sfi*I and blotting, the filter was hybridised with a probe matching the left border of T-DNA. b) The presence of T-DNA insertion in WT and mutant plants was monitored by PCR. In row # 1 a primer specific for the left border of T-DNA and a primer matching upstream the T-DNA insertion were used for the amplification. In row # 2 primers specific for the gene, one matching upstream and the other one downstream the T-DNA insertion, were used for the amplification. All mutants resulted to be homozygous for the T-DNA insertion, while the WT plants were either heterozygous for the T-DNA insertion or without any insertion. c) The *At2g38130* gene is disrupted by the insertion of the 5.8 Kb *AC106* in the third intron. The T-DNA insertion is not drawn to scale. Lower case letters indicate plant DNA sequence flanking the T-DNA. d) Northern analysis of the *At2g38130* transcript in mutant and WT plants. 30 μ g samples of total RNA were analysed using as probe a fragment of *At2g38130* cDNA. To control for RNA loading, the blot was re-probed with a cDNA fragment derived from the *APT1* gene, which is expressed at a low level in all tissues of *Arabidopsis* (Moffat et al., 1994).

The wild-type phenotype could be fully restored by *Agrobacterium tumefaciens* mediated transformation of *pam21* plants with the *At2g38130* genomic DNA together with 1 Kb of the native promoter region. In all of the transformants effective quantum yield of PSII (Φ_{II}), pigmentation and growth behaviour did not differ from wild-type plants. Moreover, in the transformant progenies the wild-type phenotype segregated with the transgene (Figure 6.7).

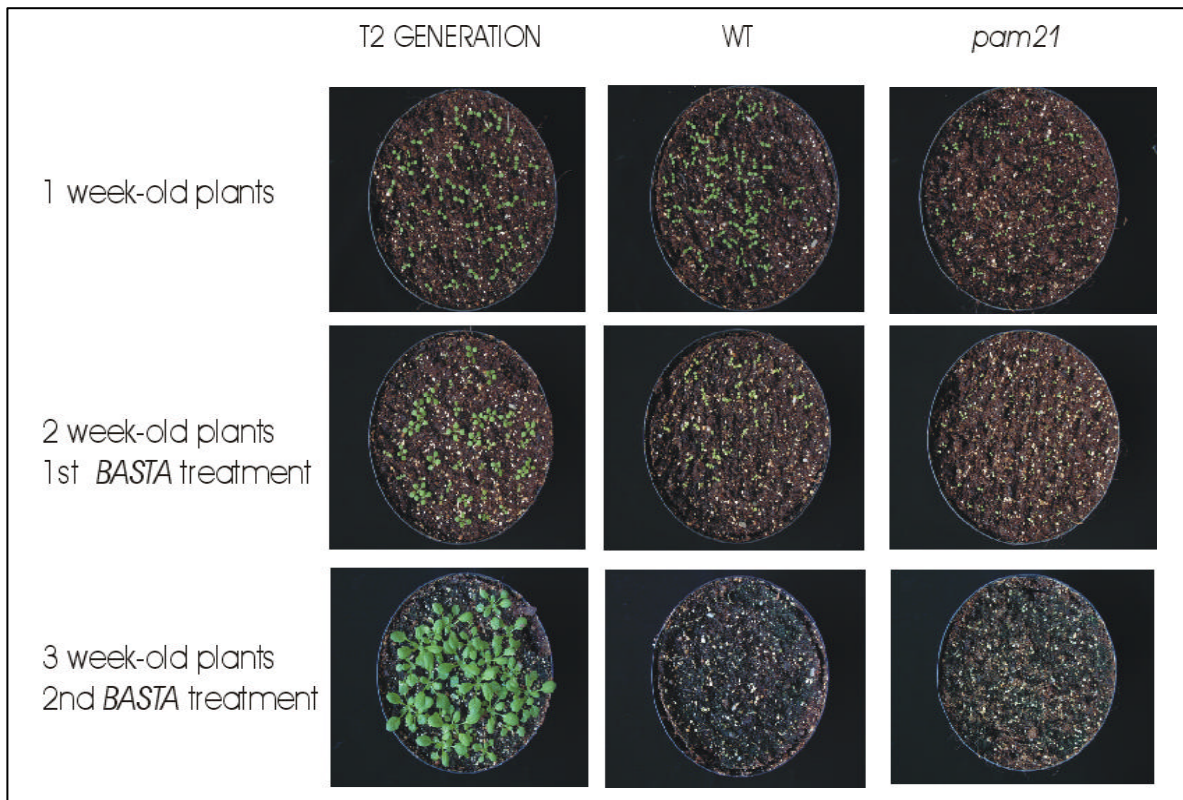


Figure 6.7 Complementation test. Mutant plants were transformed with *At2g38130* genomic DNA together with the native promoter ligated into the plant expression vector pP001-VS. Transgenic plants were selected on the basis of their resistance to *BASTA* herbicide. Successful complementation was tested in T2 generation by measurements of chlorophyll fluorescence and growth.

Database searches of the completely sequenced *Arabidopsis* genome revealed that *At2g38130* is a single-copy gene. The predicted coding region is entirely covered by overlapping ESTs. The encoded protein of 190 amino acid residues shares sequence homology with two dozens of eukaryotic proteins belonging to *Metazoa*, *Mycetozoa*, *Euglenozoa* and *Fungi*, including the yeast *N*-terminal acetyltransferases Ard1p, Nat3p and Mak3p, as well as five archaeobacterial protein sequences (Figure 6.8). *At2g38130* was most homologous to a human protein (60/68%), two *Drosophila* proteins (60/66% and 55/62%, respectively), Mak3p of *S. cerevisiae* (52/62% identity/similarity), a protein of *S. pombe*

(50/63%), and a *C. elegans* protein (48/59%) (Figure 6.9). All four domains indicative for *N*-acetyltransferases (Neuwald and Landsman, 1997) are present in *At2g38130*. Positions at which in *S. cerevisiae* point mutations abolish Mak3p function (Tercero et al., 1992) are strictly conserved in all proteins considered in Figure 6.8.

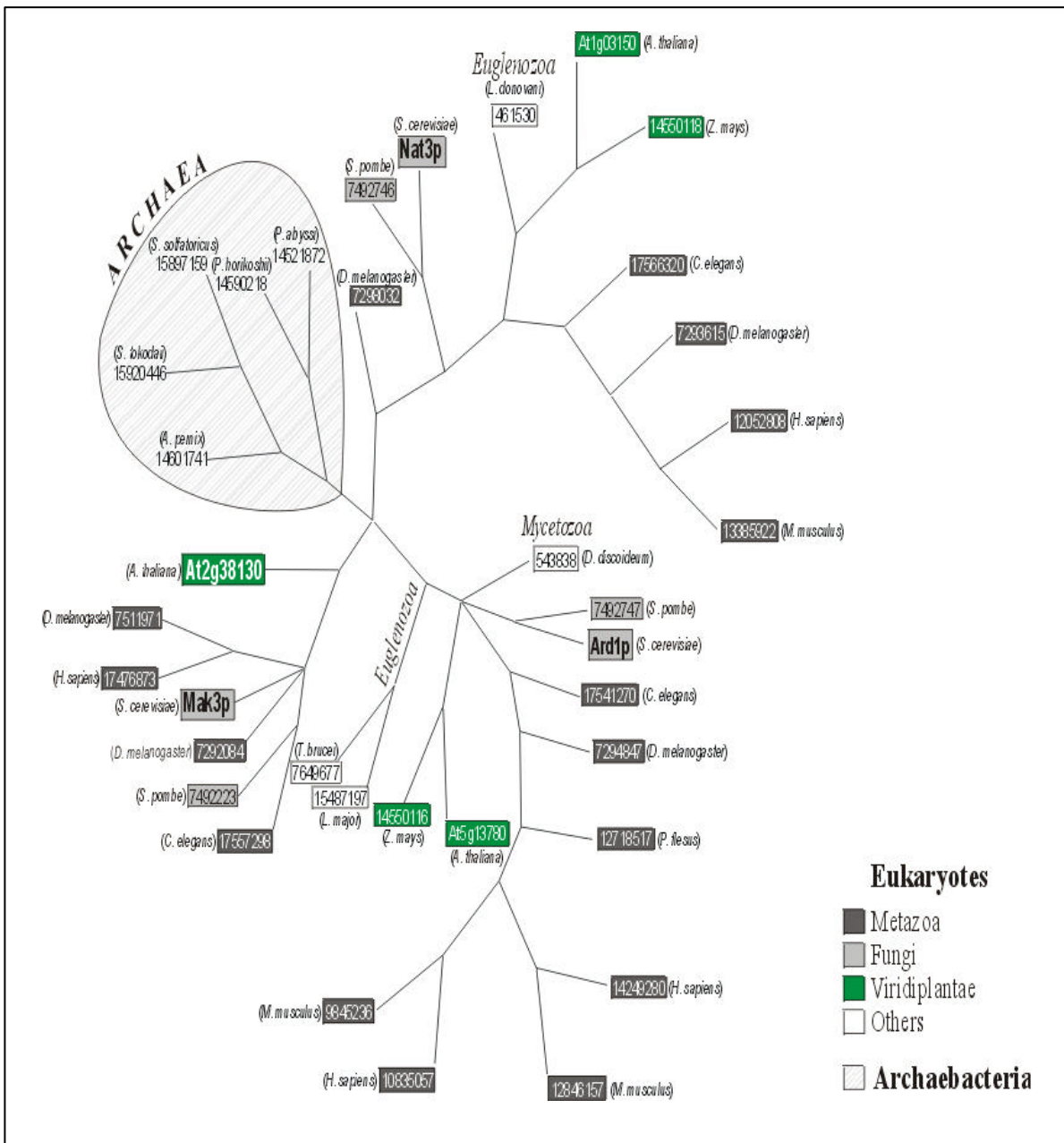


Figure 6.8 Phylogenetic tree of homologues of *At2g38130* based on distance-matrix phylogeny calculations. Protein GI accession numbers are provided with the exception of the *A. thaliana* proteins, for which the MIPS-code (<http://mips.gsf.de/proj/thal/db/index.html>) is given. The archaeobacterial clade is highlighted by grey hatching, while GIs of eukaryotic sequences are indicated by different colours or backgrounds: metazoans, white on grey background; fungi, black on a grey background; flowering plants, white on a green background, and mycetozoa or euglenozoa are indicated by boxes without filling. The tree is unrooted.

7292084	(<i>D. melanogaster</i>)	MSGKRTRSFKCAVHHRDREVCSSENFQVLVNEPPLFRKMVHAVAMEILPEERDRKYYADR 60 YTCCPPFFFIILVTLVELGFFVYHSVVTGEAAPRGPIPSDSMF IYRDKRHEIWRFLFYM 120
7511971	(<i>D. melanogaster</i>)	-----MADAQAAAAGKKYKNNKNSAEKNPNHNPNS SGQVFAQTPSNG 43
7292084	(<i>D. melanogaster</i>)	VLHAGWLHLGFNVAVQLVFLGPLLEMHVHGSTRACIYFSGVLAGSLGTSIFDPLVFLVGAS 180
7511971	(<i>D. melanogaster</i>)	HVQHQQEEEBATEDQEPACELRGLLKKMHL CNGHGHKEQEARPLGEVNVNCHAHGHSNNNHHR 103
7292084	(<i>D. melanogaster</i>)	GGVYALLAAHLAVLLN YHQMRVYGV LKLLHLILVVFVSD FGFAYARYA GDELQLGSSSEF 240
7511971	(<i>D. melanogaster</i>)	CTSGSSNNNNSTHNNNSVDSNNNRKQRREGGDCGSDSN SLKPEEKPITATSKTTANLH 163
7292084	(<i>D. melanogaster</i>)	LAIDQAEATAGAVSYVAHL AGAIAGLTIGLLV KSFEOQLHEQLVWIAH GTYLALVVFVFI 300
17557298	(<i>C. elegans</i>)	-----LATGVQKKTSTPDLVGTQEPEINLEKTIIG 29
AT2g38130	(<i>A. thaliana</i>)	-----MEKEMEDKLE 10
7511971	(<i>D. melanogaster</i>)	PTTTTDPKPKVSELVAVEQCVHVA TGSCHSREQERKQPSDYAEGATPILTAQLQLPEPA 223
7292084	(<i>D. melanogaster</i>)	AFNIMNGFAMFNIRVEKIRVTEIFENFOELSDKDSQEKMDLVTKNLPFAEKIVLPEND 360
17557298	(<i>C. elegans</i>)	TLRRCLQIAGT ENKPGSRSAKNSISEESNDLIMEESVPEASKWPHCOHMI SODEAPRNDE 89
AT2g38130	(<i>A. thaliana</i>)	-----C-----+ FDEGELEYSYAGEHHLP-----LIMS LVDQELSEPYSIF 45
Mak3p	(<i>S. cerevisiae</i>)	---MEIVYKPLDIRNEEQ-----FASIKKLLDADLSEPYSIY 34
7492223	(<i>S. pombe</i>)	-----MVLIVPYSHOY-----LKDILCOLIQKDLSEPYSKY 30
7511971	(<i>D. melanogaster</i>)	ISADEIVYKEYEAEHQHVVSTSKYDQVVRTVNTYLIPRISNTQDIMRLIQAEELSEPYSIY 283
7292084	(<i>D. melanogaster</i>)	TAAKSEGTIFQVPHDESQ-----LKVLMCLIDKELSEPYSIY 397
17557298	(<i>C. elegans</i>)	LASPNTRIVAVKDESQIN-----DIMRLITKDLSEPYSIY 124
AT2g38130	(<i>A. thaliana</i>)	-----D-----+-----A-----+ TYRYFVNLWPQLCFLEHFKG----KOVCTIVCKMGDHRQTER-GYIAMLVVIKPYRGRG 99
Mak3p	(<i>S. cerevisiae</i>)	VYRYFLNWPETLYTAVDNKSGTENIPGCCIVCKMDPHRNVLRGYIGMLAVESTYRCHG 94
7492223	(<i>S. pombe</i>)	VYRYFVHWPPESEFVALDNDNR----FTGAVICKQDVHRGTTLRGYIAMLAVKEYRKG 85
7511971	(<i>D. melanogaster</i>)	TYRYFTYNWPKLCEFLASHDN-----CYVGATVCKLDMHVNVRG-GYIAMLAVRKEYRKLK 337
7292084	(<i>D. melanogaster</i>)	TYRYFVNLWNPDLCEFLALD GDR----YVGVIVCKLEAKRDGYLGYIAMLAVDAEYRKRK 452
17557298	(<i>C. elegans</i>)	TYRYFLHNWPEVCFEFLAVDCTN----NTYTGAVLCKLELDYMGRCRKYIAMLAVDESRRIG 181
17476873	(<i>H. sapiens</i>)	-----LVGE-----EQVGATVCKLDMHVKVFRGYIAMLAVDSKYRNRG 39
AT2g38130	(<i>A. thaliana</i>)	-----A-----+-----B-----+-----+-----+ IASSELVTRAIKAMMESGCEVITLBAEVSNK GALALYGRLLGFIRAKRLYHYYLNGMDAFRL 159
Mak3p	(<i>S. cerevisiae</i>)	IATKLVETLADKMGREH CDEITMLETEVENS AALNLYEGMGFIRKRMFRYYLNEGDAFRL 154
7492223	(<i>S. pombe</i>)	IATKLTQASLDVMKNRCAQETVLETEVDNEAAMSFYBRLGFORVKRLVRYYLNGIDAFRY 145
7511971	(<i>D. melanogaster</i>)	IGTTLVTKATEAMLADNADEVVLETEVRNQPALRLYENLGFVRDKRLFRYYLNGVDALRL 397
7292084	(<i>D. melanogaster</i>)	IGRALSEMALDAMAIRDAAMTVLETELSNKPALALYCSLGFIRERRFLRYYLNGMDAFHL 512
17557298	(<i>C. elegans</i>)	IGTRLVRRALDAMCSKGCDEVVLETEVSNKNAORLYSNLGFIRQKRLKYYLNGDAFRL 241
17476873	(<i>H. sapiens</i>)	IGTNLVKKAATYAMVEGDCDEVVLETEITNKSAKLYENLGFVRDKRLFRYYLNGVDALRL 99
AT2g38130	(<i>A. thaliana</i>)	KLLFPKBRVPOIPSOVCTQOEYETFP RPRVP----- 190
Mak3p	(<i>S. cerevisiae</i>)	ILPLTERSCIRSTFLMHGRLAT----- 176
7492223	(<i>S. pombe</i>)	ILVLPN----- 150
7511971	(<i>D. melanogaster</i>)	KLWLR----- 402
7292084	(<i>D. melanogaster</i>)	KLMLHDFIDSSLNEV----- 527
17557298	(<i>C. elegans</i>)	KLIFTSRRVRSLNNOENYQPRCRVNEDDTPDEEGTY 278
17476873	(<i>H. sapiens</i>)	KLWLR----- 104

Figure 6.9. Comparison of Mak3p-like sequences from eukaryotes. The amino acid sequence of the At2g38130 protein was compared with orthologous sequences from *S. cerevisiae* (Mak3p), *S. pombe* (GI: 7492223), *D. melanogaster* (GI: 7511971; GI: 7292084), *C. elegans* (GI: 17557298), and *H. sapiens* (GI: 17476873). Black boxes indicate strictly conserved amino acids; grey boxes closely related amino acids. The symbol '+' refers to positions of point mutations that abolish Mak3p function (Tercero et al., 1992). Conserved sequence stretches (motifs A to D) which are involved presumably in the binding of acetyl-CoA are indicated according to Neuwald and Landsman, (1997).

6.5 THE *At2g38130* PROTEIN IS LOCATED IN THE CYTOSOL AND CAN FUNCTIONALLY REPLACE Mak3p IN YEAST

The *At2g38130* protein sequence did not show any recognisable transit peptide for the import into chloroplasts or mitochondria suggesting that the protein is located in the cytosol. In order to verify that, *At2g38130* was fused with the red fluorescence protein (RFP) from reef corals and the construct was used to transfect tobacco protoplasts (see Materials and Methods: chapter 2.13). Cells harbouring the *At2g38130*-RFP fusion protein showed readily detectable red fluorescence with a cytosolic distribution (Figure 6.10a-b), thereby confirming the cytosolic localisation of *At2g38130* protein. As a control, tobacco protoplasts were transfected with RFP and the reporter protein could be localised in the cytosol and due to its small size also in the nucleus (Figure 6.10c-d).

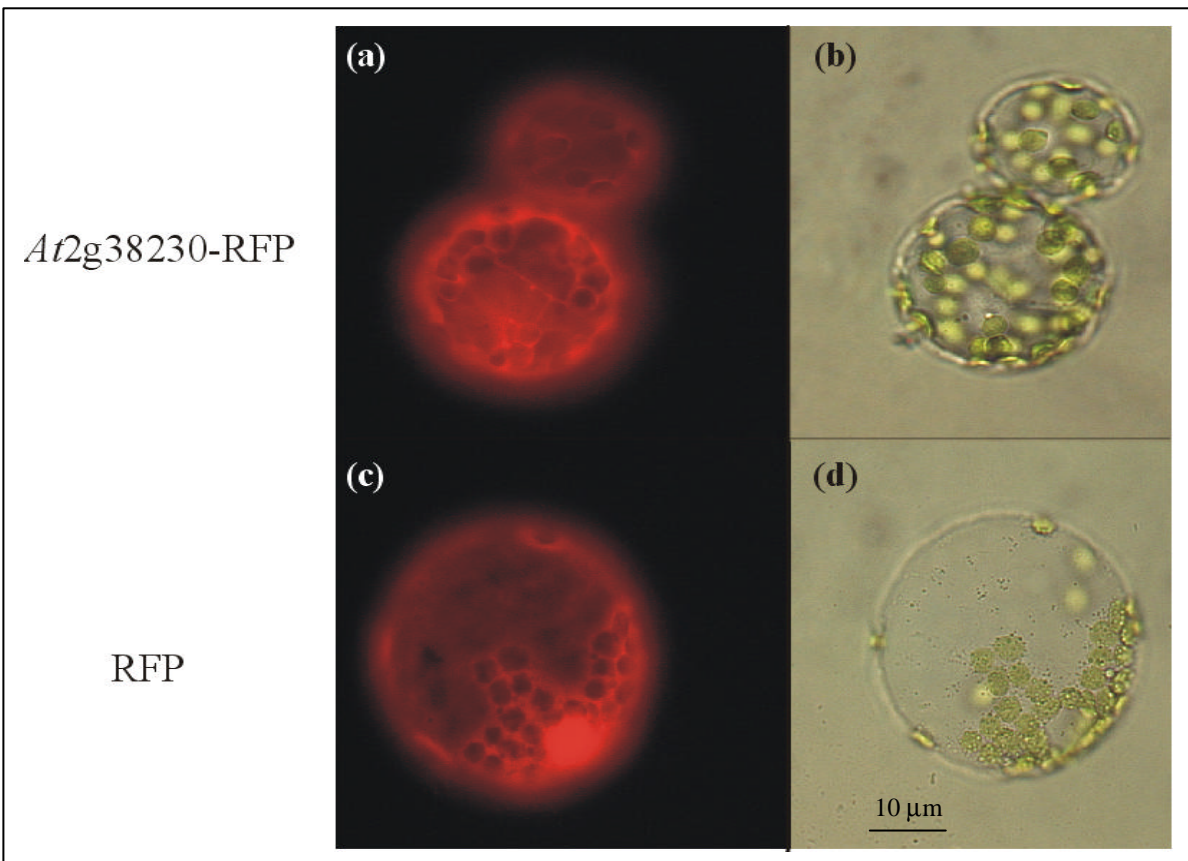


Figure 6.10 Fluorescence microscopy of mesophyll tobacco protoplasts (SR1) transfected with the *At2g38230*-RFP fusion protein (a) or with the red fluorescence protein (RFP) (c). Bright field (b-d) are presented as references for the different optical section being viewed. Scale bar, 10 μm.

The high sequence homology between *At2g38130* protein and Mak3p from *S. cerevisiae* indicated a similar function for the two proteins. In order to verify that, a yeast strain defective for Mak3p activity (*mak3-1*) was transformed with the pH7 expression vector (Edskes et al., 1999) carrying the cDNA of *At2g38130* gene under control of the ADH1 promoter, and then tested for its capacity to propagate the L-A-HN, M₁ dsRNA virus (see Materials and Methods: chapter 2.8). The virus killer assay (Figure 6.11) showed that the yeast strain, harbouring the *Arabidopsis* gene (*mak3-1/pAtMAK3*) behaved like the wild-type yeast strain (*mak3-1/pScMAK3*): killing zones (white circles) were present around the yeast colonies, proving that the *At2g38130* protein is an *N*-terminal acetyltransferase enzyme orthologous of yeast Mak3p. Because the *PAM21* locus corresponds to the *At2g38130* gene that encodes the *Arabidopsis* orthologue of Mak3p, the *At2g38130* protein was called AtMAK3 and the *pam21* mutant was renamed *atmak3-1*.

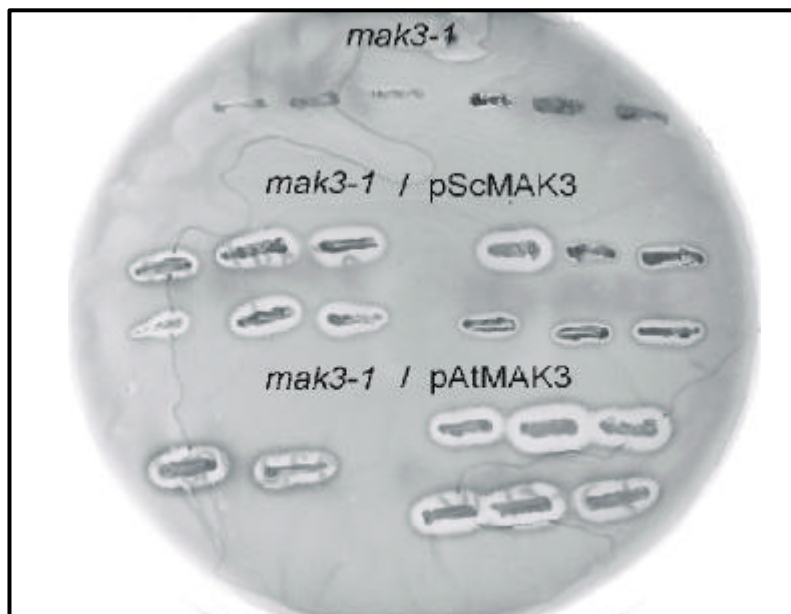


Figure 6.11 Yeast complementation test. The mutant yeast strain *mak3-1* was transformed with the *Saccharomyces cerevisiae* *MAK3* gene (*mak3-1/pScMAK3*) and with the *Arabidopsis* orthologue of *MAK3* (*mak3-1/pAtMAK3*). After cytoduction (Ridley et al., 1984), the three yeast strains were tested for their capacity to propagate the L-A-HN M₁ dsRNA virus. The *mak3-1/pScMAK3* strain and the strain carrying the *At2g38130* gene (*mak3-1/pAtMAK3*) were able to propagate the virus as shown by the presence of the killing zones (white circles) surrounding the yeast colonies

6.6 *At*MAK3 INTERACTS WITH THE *ARABIDOPSIS* ORTHOLOGUE OF Mak10p

The yeast Mak3p protein forms with Mak10p and Mak31p the *N*-terminal acetyltransferase C complex (NatC complex) (Polevodova and Sherman, 2001). In particular, a proteome-wide analysis of protein-protein interactions in *S. cerevisiae* showed that Mak3p interacts with Mak10p, and that Mak31p can interact with Mak10p (Uetz et al., 2000). Moreover, the Mak3p-Mak10p-Mak31p trimeric complex was isolated by using a tandem affinity purification method (Rigaout et al., 1999).

In order to investigate whether the NatC complex exists also in *Arabidopsis*, orthologues of Mak10p and Mak31p were searched within the *Arabidopsis* protein database. The yeast Mak10p amino acid sequence showed 35% similarity with the *Arabidopsis At2g11000* protein (Figure 6.12a), an unknown protein having a domain similar to the lipid attachment site of prokaryotic membrane lipoproteins. The yeast Mak31p had 52% similarity with two *Arabidopsis* snRNP Sm-like proteins, *At3g11500* and *At2g23930* sharing 99% of identity (Figure 6.12b). The Sm-like proteins (spliceosomal-like proteins) are small nuclear ribonucleoproteins (snRNP) involved in various functions including pre-mRNA splicing, tRNA processing, rRNA maturation, telomeric DNA synthesis. However, the *At3g11500* and *At2g23930* proteins lacked a glycine or cysteine at position 107, as numbered according to the alignment of Sm domains, which is present in all the other members of the Sm protein family (Seraphin, 1995). Moreover, Mak31p did not precipitate any of the tested RNAs (Seraphin, 1995), indicating that Mak31p and its *Arabidopsis* orthologues do not belong to the Sm-like protein family.

Subsequently, the existence of interactions among *At*MAK3, *At2g11000* and *At3g11500* were tested by two hybrid assays (see Materials and Methods: chapter 2.9). The *At*MAK3 fused to the GAL4 DNA binding domain was expressed in yeast together with the *At2g11000* protein fused to the GAL4 activation domain. Yeast cells were able to grow very robustly in medium lacking histidine and adenine and they became blue in the *LacZ* test indicating that *At*MAK3 and *At2g11000* interact (Figure 6.13a). However, no interaction could be observed between *At3g11500* and *At2g11000* (Figure 6.13b) and between *At*MAK3 and *At3g11500* (Figure 6.13c).

(a)

Mak10p YEAST	-----MEVDSILGSLSTITDDFDQLVDVLSLFDDELCSKTKPEALVKDPRDL	46
At2g11000	MQSVREDEDSSSPIHHSKTSSTSSIPSGDNNSVWADVLPILLSAACSDIQEGELINGDNENL	60
Mak10p YEAST	EEGTHSLEVNNSKIDS--SLIELTAEIEIEFDVN----VAYDPPIASVAALADRIILRCV	98
At2g11000	EAAMSALEIMDPKMDSGMVSIFYSIDAEIESGFAPVPISSDSTVNVQSIIDIMDHLLAGE	120
Mak10p YEAST	ISWLNQYQTLPTTVLSGRYTESLLS SLVKGTAGS SWCTGNILYDKVIGSCILGVCYLTK	158
At2g11000	ATWHMG-HSLACTVFSCLIVLRLPER--TSSQALLHSYCRVIRATCRVAVSVVSDARTNEE	177
Mak10p YEAST	FVQKLSAAGIVSEEBELNFNNGFNTEFDNLPGQDVVINSLETSLQITPEAYSDDSLHLTMI	218
At2g11000	EDLFTMYGLPESGEBDAKGLILLNAVEETICRQLRACKAIDRRRMLEDAELEPLQSNPHL	237
Mak10p YEAST	KH-ILKILICLVHLEDLIT-----DYSTKTSHEDELLENANSVNGIFPOLQIS	265
At2g11000	EESFCRSLICRIRFRKIFLHALNCMRRPQGRGLELARKHIGYCHISELDSVLDSAEFLRID	297
Mak10p YEAST	PPKGFSTYIQKHRSNQFPFRKIKITKLPDYSGFITLANDVKTIILLVDKAEESAEITYQFAK	325
At2g11000	IFENGVNEIEESTTASGRSPIGFDPTLNKRLSAPTPPRAIKLISWKKAIDYYVLLHNLND	357
Mak10p YEAST	FFNKLEQRHVVARILFFIFFIRDDRTVLGKFSYTOFVLLHVKEFS--AQTPSEFESSIGN	383
At2g11000	KICAFSLEPDEAVLEFVIQFQKSRPDIVARAHLQLLLVQDGKLYGRDTFLICARSLAL	417
Mak10p YEAST	EIIQESSNMLLEWYQNCSONTCRYRQGFNRQLLWDSLQAQFESVNSQVYCSWTYFMKLS	443
At2g11000	DVSKNHGLHTNEYILQLNQMGIAVGQMMQODTSRSSKNGDKSLILLNHLYG-GLEEQINW	476
Mak10p YEAST	SMIEFSIKGFDLDIYKFEFAYSMFWYVYVLSHHLETFLKDSQNDIESNIMAIHSMNKKLK	503
At2g11000	VAIRFLMLGFDLDLYSESEYCMVYVYVYII---LWKLAERARFRVLIVVNTTEERKAKENK	476
Mak10p YEAST	KLKAGEKQDQLRLKRFAMDNEMEQLQATKQFLNYLLKEINITKSLCLIEVFQFAILKSF	563
At2g11000	EYSRDMAREDRISLWVLFKQCOTCLAQGLTVMIAALRNEGMSLK-----	577
Mak10p YEAST	GLIDNKNSIPSKFSNBRLIHNRKPFNSIGVPELPEYEVFQQILKDFVIEKGAAFDIK	623
At2g11000	-----SQGFENTENKFIQHFELLOKASLPEYDAYESEFSKSTSHARLD-----	620
Mak10p YEAST	LERATNFIETERNVSSIDETMQGIRGCDNNGVLVTGTRLVQELSIEYYCKIKHTSKAL	683
At2g11000	-----YLPVYEFHDAQKIAKDKVVCYAN-----DPDKIAEVTGTEKVAERN	662
Mak10p YEAST	SVNSKIVIVNTLKKNKKNKDSIEYKVELVHTTEGWNVSPIQTRIKQDRYK	733
At2g11000	IVAVNIFCQDRSLKVSFEFTIHP-----YEATAVVRSS-----	695

(b)

Mak31p YEAST	----MDILKLSDFIGNTLIVSITEDRILVGSIVAVDAQMNLLDHVEERMSSSRM-MGLIV	55
At3g11500	MRSRGQPPDLKKYMDKKLQIKINANRMVVGITRGFDQFMNLVVDNTVEVNGDDKTDICMV	60
At2g23930	MRSRGQPPDLKKYMDKKLQIKINANRMVVGITRGFDQFMNLVVDNTVEVNGNDKTDICMV	60
Mak31p YEAST	SVPRRSVKTIIMIDKPVLQELTANKVELMANIV	87
At3g11500	VIRGNSIVTVEALEPVGRS-----	79
At2g23930	VIRGNSIVTVEALEPVGRSS-----	80

Figure 6.12 Amino acid sequence comparison of yeast Mak10p (a) and yeast Mak31p (b) with orthologous sequences from *Arabidopsis thaliana*. Black boxes indicate strictly conserved amino acids; grey boxes closely related amino acids.

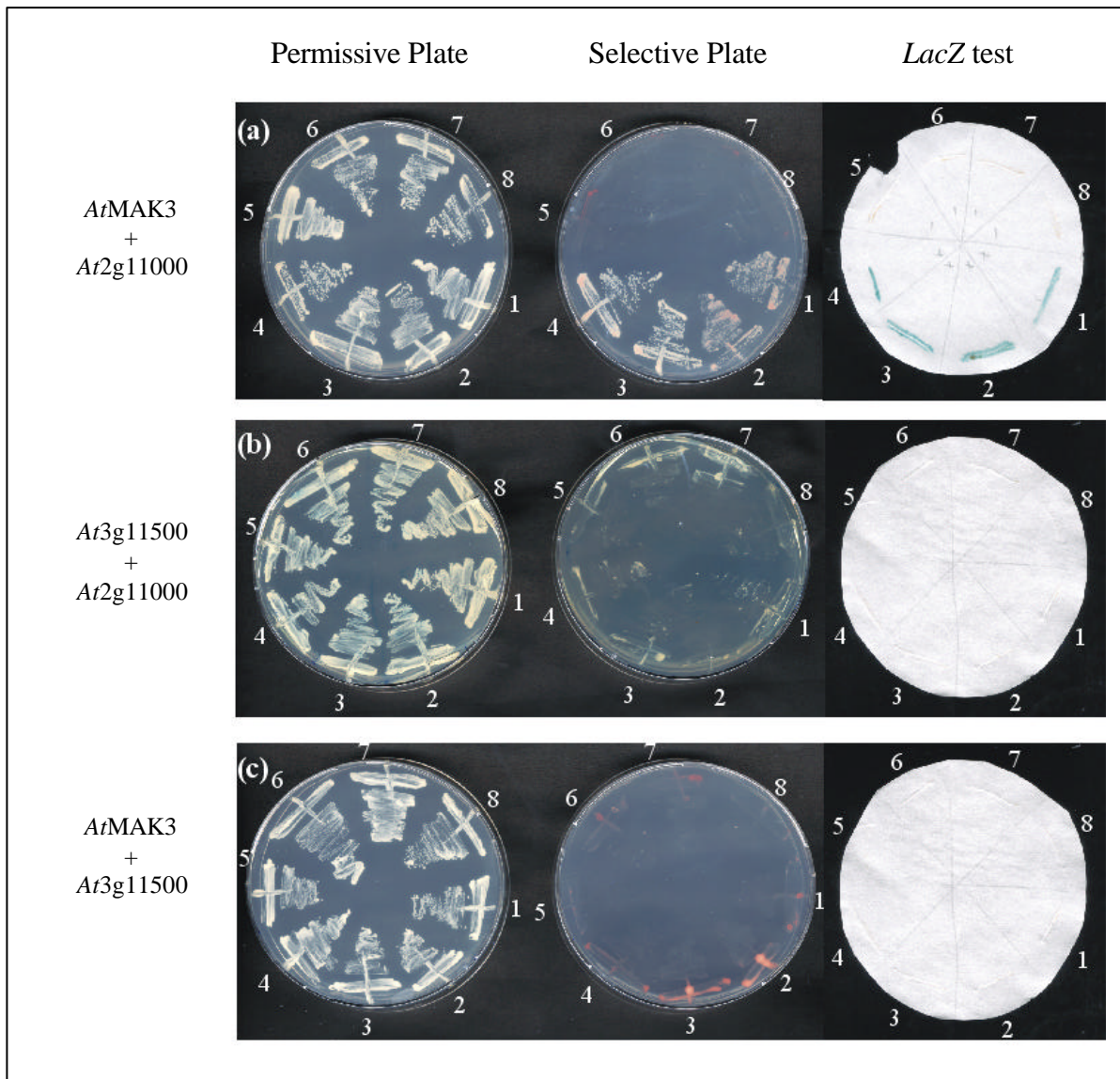


Figure 6.13 a) *AtMAK3* cloned into the pAS2-1 vector (bait vector) was tested for interaction with *At2g11000* cloned either into pGAD424 (1 and 2) or pGADT7 (3 and 4). Colonies 5, 6, 7, 8 are controls: #5 contains *AtMAK3*-pAS2-1 together with empty pGAD424; #6 contains empty pAS2-1 together with *At2g1100*-pGAD424; #7 contains *AtMAK3*-pAS2-1 together with empty pGADT7; #8 contains empty pAS2-1 together with *At2g1100*-pGADT7. b) *At3g11500* cloned into pAS2-1 vector (bait vector) was tested for interaction with *At2g11000* cloned either into pGAD424 (1 and 2) or pGADT7 (3 and 4). Colonies 5, 6, 7, 8 are controls: #5 contains *At3g11500*-pAS2-1 together with empty pGAD424; #6 contains empty pAS2-1 together with *At2g1100*-pGAD424; #7 contains *At3g11500*-pAS2-1 together with empty pGADT7; #8 contains empty pAS2-1 together with *At2g1100*-pGADT7. c) *AtMAK3* cloned into pAS2-1 vector (bait vector) was tested for interaction with *At3g11500* cloned either into pGAD424 (1 and 2) or pGADT7 (3 and 4). Colonies 5, 6, 7, 8 are controls: #5 contains *AtMAK3*-pAS2-1 together with empty pGAD424; #6 contains empty pAS2-1 together with *At3g11500*-pGAD424; #7 contains *AtMAK3*-pAS2-1 together with empty pGADT7; #8 contains empty pAS2-1 together with *At3g11500*-pGADT7. The AH109 yeast strain carrying reporter genes involved in the biosynthesis of histidine and adenine was used to test growth on selective plates. The Y190 yeast strain carrying the *b*-galactosidase reporter gene was used in the *LacZ* test.

DISCUSSION

The *pam21* mutation is due to a T-DNA insertion in the third intron of the *At2g38230* gene. *At2g38230* mRNA could not be detected in the mutant and complementation of *pam21* with the *At2g38230* genomic DNA together with the native promoter resulted in the restoration of the wild-type phenotype. The *At2g38230* gene product is located in the cytosol as predicted and its amino acid sequence shows high similarity to proteins of *H. sapiens*, *Drosophila*, *C. elegans*, *S. pombe* and to the *N*-terminal acetyltransferase Mak3p of *S. cerevisiae*. Complementation of the yeast *mak3-1* strain with the *At2g38230* cDNA indicated that the *At2g38230* (*AtMAK3*) protein is a *N*-terminal acetyltransferase.

N-terminal acetyltransferases have been extensively described in yeast. In particular, *S. cerevisiae* contains three types of *N*-terminal acetyltransferases, designated as NatA, NatB and NatC each acetylating a different set of proteins with different *N*-terminal regions (Polevoda et al., 1999; Polevoda and Sherman, 2001). The NatC complex is a trimer, formed by the association of Mak10p, Mak31p and the catalytic subunit, Mak3p (Rigaut et al., 1999), and it is required for the *N*-terminal acetylation of the killer viral major coat protein, GAG, that has a mature Ac-Met-Leu-Arg-Phe terminus (Tercero and Wickner, 1992; Tercero et al., 1993). The absence of Mak3p in yeast mutant strains prevents the assembly and propagation of L-A-HN, M₁ dsRNA viral particles and reduces growth on media containing nonfermentable carbon sources, such as glycerol (Tercero et al., 1993).

In *Arabidopsis*, the disruption of the *AtMAK3* causes a complex phenotype: plants are slightly pale green, the growth rate is decreased and the photosynthetic performance is impaired. The altered phenotype is present only in young developing plants, while in 5-6 week-old plants photosynthesis and pigment content of leaves are identical to wild-type plants. Analyses of thylakoid polypeptide composition showed a reduced amount of PSI, PSII core and α - and β -subunits of ATPase, explaining the altered values of Fv/Fm and Φ_{II} observed in *atmak3-1* plants. In contrast, the *atpA* transcript amount increased in mutant plants, while the abundance of *psbA*, *psbC*, *psaB*, *atpB* mRNAs was unaltered. The *psaA* transcripts showed an increased amount of the 5.2 kb band in mutant plants together with a reduction in the abundance of the bands smaller than 2 kb, indicating an alteration in the mRNA maturation process. A similar alteration could be also observed in the *psbB* transcripts where an increased amount of the 5.7 kb band was visible. Interestingly, the

altered maturation of the *psbB* transcripts was also present in the *prpl11-1* mutant affected in the chloroplast translation (see Chapter 4).

Taken together, the data indicate that the altered photosynthetic phenotype of *atmak3-1* plants is caused by a post-transcriptional defect such as mRNA maturation, reduced protein synthesis or increased protein degradation. To clarify this aspect, *in vivo* translation assays were performed and a drastic reduction of labelled D1 and CP47 subunits could be observed in mutant plants while CP43 and most of the other thylakoid subunits were present at wild-type levels. The concomitant reduction of D1 and CP47 synthesis is a well-known phenomenon termed control by epistasy of protein synthesis (CES) (Choquet and Vallon, 2000). In particular, it has been reported that the translation rate of CP47 is regulated according to the amount of D1 in order to prevent accumulation of antenna proteins not directly associated with the PSII reaction center (de Vitry et al., 1989). The possibility that a defect in D1 synthesis in *atmak3-1* could reduce the synthesis of CP47 was supported by polysome association analysis. Indeed, the *psbA* transcripts of mutant plants migrated in a larger amount with the heavier polysome particles indicating a defect during the translation elongation. Contrarily, the *psbB* transcripts were associated with lighter polysome particles, most probably due to the down-regulation of translation initiation. Moreover, the translation rate of PsaA, PsaB, and α - and β -subunits of ATPase was not altered in mutant plants, indicating that the reduced amount of these polypeptides observed by densitometric and immunoblot analyses had to be attributed to an increased degradation. Although the defect in D1 and CP47 protein translation can easily explain the altered photosynthetic performances of *atmak3-1*, it is more difficult to understand how the absence of a cytosolic *N*-terminal acetyltransferase can affect photosynthesis. The possibility that the altered photosynthetic phenotype observed in *atmak3-1* plants is a secondary effect of a major alteration in mitochondria has to be considered. Indeed, Tercero et al. (1993) suggested that the reduced growth of *mak3-1* yeast strain on glycerol medium had to be attributed to the lack of *N*-terminal acetylation of the mitochondrial proteins kdg1p (α -ketoglutarate dehydrogenase), Fum1p (fumarate hydratase), and Mrp1p (a mitochondrial ribosomal protein) that all contain Met-Leu-Arg-Phe termini, similar to GAG protein. However, the only way to explain the altered photosynthetic phenotype is to identify proteins acetylated by AtMAK3. For this purpose, the *N*-terminal sequences of proteins acetylated by NatC in

yeast could be a useful tool to identify possible targets in *Arabidopsis*. Additionally, the isolation of proteins from wild-type and *atmak3-1* leaves labelled with [C^{14}]acetate is certainly another strategy to consider in order to identify the targets of acetylation and therefore to clarify the role of *AtMAK3*.

SUMMARY

Photosynthesis enables life on earth by producing organic materials to the biosphere. Although the photosynthetic process has been extensively studied, many aspects still remain to be clarified. The isolation of photosynthetic mutants and the identification of the affected genes are important steps to increase the knowledge of this process. In this thesis, photosynthetic mutants were isolated, based on their altered values of photosystem II effective quantum yield (Φ_{II}). During the screening of more than 2000 insertion tagged lines, 18 *photosynthesis affected mutants* (*pam*) have been identified, and for five of them the disrupted genes were isolated. The corresponding genes are involved in different levels of chloroplast functions, including chloroplast translation (*pam14/prpl11-1* and *pam15/PROLYL tRNA SYNTHETASE*), thylakoid electron transport (*pam4/psae1-1*), heme biosynthesis (*pam20/hy1*) and co-translational protein modification (*pam21/atmak3-1*). Three of the mutants were characterised in detail at the molecular and physiological level. The *prpl11-1* mutant was disrupted in the gene coding for the L11 subunit of chloroplast ribosomes. The complete absence of this protein did not affect the ribosome stability and polysome assembly, however a drastic reduction of the chloroplast translation rate could be observed. The *psae1-1* mutant showed a marked decrease in the levels of E subunit of photosystem I (PSI). Electron transport measurements indicated that the E subunit is essential for the electron flow through PSI. Moreover, the almost complete absence of PsaeE drastically inhibits photosynthetic state transitions. In particular, a permanent phosphorylation of a fraction of light harvesting complex of photosystem II (LHCII), together with the formation of a stable complex between phosphorylated LHCII and PSI, was observed. In fact, this is the first time that such a complex could be isolated. *atmak3-1* was the only mutant isolated in this thesis, which was affected in a protein located in the cytosol. The disrupted gene encodes an orthologue of the *S. cerevisiae* N-terminal acetyltransferase Mak3p, and causes a drastic reduction of the translation rate of D1 and CP47. Complementation analysis revealed that *AtMAK3* can functionally replace the yeast protein. Moreover, the *AtMAK3* interacts with the *Arabidopsis* orthologue of the yeast Mak10p in two hybrid experiments, implying that a yeast NatC-like complex also operates in higher plants.

ZUSAMMENFASSUNG

Photosynthese ermöglicht das Leben auf der Erde durch die Produktion von organischem Material für die Biosphäre. Obwohl der photosynthetische Prozeß sehr genau studiert wurde, sind noch viele Aspekte zu klären. Die Isolierung photosynthetischer Mutanten und die Identifizierung der betroffenen Gene ist ein entscheidender Schritt das Wissen über die Kenntnis dieses Prozesses zu vergrößern. Im Rahmen dieser Arbeit wurden photosynthetische Mutanten, basierend auf ihren veränderten Werten für den Quantum-Ertrag von Photosystem II isoliert. Bei der Durchmusterung von mehr als 2000 Insertions-markierten Linien (insertion-tagged lines) wurden 18 *Photosynthese betroffene Mutanten* (*pam*) identifiziert. Für fünf von diesem wurden die unterbrochenen Gene isoliert. Die korrespondierenden Gene sind auf verschiedenen Niveaus plastidärer Funktionen involviert, einschließlich Chloroplasten-Translation (*pam14/prpl11-1* und *pam15/PROLYL tRNA SYNTHETASE*), thylakoidärem Elektronentransport (*pam4/psae1-1*), Häm-Biosynthese (*pam20/hy1*) and co-translationaler Proteinmodifikation (*pam21/atmak3-1*). Drei dieser Mutanten wurden im Detail auf molekularer und physiologischer Ebene untersucht. Die *prpl11-1* Mutante hat eine Insertion im Gen für die L11-Untereinheit von Chloroplasten-Ribosomen. Das gänzliche Fehlen dieses Proteins beeinträchtigt die Ribosomen-Stabilität und das Polysomen-"assembly" nicht. Es ließ sich jedoch eine drastische Reduktion der Chloroplasten-Translationsrate beobachten. Die *psae1-1* Mutanten zeigte eine deutliche Abnahme in der Menge der E Untereinheit von Photosystem I (PSI). Messungen des Elektronentransports zeigten, daß die E-Untereinheit essentiell für die Elektronenfluß durch PSI ist. Außerdem inhibiert die nahezu gänzliche Abwesenheit von PsaE drastisch die Transitionen des photosynthetischen Zustandes. Im Besonderen ließ sich eine permanente Phosphorylierung einer Fraktion des "light harvesting complex" von Photosystem II (LHCII) zusammen mit der Bildung eines stabilen Komplexes zwischen phosphoryliertem LHCII und PSI beobachten. Tatsächlich ist dies das erste Mal, daß ein solcher Komplex isoliert werden konnte. *atmak3-1* ist die einzige Mutante in dieser Arbeit, die durch ein im Cytosol lokalisiertes Protein beeinträchtigt wird. Das unterbrochene Gen kodiert ein Orthologes der *S.cerevisiae* N-terminalen Acetyltransferase Mak3p und verursacht eine drastische Reduktion der Translationsrate von D1 und CP47. Die Komplementationsanalyse zeigte, daß *AtMAK3* das Hefeprotein funktionell ersetzen kann. Außerdem interagiert

*At*MAK3 in 2-hybrid Experimenten mit dem Arabidopsis-Orthologen des Hefe Mak10p, was darauf hindeutet, daß der Hefe NatC-ähnliche Komplex auch in höheren Pflanzen arbeitet.

REFERENCES

A

- Albertsson P-A., The structure and function of the chloroplast photosynthetic membrane, a model for the domain organization, *Photosynth. Res.* 46 (1995) 141-149.
- Allen J.F., Protein phosphorylation in regulation of photosynthesis, *Biochim. Biophys. Acta* 1098 (1992a) 275-335.
- Allen J.F., How does protein phosphorylation regulate photosynthesis?, *Trends Biochem. Sci.* 17 (1992b) 12-17.
- Allen J.F. and Forsberg J., Molecular recognition in thylakoid structure and function, *Trends Plant Sci.* 6 (2001) 317-326.
- Anderson J.M., Photoregulation of the composition, function and structure of thylakoid membranes, *Annu. Rev. Plant Physiol.* 37 (1986) 93-136.

B

- Ban N., Nissen P., Hansen J., Capel M., Moore P.B. and Steitz T.A., Placement of protein and RNA structures into a 5 Å-resolution map of the 50S ribosomal subunit, *Nature* 400 (1999) 841-847.
- Barber J., Regulation of energy-transfer by cations and protein- phosphorylation in relation to thylakoid membrane organization, *Photosynth. Res.* 10 (1986) 243-253.
- Barkan A., Nuclear mutants of maize with defects in chloroplast polysome assembly have altered chloroplast RNA metabolism, *Plant Cell* 5 (1993) 389-402.
- Barkan A., Approaches to investigating nuclear genes that function in chloroplast biogenesis in land plants, *Meth. Enzimol* 297 (1998) 38-57.
- Bartel P.L., Chien C.T., Sterglanz R. and Fields S., Using the two-hybrid system to detect protein-protein interactions, In cellular interactions in Development: A Practical Approach ed. Hartley D.A. (Oxford University Press, Oxford) 153-179.
- Bassi R., dal Belin Peruffo A., Barbato R. and Ghisi R., Differences in chlorophyll-protein complexes and composition of polypeptides between thylakoids from bundle sheaths and mesophyll cells in maize, *Eur. J. Biochem.* 146 (1985) 589-595.

-
- Bassi R., Pineau B., Dainese P., and Marquardt J., Carotenoid-binding proteins of photosystem II, *Eur. J. Biochem.* 212 (1993) 297-303.
 - Bassi R. and Yamamoto H.Y., Carotenoids: localization and function in photosynthetic apparatus of higher plants, *In photosynthetic antenna systems*, Yocum C., ed. Springer-Verlag, Heidelberg (1995) 1-35.
 - Bauer J., Hiltbrunner A. and Kessler F., Molecular biology of chloroplast biogenesis: gene expression, protein import and intraorganellar sorting, *Cell. Mol. Life Sci.* 58 (2001) 420-433.
 - Bendall D.S., Photosynthetic cytochromes of oxygenic organisms, *Biochim. Biophys. Acta* 683 (1982) 119-151.
 - Bennett J., Protein phosphorylation in green plant chloroplast, *Annu. Rev. Plant. Physiol. Plant. Mol. Biol.* 42 (1991) 281-311.
 - Bennoun P. and Levine R.P., Detecting mutants that have impaired photosynthesis by their increased level of fluorescence, *Plant Physiol.* 42 (1967) 1284-1287.
 - Boekema E.J., Jensen P.E., Schlodder E., van Breemen J.F.L., van Roon H., Scheller H.V. and Dekker J.P., Green plant photosystem I binds light-harvesting complex I on one side of the complex, *Biochemistry* 40 (2001) 1029-1036.
 - Bruce B.D., Chloroplast transit peptides: structure, function and evolution, *Trends Cell Biol.* 10 (2000) 440-447.
 - Brutnell T.P., Sawers R.J., Mant A. and Langdale J.A., BUNDLE SHEATH DEFECTIVE2, a novel protein required for post-translational regulation of the *rbcl* gene of maize, *Plant Cell* 11 (1999) 849-864.
 - Burlacu-Miron S., Perrier V., Gilles A.M., Pistotnik E. and Craescu C.T., Structural and energetic factors of the increased thermal stability in a genetically engineered *Escherichia coli* adenylate kinase, *J. Biol. Chem.* 24 (1998) 19102-19107.

C

- Casazza A.P., Tarantino D. and Soave C., Preparation and functional characterization of thylakoids from *Arabidopsis thaliana*, *Photosynth. Res.* 68 (2001) 175-180.
- Choquet Y. and Vallon O., Synthesis, assembly and degradation of thylakoid membrane proteins, *Biochimie* 82 (2000) 615-634.
- Clayton R.K., Photosynthesis: Physical mechanisms and chemical patterns, Cambridge University Press, Cambridge, England (1980).

-
- Clough S.J. and Bent A.F., Floral dip: a simplified method for *Agrobacterium*-mediated transformation of *Arabidopsis thaliana*, *Plant J.* 16 (1998) 735-743.

D

- Davis S.J., Kurepa J., Vierstra R.D., The *Arabidopsis thaliana* *HY1* locus, required for phytochrome-chromophore biosynthesis, encodes a protein related to heme oxygenases, *Proc. Natl. Acad. Sci. USA* 96 (1999) 6541-6546.
- Demmig-Adams B. and Adams III W.W., Photoprotection and other responses of plants to high light stress, *Annu. Rev. Plant Physiol. Plant Mol. Biol.* 43 (1992) 599-626.
- Devereux J., Haeberli P. and Smithies O., A comprehensive set of sequence analysis programs for the VAX, *Nucleic Acids Res.* 12 (1984) 387-395.
- de Vitry C., Olive J., Drapier D., Recouvreur M. and Wollman F.A., Posttranslational events leading to the assembly of photosystem II protein complex: a study using photosynthesis mutant from *Chlamydomonas reinhardtii*, *J. Cell Biol.* 109 (1989) 991-1006.
- Douglas S.E., Plastid evolution: origins, diversity, trends, *Curr. Opin. Genet. Dev.* 8 (1998) 655-661.

E

- Edskes H.K., Gray V.T. and Wickner B.R., The (URE3) prion is an aggregated form of Ure2p that can be cured by overexpression of Ure2p fragments, *Proc. Natl. Acad. Sci.* 96 (1999) 1498-1503.
- Elich T.D., Edelman M. and Mattoo A.K., Evidence for light-dependent and light-independent protein dephosphorylation in chloroplasts, *FEBS Lett.* 411 (1997) 236-238.
- Emanuelsson O., Nielsen H., Brunak S. and von Heijne G., Predicting subcellular localization of proteins based on their *N*-terminal amino acid sequence, *J. Mol. Biol.* 300 (2000) 1005-1016.
- Expert-Bezançon A., Barritault D., Milet M. and Hayes D.H., Close proximity of *Escherichia coli* 50S subunit proteins L7/L12 and L10 and L11, *J. Mol. Biol.* 108 (1976) 781-787.

F

- Färber A., Young A.J., Ruban A.V., Horton P. and Jahns P., Dynamics of xanthophyll-cycle activity in different antenna subcomplexes in the photosynthetic membranes of higher plants: the relationship between zeaxanthin conversion and nonphotochemical fluorescence quenching, *Plant Physiol.* 115 (1997) 1609-1618.

-
- Forti G. and Elli G., The function of ascorbic acid in photosynthetic phosphorylation, *Plant Physiol.* 109 (1995) 1207-1211.
 - Frey M., Stettner C. and Gierl A., A general method for gene isolation in tagging approaches: Amplification of insertion mutagenised sites (AIMS), *Plant J.* 13 (1998) 717-721.
 - Fulgosi H., Vener A.V., Altschmied L., Herrmann R.G. and Andersson B., A novel multi-functional chloroplast protein: identification of a 40 kDa immunophilin-like protein located in the thylakoid lumen, *EMBO J.* 17 (1998) 1577-1587.

G

- Gal A., Zer H. and Ohad I., Redox-controlled thylakoid protein phosphorylation: news and views, *Physiol. Plant.* 100 (1997) 869-885.
- Genty B., Briantais J.M. and Baker N.R., The relationship between the quantum yield of photosynthetic electron-transport and quenching of chlorophyll fluorescence, *Biochim. Biophys. Acta* 990 (1989) 87-92.
- Ghanotakis D.F. and Yocum C.F., Photosystem II and the oxygen evolving complex, *Annu. Rev. Plant Phys.* 41 (1990) 255-276.
- Gietz D., St Jean A., Woods R.A. and Sciestl R.H., Improved method for high efficiency transformation of intact yeast cells, *Nucleic Acids Res.* 20 (1992) 1425.
- Gross E., Plastocyanin-structure and function, *Photosynth. Res.* 37 (1993) 103-116.

H

- Haehnel W., The reduction kinetics of chlorophyll a as an indicator for proton uptake between the light reactions in chloroplasts, *Biochim. Biophys. Acta* 440 (1976) 506-521.
- Haldrup A., Naver H. and Scheller H.V., The interaction between plastocyanin and photosystem I is inefficient in transgenic *Arabidopsis* plants lacking the PSI-N subunit of photosystem I, *Plant J.* 17 (1999) 689-698.
- Haldrup A., Simpson D.J. and Scheller H.V., Down-regulation of the PSI-F subunit of photosystem I in *Arabidopsis thaliana*. The PSI-F subunit is essential for photoautotrophic growth and antenna function, *J. Biol. Chem.* 275 (2000) 31211-31218.
- Hankamer B., Morris E., Nield J., Gerle C. and Barber J., Three-dimensional structure of the Photosystem II core dimer of higher plants determined by electron microscopy, *J. Struct. Biol.* 135 (2001) 262-269.
- Harper J.W., Adami G.R., Wie N., Keyomarsi K. and Elledge S.J., The p21 Cdk-interacting protein Cip1 is a potent inhibitor of G1 cyclin-dependent Kinases, *Cell* 75 (1993) 805-816.

- Hauska G., Riedel A. and Nitschke W., The Rieske FeS-centers of cytochrome B6F/BC1 complexes, *Photosynth. Res.* 34 (1992) 89-98.
- Hill R. and Bendall F., Function of the two cytochrome components in chloroplast: a working hypothesis, *Nature* 186 (1960) 136-137.
- Holzwarth A.R., Lehner H., Braslavsky S.E. and Schaffner K., Phytochrome models 2. Fluorescence of biliverdin dimethyl ester, *Liebigs Ann. Chem.* 12 (1978) 2002-2017.
- Horton P., Ruban A.V. and Walters R.G., Regulation of light harvesting in green plants, *Annu. Rev. Plant Physiol. Plant Mol. Biol.* 47 (1996) 655-684.

I

J

- Jach G., Binot E., Frings S., Luxa K. and Schell J., Use of the red fluorescent protein from *Discosoma* sp. (dsRED) as a reporter for plant gene expression, *Plant J.* 28 (2001) 483-491.
- James P., Halladay J. and Craig E.A., Genomic libraries and a host strain designed for highly efficient two-hybrid selection in yeast, *Genetics* 144 (1996) 1425-1436.
- Jensen P.E., Gilpin M., Knoetzel J. and Scheller H.V., The PSI-K subunit of photosystem I is involved in the interaction between light-harvesting complex I and the photosystem I reaction center core, *J. Biol. Chem.* 275 (2000) 24701-24708.
- Jensen P.E., Rosgaard L., Knoetzel J. and Scheller H.V., Photosystem I activity is increased in the absence of the PSI-G subunit, *J. Biol. Chem.* 277 (2002) 2798-2803.
- Joliot P. and Kok B., In "*Bioenergetics of photosynthesis*", Govindjee ed., Academic Press, New York (1975) 387-412.
- Joliot P. and Joliot A., Mechanism of proton-pumping in the cytochrome b/f complex, *Photosynth. Res.* 9 (1986) 113-124.

K

- Kenny J.W., Lambert J.M. and Traut R.R., Cross-linking of ribosomes using 2-iminothiolane (methyl 4-mercaptobutyrimidate) and identification of cross-linked proteins by diagonal polyacrylamide/sodium dodecyl sulfate gel electrophoresis, *Meth. Enzymol.* 59 (1979) 534-550.
- Klaff P. and Gruissem W., Changes in chloroplast mRNA stability during leaf development, *Plant Cell* 3 (1991) 517-529.

-
- Koncz C., Mayerhofer R., Koncz-Kalman Z., Nawrath C., Reiss B., Redei G.P. and Schell J., Isolation of a gene encoding a novel chloroplast protein by T-DNA tagging in *Arabidopsis thaliana*, *Embo J.* 9 (1990) 1337-1346.
 - Krause G.H. and Weis E., Chlorophyll fluorescence and photosynthesis: the basics, *Annu. Rev. Plant Physiol. Plant Mol. Biol.* 42 (1991) 313-349.
 - Krisan P.J., Young J.C. and Sussman M.R., T-DNA as an insertional mutagen in *Arabidopsis*, *Plant Cell* 11 (1999) 2283-2290.

L

- Leister D., Varotto C., Pesaresi P., Niwergall A. and Salamini F., Large-scale evaluation of plant growth in *Arabidopsis thaliana* by non-invasive image analysis, *Plant Physiol. Biochem.* 37 (1999) 671-678.
- Li T.Z., Lou S., Lin. M. and Kuang T., Organization of reaction center and internal and peripheral antennae chlorophyll-protein complexes of photosystem II, *Photobiochem. Photobiophys.* 11 (1986) 19-28.
- Li X.P., Bjorkman O., Shih C., Grossman A.R., Rosenquist M., Jansson S. and Niyogi K.K., A pigment-binding protein essential for regulation of photosynthetic light harvesting, *Nature* 403 (2000) 391-395.
- Lin X. et al., Sequence and analysis of chromosome 2 of the plant *Arabidopsis thaliana*, *Nature* 402 (1999) 761-768.
- Littlechild J., Dijk J. and Garrett R.A., The identification of new RNA-binding proteins in the *Escherichia coli* ribosome, *FEBS Lett.* 74 (1977) 292-294.
- Liu Y.G., Mitsukawa N., Oosumi T. and Whittier R.F., Efficient isolation and mapping of *Arabidopsis thaliana* T-DNA insert junctions by thermal asymmetric interlaced PCR, *Plant J.* 8 (1995) 457-463.
- Lunde C., Jensen P.E., Haldrup A., Knoetzel J. and Scheller H.V., The PSI-H subunit of photosystem I is essential for state transitions in plant photosynthesis, *Nature* 408 (2000) 613-615.

M

- Maliga P., Sz. -Bresnovits A., Marton L. and Joo F., Non-mendelian streptomycin-resistant tobacco mutant with altered chloroplasts and mitochondria, *Nature* 255 (1975) 401-402.
- Mans R.J. and Novelli G.D., Measurements of the incorporation of radioactive amino acids into protein by a filter-paper disk method, *Arch. Biochem. Biophys.* 94 (1961) 48-53.
- Mayer K. et al., Sequence and analysis of chromosome 4 of the plant *Arabidopsis thaliana*, *Nature* 402 (1999) 769-777.

-
- McElwain K.B., Boynton J.E. and Gillham N.V., A nuclear mutation conferring thiostrepton resistance in *Chlamydomonas reinhardtii* affects a chloroplast ribosomal protein related to *Escherichia coli* ribosomal protein L11, *Mol. Gen. Genet.* 241 (1993) 564-572.
 - Meinke D.W., Cherry J.M., Dean C., Rousley S.D. and Koornneff M., *Arabidopsis thaliana*: a model plant for genome analysis, *Science* 282 (1998) 662-665.
 - Meurer J., Meierhoff K. and Westhoff P., Isolation of high-chlorophyll-fluorescence mutants of *Arabidopsis thaliana* and their characterisation by spectroscopy, immunoblotting and northern hybridisation, *Planta* 198 (1996) 385-396.
 - Moffatt B.A., McWhinnie E.A., Agarwal S.K. and Schaff D.A., The adenine phosphoribosyltransferase-encoding gene of *Arabidopsis thaliana*, *Gene* 143 (1994) 211-216.
 - Morais F., Barber J. and Nixon P.J., The chloroplast-encoded α subunit of cytochrome *b-559* is required for assembly of the photosystem II complex in both the light and the dark in *Chlamydomonas reinhardtii*, *J. Biol. Chem.* 273 (1998) 29315-29320.
 - Muramoto T., Kohchi T., Yokota A., Hwang I. and Goodman H.M., The *Arabidopsis* photomorphogenic mutant *hyl* is deficient in phytochrome chromophore biosynthesis as a result of a mutation in a plastid heme oxygenase, *Plant Cell* 11 (1999) 335-348.

N

- Naver H., Haldrup A. and Scheller H.V., Cosuppression of photosystem I subunit PSI-H in *Arabidopsis thaliana*. Efficient electron transfer and stability of photosystem I is dependent upon the PSI-H subunit, *J. Biol. Chem.* 274 (1999) 10784-10789.
- Naver H., Scott M.P., Adersen B., Moller B.L. and Scheller H.V., Reconstitution of barley photosystem-I reveals that the *N*-terminus of the PSI-D subunit is essential for tight binding of PSI-C, *Physiol. Plant.* 95 (1995) 19-26.
- Negrutiu I., Shillito R., Potrykus I., Biasini G. and Sala F., Hybrid genes in the analysis of transformation conditions, *Plant Mol. Biol.* 8 (1987) 363-373.
- Neuwald A.F. and Landsman D., GCN5-related histone *N*-acetyltransferases belong to a diverse superfamily that includes the yeast SPT10 protein, *Trends Biochem. Sci.* 22 (1997) 154-155.
- Nield J., Balsera M., De Las Rivas J. and Barber J., 3D cryo-EM study of the extrinsic domains of the oxygen evolving complex of spinach: Assignment of the PsbO protein, *J. Biol. Chem.* (2002) published as manuscript M110549200.
- Niyogi K.K., Photoprotection revisited: Genetic and molecular approaches, *Annu. Rev. Plant Physiol. Plant Mol. Biol.* 50 (1999) 333-359.

-
- Niyogi K.K., Grossman A.R. and Bjorkman O., *Arabidopsis* mutants define a central role for the xanthophyll cycle in the regulation of photosynthetic energy conversion, *Plant Cell* 10 (1998) 1121-1134.

O

P

- Parinov S., Sevugan M., De Y., Yang W.C., Kumaran M. and Sundaresan V., Analysis of flanking sequences from *Dissociation* insertion lines. A database for reverse genetics in *Arabidopsis*, *Plant Cell* 11 (1999) 2263-2270.
- Parinov S. and Sundaresan V., Functional genomics in *Arabidopsis*: large-scale insertional mutagenesis complements the genome sequencing project, *Curr. Opin. Biotechnol.* 11 (2000) 157-161.
- Pesaresi P., Morales F., Moya I. and Bassi R., Xanthophyll cycle pigments in wild-type *Arabidopsis* and in *aba* mutants blocked in zeaxanthin epoxidation, in: P.Mathis (Ed), Photosynthesis. From light to biosphere, IV, Kluwer Academic Publisher, Dordrecht, The Netherlands, (1995) 95-98.
- Peter G.F. and Thornber J.P., Biochemical composition and organisation of higher plant photosystem II light-harvesting pigment-proteins, *J. Biol. Chem.* 266 (1991) 16745-16754.
- Pfannschmidt T., Nilsson A. and Allen J.F., Photosynthetic control of chloroplast gene expression. *Nature* 397 (1999) 625-628.
- Pierre Y., Breyton C., Kramer D. and Popot J.L., Purification and characterisation of the cytochrome B(6)F complex from *Chlamydomonas reinhardtii*, *J. Biol. Chem* 270 (1995) 29342-29349.
- Polevoda B., Norbeck J., Takakura H., Blomberg A. and Sherman F., Identification and specificities of N-terminal acetyltransferase from *Saccharomyces cerevisiae*, *Embo J.* 18 (1999) 6155-6168.
- Polevoda B. and Sherman F., NatC N^α-terminal acetyltransferase of yeast contains three subunits, Mak3p, Mak10p and Mak31p., *J. Biol. Chem.* 276 (2001) 20154-20159.
- Porse B.T., Cundliffe E. and Garrett R.A., The antibiotic micrococcin acts on protein L11 at the ribosomal GTPase centre, *J. Mol. Biol.* 287 (1999) 33-45.
- Porra R., Thompson W. and Kriedemann P., Determination of accurate extinction coefficients and simultaneous equations for assaying chlorophyll a and b extracted with four different solvents: verification of the concentration of chlorophyll standards by atomic absorption spectroscopy, *Biochim. Biophys. Acta*, 975 (1989) 384-394.
- Powles S.B., Photoinhibition of photosynthesis induced by visible light, *Annu. Rev. Plant Physiol. Plant Mol. Biol.*, 35 (1984) 15-44.

Q

R

- Renger G. and Govindjee M., The mechanism of photosynthetic water oxidation, *Photosynth. Res.* 6 (1985) 33-55.
- Ridley S.P., Sommer S.S. and Wickner R.B., Superkiller mutations in *Saccharomyces cerevisiae* suppress exclusion of M₂ double stranded RNA by L-A-HN and confer cold sensitivity in the presence of M and L-A-HN, *J. Biol. Chem.* 4 (1984) 761-770.
- Rigaut G., Shevchenko A., Rutz B., Wilm M., Mann M. and Seraphin B., A generic protein purification method for protein complex characterization and proteome exploration, *Nature Biotech.* 17 (1999) 1030-1032.
- Robinson C., Simon J., Thompson S.J. and Woolhead C., Multiple pathways used for the targeting of thylakoid proteins in chloroplast, *Traffic* 2 (2001) 245-251.
- Rodermel S., Haley J., Jiang C.Z., Tsai C.H. and Bogorad L., A mechanism for intergenomic integration: abundance of ribulose biphosphate carboxylase small-subunit protein influences the translation of the large-subunit mRNA, *Proc Natl Acad Sci USA* 93 (1996) 3881-3885.
- Rodnina M.V., Savelsbergh A., Matassova N.B., Katunin V.I., Semenov Y.P. and Wintermeyer W., Thiostrepton inhibits the turnover but not the GTPase of elongation factor G on the ribosome, *Proc. Natl. Acad. Sci. USA.* 96 (1999) 9586-9590.
- Rutherford A.W. and Heathcote P., Primary photochemistry in photosystem I, *Photosynth. Res.* 6 (1985) 295-316.
- Ryan P.C., Lu M. and Draper D.E., Recognition of the highly conserved GTPase center of 23S ribosomal RNA by ribosomal protein L11 and the antibiotic thiostrepton, *J. Mol. Biol.* 221 (1991) 1257-1268.

S

- Salanoubat M. et al., Sequence and analysis of chromosome 3 of the plant *Arabidopsis thaliana*, *Nature* 408 (2000) 820-822.
- Sambrook J., Fritsch E.F. and Maniatis T., *Molecular cloning: A laboratory manual.* 2nd Ed. Plainview, NY: Cold Spring Harbor Laboratory Press (1989).

-
- Samson G., and Bruce D., Complementary changes in absorption cross-sections of photosystem I and II due to phosphorylation and Mg²⁺-depletion in spinach thylakoids, *Biochim. Biophys. Acta.* 1232 (1995) 21-26.
 - Sander G., Ribosomal protein L11 from *Escherichia coli* its role in the binding of tRNA to the ribosome and in elongation factor G-dependent GTP hydrolysis, *J. Biol. Chem.* 258 (1983) 10098-10103.
 - Sanguinetti C.J., Dias Neto E. and Simpson A.J., Rapid silver staining and recovery of PCR products separated on polyacrylamide gels, *Biotechniques* (1994) 914-21.
 - Santini C., Tidu V., Tognon G., Ghiretti Magaldi A. and Bassi R., Three-dimensional structure of the higher-plant photosystem II reaction centre and evidence for its dimeric organization *in vivo*, *Eur. J. Biochem.* 221(1994) 307-315.
 - Sauer K., Primary events and the trapping of energy. *In Bioenergetics of Photosynthesis*, Govindjee, ed., Academic Press, New York (1975) 116-181.
 - Schägger H. and von Jagow G., Tricine-sodium dodecyl sulfate-polyacrylamide gel electrophoresis for the separation of proteins in the range from 1 to 100 kDa., *Anal. Biochem.* 166 (1987) 368-379.
 - Schägger H., Electrophoretic isolation of membrane proteins from acrylamide gels, *Appl. Biochem. Biotech.* 48 (1994) 185-203.
 - Scheller H.V., Jensen P.E., Haldrup A., Lunde C. and Knoetzel J., Role of subunits in eukaryotic photosystem I, *Biochim. Biophys. Acta* 1507 (2001) 41-60.
 - Schreiber U., Schliwa U. and Bilger W., Continuous recording of photochemical and non-photochemical chlorophyll fluorescence quenching with a new type of modulation fluorometer, *Photosynth. Res.* 10 (1986) 51-62.
 - Schrier P.I. and Möller W., The involvement of 50S ribosomal protein L11 in the EF-G dependent GTP hydrolysis of *E.coli* ribosomes, *FEBS Lett.* 54 (1975) 130-134.
 - Schultes N.P., Sawers R.J., Brutnell T.P. and Krueger R.W., Maize *high chlorophyll fluorescent 60* mutation is caused by an *Ac* disruption of the gene encoding the chloroplast ribosomal small subunit protein 17, *Plant J.* 21 (2000) 317-327.
 - Seraphin B., Sm and Sm-like proteins belong to a large family: identification of proteins of the U6 as well as the U1, U2, U4, and U5 snRNPs, *EMBO J.* 14 (1995) 2089-2098.
 - Shikanai T., Munekage Y., Shimizu K., Endo T. and Hashimoto T., Identification and characterization of *Arabidopsis* mutants with reduced quenching of chlorophyll fluorescence, *Plant Cell Physiol.* 40 (1999) 1134-1142.

-
- Silverstein T., Cheng L. and Allen J.F., Chloroplast thylakoid protein phosphatase reactions are redox-independent and kinetically heterogeneous, *FEBS Lett.* 334 (1993) 101-105.
 - Smooker P.M., Schmidt J. and Subramanian A.R., The nuclear-organelle distribution of chloroplast ribosomal proteins genes. Features of a cDNA clone encoding the cytoplasmic precursor of L11, *Biochimie* 73 (1991) 845-851.
 - Snyders S. and Kohorn B.D., TAKs, thylakoid membrane protein kinases associated with energy transduction, *J. Biol. Chem.* 274 (1999) 9173-9140.
 - Snyders S. and Kohorn B.D., Disruption of thylakoid-associated kinase 1 leads to alteration of light harvesting in *Arabidopsis*, *J. Biol. Chem.* 276 (2001) 32169-32176.
 - Somerville C.R., Analysis of photosynthesis with mutants of higher plants and algae, *Annu. Rev. Plant. Physiol.* 37 (1986) 467-507.
 - Speulman E., Metz P.L., van Arkel G., Lintel Hekkert B., Stiekema W.J. and Pereira A., A two component enhancer-inhibitor transposon mutagenesis system for functional analysis of the *Arabidopsis* genome, *Plant Cell* 11 (1999) 1853-1866.
 - Stark M. and Cundliffe E., On the biological role of ribosomal protein BM-L11 of *Bacillus megaterium*, homologous with *Escherichia coli* ribosomal protein L11, *J. Mol. Biol.* 134 (1979) 767-769.
 - Stark M.J., Cundliffe E., Dijk J. and Stoffler G., Functional homology between *E. coli* ribosomal protein L11 and *B. megaterium* protein BM-L11, *Mol. Gen. Genet.* 180 (1980) 11-15.
 - Steiner-Lange S., Gremse M., Kuckenbergh M., Nissing E., Schachtele D., Spenrath N., Wolff M., Saedler H. and Dekker K., Efficient identification of *Arabidopsis* knockout mutants using DNA-arrays of transposon flanking sequences, *Plant Biology* 3 (2001) 391-397.
 - Steinback K.E., Bose S. and Kyle D.J., Phosphorylation of the light-harvesting chlorophyll-protein regulates excitation energy distribution between photosystem II and photosystem I, *Arch. Biochem. Biophys.* 216 (1982) 356-361.
 - Swofford D.L., Phylogenetic analysis using parsimony (*and other methods). Version 4, Sinauer Associates, Sunderland, Massachusetts 2000.

T

- Tabata S. et al., Sequence and analysis of chromosome 5 of the plant *Arabidopsis thaliana*, *Nature* 408 (2000) 820-822.

-
- Tate W.P., Schulze H. and Nierhaus K.H., The *Escherichia coli* ribosomal protein L11 suppresses release factor 2 but promotes the release factor 1 activities in peptide chain termination *J. Biol. Chem.* 258, (1983) 12816-12820.
 - Tercero J.C., Riles L.E. and Wickner R.B., Localized mutagenesis and evidence for post-transcriptional regulation of Mak3p, *J. Biol. Chem.* 267 (1992) 20270-20276.
 - Tercero J.C. and Wickner R.B., Mak3P encodes an *N*-acetyltransferase whose modification of the L-A GAG NH₂ terminus is necessary for virus particle assembly, *J. Biol. Chem.* 267 (1992) 20277-20281.
 - Tercero J.C., Dinman J.D. and Wickner B.R., Yeast Mak3p *N*-acetyltransferase recognizes the *N*-terminal four amino acids of the major coat protein (GAG) of the L-A double stranded RNA virus, *J. Bacteriol.* 175 (1993) 3192-3194.
 - The *Arabidopsis* Genome Initiative, Analysis of the genome sequence of the flowering plant *Arabidopsis thaliana*, *Nature* 408 (2000) 796-815.
 - Theologis A. et al., Sequence and analysis of chromosome 1 of the plant *Arabidopsis thaliana*, *Nature* 408 (2000) 816-820.
 - Thompson J.D., Higgins D.G. and Gibson T.J., CLUSTAL W: improving the sensitivity of progressive multiple sequence alignment through sequence weighting, position-specific gap penalties and weight matrix choice, *Nucleic Acids Res.* 22 (1994) 4673-4680.

U

- Uetz et al., A comprehensive analysis of protein-protein interactions in *Saccharomyces cerevisiae*, *Nature* 403 (2000) 623-627.

V

- Vallon O., Bulte L., Dainese P., Olive J., Bassi R. and Wollman F.A., Lateral redistribution of cytochrome b6/f complexes along thylakoid membranes upon state transitions, *Proc. Natl. Acad. Sci. USA* 88 (1991) 8262-8266.
- Varotto C., Pesaresi P., Meurer J., Oelmüller R., Steiner-Lange S., Salamini F. and Leister D., Disruption of the *Arabidopsis* photosystem I gene *psaeI* affects photosynthesis and impairs growth, *Plant J.* 22 (2000) 115-124.
- Vener A.V., VanKan P.J.M., Rich P.R., Ohad I. and Andersson B., Plastoquinol at the quinol oxidation site of reduced cytochrome *bf* mediates signal transduction between light and protein phosphorylation: Thylakoid protein kinase deactivation by a single-turnover flash, *Proc. Natl. Acad. Sci. USA* 94 (1997) 1585-1590.

- Vener A.V., Ohad I. and Andersson B., Protein phosphorylation and redox sensing in chloroplast thylakoids, *Curr. Opin. Plant Biol.* 1 (1998) 217-223.
- von Heijne G., Steppuhn J. and Herrmann R.G., Domain structure of mitochondrial and chloroplast targeting peptides, *Eur. J. Biochem.* 180 (1989) 535-545.

W

- Walden R., Fritze K., Hayashi H., Miklashevichs E., Harling H. and Schell J., Activation Tagging: a means of isolating genes implicated as playing a role in plant growth and development, *Plant Mol. Biol.* 26 (1994) 1521-1528.
- Walters R.G. and Horton P., Acclimation of *Arabidopsis thaliana* to the light environment - changes in composition of the photosynthetic apparatus, *Planta* 195 (1994) 248-256.
- Weis E., Chlorophyll fluorescence at 77K in intact leaves: Characterization of a technique to eliminate artifacts related to self-absorption, *Photosynth. Res.* 6 (1985) 73-86.
- Wisman E., Hartmann U., Sagasser M., Baumann E., Palme K., Hahlbrock K., Saedler H. and Weisshaar B., Knock-out mutants from an En-1 mutagenized *Arabidopsis thaliana* population generate phenylpropanoid biosynthesis phenotypes, *Proc. Natl. Acad. Sci. USA* 95 (1998) 12432-12437.
- Wollman F.A., State transitions reveal the dynamics and flexibility of the photosynthetic apparatus, *EMBO J.* 20 (2001) 3623-3630.

X

Y

- Yamaguchi K. and Subramanian A.R., The plastid ribosomal proteins. Identification of all the proteins in the 50 S subunit of an organelle ribosome (chloroplast), *J. Biol. Chem.* 275 (2000) 28466-28482.
- Yamaguchi K., von Knoblauch K. and Subramanian A.R., The plastid ribosomal proteins. Identification of all the proteins in the 30S subunit of an organelle ribosome (chloroplast), *J. Biol. Chem.* 275 (2000) 28455-28465.

Z

- Zito F., Finazzi G., Delosme R., Nitschke W., Picot D. and Wollman F.A., The Qo site of cytochrome b₆f complexes controls the activation of the LHCII kinase, *EMBO J.* 18 (1999) 2961-2969.

APPENDIX

ERKLÄRUNG

“Ich versichere, daß ich die von mir vorgelegte Dissertation selbständig angefertigt, die benutzten Quellen und Hilfsmittel vollständig angegeben und die Stellen der Arbeit –einschließlich Tabellen, Karten und Abbildungen –, die anderen Werken im Wortlaut oder dem Sinn nach entnommen sind, in jedem Einzelfall als Entlehnung kenntlich gemacht habe; daß diese Dissertation noch keiner anderen Fakultät oder Universität zur Prüfung vorgelegen hat; daß sie – abgesehen von unten angegebenen Teilpublikationen – noch nicht veröffentlicht

worden ist sowie, daß ich eine solche Veröffentlichung vor Abschluß des Promotionsverfahrens nicht vornehmen werde.

Die Bestimmungen dieser Promotionsordnung sind mir bekannt. Die von mir vorgelegte Dissertation ist von Prof. Dr. Francesco Salamini betreut worden.”

Köln, den 25.4.2002

Paolo Pesaresi

TEILPUBLIKATIONEN:

- 1 Leister D, Varotto C, Pesaresi P, Niwergall A, Salamini F., Large-scale evaluation of plant growth in *Arabidopsis thaliana* by non-invasive image analysis, *Plant Physiol. Bioch.* 37 (1999) 671-678.
- 2 Varotto C., Pesaresi P., Maiwald D., Kurth J., Salamini F., Leister D., Identification of photosynthetic mutants of *Arabidopsis* by automatic screening for altered effective quantum yield of photosystem II, *Photosynthetica* 38 (2000) 497-504.
- 3 Varotto C., Pesaresi P., Meurer J., Oelmüller R., Steiner-Lange S., Salamini F., Leister D., Disruption of the *Arabidopsis* photosystem I gene *psaE1* affects photosynthesis and impairs growth, *Plant J.* 22 (2000) 115-24.
- 4 Pesaresi P, Varotto C, Meurer J, Jahns P, Salamini F, Leister D., Knock-out of the plastid ribosomal protein L11 in *Arabidopsis*: effects on mRNA translation and photosynthesis, *Plant J.* 27 (2001) 179-189.
- 5 Pesaresi P., Varotto C., Richly E., Kurth J., Salamini F., Leister D., Functional genomics of *Arabidopsis* photosynthesis, *Plant Physiol. Bioch.* 39 (2001) 285-294.

LEBENS LAUF

Name

Paolo Pesaresi

Adresse

Max-Planck-Institut für Züchtungsforschung
 Carl-von-Linne Weg 10
 D-50829 Köln
 Tel: +49-221-5062-416
 Fax: +49-221-5062-413
 e-mail: pesaresi@mpiz-koeln.mpg.de

Geburtsdatum und -ort

17.05.1971 Jesi (Ancona)
 Italien

Nationalität

italienisch

Ausbildung

1977-1982	Grundschule
1982-1990	Gymnasium
1990	Abitur
1990-1996	Studium der Biologie an der Universität Urbino, Italien
09/1994-10/1996	Diplomarbeit an der Universität Verona, Prof. R. Bassi, Thema: "Role of carotenoids and antenna proteins in the zeaxanthin dependent photoprotective mechanism."
07.11.1996	Diplomprüfung
01/1999	Beginn der Doktorarbeit am Max-Planck Institut für Züchtungs-forschung, Köln, Abt. Prof. F. Salamini, Arbeitsgruppe Dr. D. Leister

Publikationen

- 1 Pesaresi P., Morales F., Moya I. and Bassi R., Xanthophyll cycle pigments in wild-type *Arabidopsis* and in *aba* mutants blocked in zeaxanthin epoxidation, in: P.Mathis Ed., Photosynthesis. From light to biosphere, IV, Kluwer Academic Publisher, Dordrecht, The Netherlands (1995) 95-98.
- 2 Pesaresi P., Sandona D., Giuffra E., and Bassi R., A single point mutation (E166Q) prevents dicyclohexylcarbodiimide binding to the photosystem II subunit CP29, *Febs Lett.* 402 (1997) 151-156.
- 3 Buffoni M., Testi M.G., Pesaresi P., Garlaschi F.M. and Jennings R.C., A study of the relation between CP29 phosphorylation, zeaxanthin content and fluorescence quenching parameters in Zee mays leaves, *Physiol. Plantarum* 102 (1998) 318-324.
- 4 Ruban A.V., Pesaresi P., Wacker U., Irrgang K.D.J., Bassi R. and Horton P., The relationship between the binding of dicyclohexylcarbodiimide and quenching of chlorophyll fluorescence in the light-harvesting proteins of photosystem II, *Biochemistry* 37 (1998) 11586-11591.
- 5 Leister D., Varotto C., Pesaresi P., Niwergall A. and Salamini F., Large-scale evaluation of plant growth in *Arabidopsis thaliana* by non-invasive image analysis, *Plant Physiol. Bioch.* 37 (1999) 671-678.
- 6 Varotto C., Pesaresi P., Maiwald D., Kurth J., Salamini F. and Leister D., Identification of photosynthetic mutants of *Arabidopsis* by automatic screening for altered effective quantum yield of photosystem II, *Photosynthetica* 38 (2000) 497-504.

-
- 7 Varotto C., Pesaresi P., Meurer J., Oelmüller R., Steiner-Lange S., Salamini F. and Leister D., Disruption of the *Arabidopsis* photosystem I gene *psaE1* affects photosynthesis and impairs growth, *Plant J.* 22 (2000) 115-24.
 - 8 Pesaresi P., Varotto C., Richly E., Kurth J., Salamini F. and Leister D., Functional genomics of *Arabidopsis* photosynthesis, *Plant Physiol. Bioch.* 39 (2001) 285-294.
 - 9 Pesaresi P., Varotto C., Meurer J., Jahns P., Salamini F. and Leister D., Knock-out of the plastid ribosomal protein L11 in *Arabidopsis*: effects on mRNA translation and photosynthesis, *Plant J.* 27 (2001) 179-189.
 - 10 Grasses T., Pesaresi P., Schiavon F., Varotto C., Salamini F., Jahns P. and Leister D., The role of Delta pH-dependent dissipation of excitation energy in protecting photosystem II against light-induced damage in *Arabidopsis thaliana*, *Plant Physiol. Bioch.* 40 (2002) 41-49.
 - 11 Kurth J., Varotto C., Pesaresi P., Biehl A., Richly E., Salamini F. and Leister D., Gene-sequence-tag expression analyses of 1800 genes related to chloroplast functions, *Planta* (*in press*).
 - 12 Varotto C., Pesaresi P., Jahns P., Leßnick A., Tizzano M., Schiavon F., Salamini F. and Leister D., Single and double knock-outs of the genes for photosystem I subunits PSI-G, -K and -H of *Arabidopsis thaliana*: effects on PSI composition, photosynthetic electron flow and state transitions, *Plant Physiol.* (*in press*)

ACKNOWLEDGMENTS

I would like to thank Prof. Dr. F. Salamini for providing me the opportunity to work in his department at the Max-Planck-Institut für Züchtungsforschung and Prof. Dr. H. Saedler for providing the fellowship for this Ph.D.

I wish to express my gratitude to Dr. Dario Leister for taking the responsibility of being my supervisor and for suggestions, discussions and encouragement during my Ph.D.

I am grateful to Claudio Varotto for his friendship and valuable help in every situation. I thank him also for teaching me many of the techniques used in this thesis.

Many thanks to all the colleagues and friends of my group for their continuous help and for the nice atmosphere in the lab: Alexander, Alexandra, Angela, Ania, Barbara, Beatrice, Daniela, Erik, Fabio, Guido, Joachim, Marianne, Marco, Martin, Oliver and Regina.

I'd like to thank also external collaborators for their precious help: Dr. Jahns for HPLC analysis, Dr. Meurer for *in vivo* translation assays, Prof. Dr. Soave for electron transport measurements, Prof. Dr. Scheller for LHCI phosphorylation assay, Prof. Dr. Wickner for the *mak3-1* complementation assay, Dr. Masiero for two-hybrid analysis.